VSB TECHNICAL UNIVERSITY OF OSTRAVA | FACULTY OF ELECTRICAL ENGINEERING AND COMPUTER SCIENCE

Sensor for pressure measurement in the pleural cavity

Senzor pro měření tlaků v pohrudniční dutině

Bc. Tomáš Mimra

Diploma thesis

Supervisor: doc. Ing. Martin Černý, Ph.D.

Ostrava, 2021

I owe my gratitude to doc. Ing. Martin Černý, Ph.D. for helping me throughout the time I have been working on the thesis and helping me reach the internship in the Université Claude Bernard Lyon 1. I would like to extend my thanks to prof. Norbert Noury who was my mentor during the internship and helped me immensely during and even after my stay. His guidance was irreplaceable.

I would also like to say thanks to my family and friends who stood with me for every step of the way. And to my amazing wife Kristina Mimrová without whom I would sooner or later descend into madness.

Abstrakt

Tato diplomová práce pojednává o návrhu systému určenému k měření tlaku v pohrudniční dutině. V úvodu práce je rozebrána anatomie a fyziologie dutiny. Následně jsou prezentována aktuální řešení čerpaná z dostupné literatury. Poté je popsáno navržení a výběr měřícího řetězce a vybrána vhodná řešení z hlediska tvaru a materiálu. Dále jsou prezentovány čtyři metody testování vytvořených měřících balónků připojené k měřícímu řetězci. První z experiment otestoval maximální měřitelnou frekvenci dýchání. Druhý test ukazuje jakou senzitivitu má měřící řetězec na změny tlaku. V třetím testu jsou podrobeny měřící balónky praktickému testu, kdy se balónky vkládají do umělé plíce připojené k plicnímu ventilátoru a úkolem měřícího řetězce je zachytit dýchací křivku. Jako poslední experiment bylo otestování vytvořeného fyzického modelu a rovněž otestování měřící schopnosti balónku. U každého z testu jsou prezentovány statistické výsledky měření jež ukazují shodu tlaku skutečného a naměřeného a také vzájemnou korelaci mezi vstupní dechovou křivkou a křivkou změřenou.

Klíčová slova: tlak, pohrudniční dutina, balónek, dechová křivka

Abstract

This diploma thesis deals with the design of a system designed to measure the pressure in the pleural cavity. The anatomy and physiology of the cavity are discussed in the introduction. Subsequently, current solutions drawn from the available literature are presented. Then the design and selection of the measuring chain are described and suitable solutions in terms of shape and material are selected. Next, four methods of testing the created measuring balloons connected to the measuring chain are presented. The first of the experiments tested the maximum measurable respiratory rate. The second test shows how sensitive the measuring chain is to pressure changes. In the third test, the measuring balloons are subjected to a practical test, in which the balloons are inserted into an artificial lung connected to a ventilator and the task of the measuring chain is to capture the breathing curve. The last experiment was to test the self-made physical model and to test the measuring ability of the balloon. For each of the tests, the statistical results of the measurements are presented, which show the agreement of the actual and measured pressure, and the mutual correlation between the input breath curve and the measured curve.

Key words: pressure, pleural pressure, intrapleural pressure, measuring balloon, breath curve

Content

List of shortcuts

FDM	Fused Deposition Modeling- method of 3D printing
SLA	Stereolithography- method of 3D printing
3D	Three-dimensional dimension
TV	Tidal volume
IRV	Inspiratory Reserve Volume
ERV	Expiratory Reserve Volume
RV	Residual Volume
TLC	Total Lung Capacity
IC	Inspiration capacity
VC	Vital capacity
FRC	Function Residual Capacity
PT product	Pressure-Time Product
WOB	Work of Breathing
FLM	First-order lung mechanics model
RLS	Recursive Least Squares
EF	Exponential forgetting
VFF-RLS	Vector-type forgetting factor
TPU	Thermoplastic polyurethane
TPE	Thermoplastic elastomer
PP	Polypropylene
PLA	Polylactic acid
PETG	Polyethylene terephthalate glycol
PTFE	Polytetrafluoroethylene
PVC	Polyvinyl chloride

Figure list

Table list

Introduction

Lungs holds their shape only due to intrapleural pressure and the shape of a chest. When a baby is born, the first breath expands the lungs and they "stick" to the parietal pleura. Here the pleural cavity is created and there is intrapleural pressure. The value of the pressure during hale is approximately -8 kPa, what is approximately -60 mmHg, and during exhale the value is approximately -3,3 kPa, what is approximately -25 mmHg.

This pressure is usually measures by the pressure sensor applied into the esophagus. The measured pressure should be the same like intrapleural pressure, but there is no any evidence that the pressure measured inside of the esophagus is completely the same like intrapleural pressure.

The aim of this thesis is to develop a measuring method of intrapleural pressure based on invasive measurements. . The proposed method is based on measuring balloons, which should be placed into intrapleural area. The pressure inside of the measuring balloons is measured by precise pressure sensors, commonly used in the biomedical engineering applications.

This work focuses on the design and testing of measuring balloons. Balloons will be designed and then printed on FDM (Fused Deposition Modeling) and SLA (Stereolithography) 3D printers. Choosing the right design and the right material is also the goal of the thesis.

The designed sensor will be verified on a set of test experiments. The first-order transfer function will be calculated values which will show the frequency sensitivity. Also the calibration experiments for different shapes of measuring balloons will be performed. In the last step measuring balloons will be tested in the experimental setup with artificial lungs and commonly used patient ventilator.

1. Theory

In this chapter is described essentials about the anatomy, physiology, and pathology of the respiratory tract. Moreover, there are described the basics of mechanics of ventilation and all lung volumes and capacities. The last and key part of this theory will be the description of the pleural cavity.

1.1. Anatomy of the respiratory tract and thorax

This section was sourced from [1−5].

Respiratory tract represents a system of organs which ensures the exchange of gases between the blood and the external environment. The respiratory system is divided into the upper and lower respiratory tract.

The upper respiratory tract is used to transport inhaled air through the nose or mouth into the lungs. Upper respiratory tract consists of the nasal cavity, paranasal sinuses, and pharynx, which is divided into three parts: the upper nasopharynx, the middle oral pharynx opening into the oral cavity and the lower and laryngeal part of the pharynx, where the interface between the larynx and esophagus. The primary function of the upper respiratory tract is to heat the air.

The larynx is an unpaired organ which belongs to the upper and lower respiratory tract. Air passes through it into the trachea and then into the lungs, so it serves for respiration and further for phonation. It is stored in the front landscape of the neck. The laryngeal wall is reinforced with cartilage, small joints, ligaments, and membranes. Cartilage is controlled by 7 pairs of muscles. The surface is covered with adventitia and the cavity is lined with mucosa, which is attached to submucosal ligament. The vocal cords are stored in the larynx.

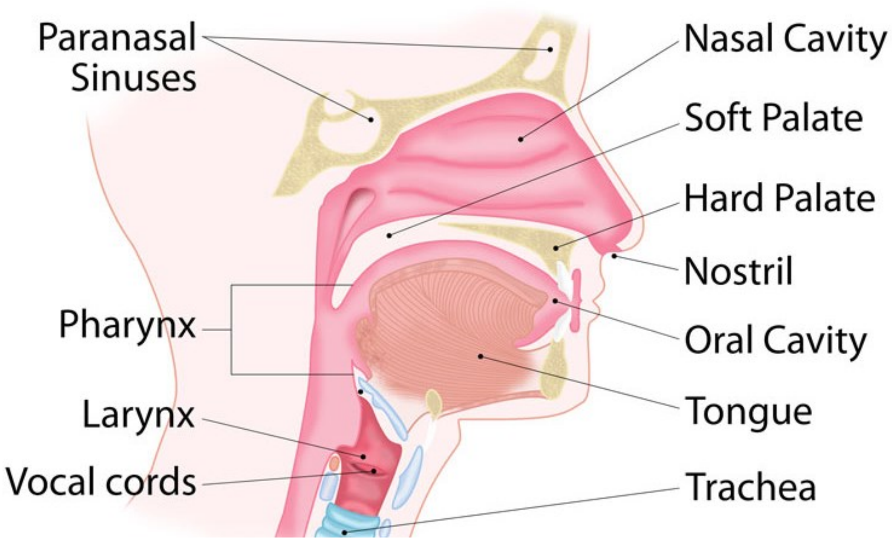

Figure 1: Upper respiratory tract [1]

The lower respiratory tract is also called the respiratory tree, or tracheobronchial tree continuing through the larynx, the trachea which further branches into the bronchi, which sink into the right and left lungs. The bronchus are divided into right and left main, also called primary bronchus, lobar bronchus and segmental bronchus. All these organs have the form of a cartilaginous tube which has flexible properties.

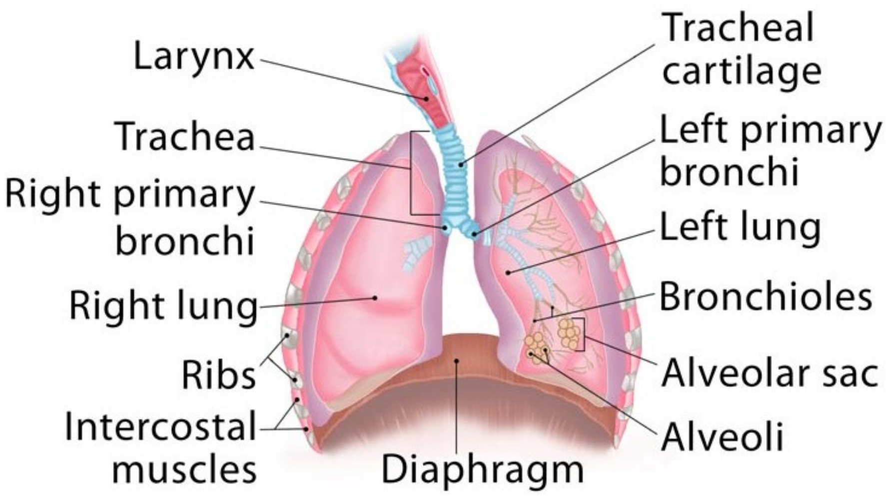

Figure 2: Lower respiratory tract [2]

In the lungs a chemical reaction occurs in which the blood is oxygenated. The lungs are divided into lobes, the right into three lobes and the left into two. The left lung is adapted to the heart by the number of lobes. The bronchus that enters the lungs is divided into bronchioles. Bronchiole is divided into conducting bronchiole, those are divided into terminal bronchiole, and those into respiratory bronchioles. The respiratory bronchiole passes into the alveolar duct which enters the alveolar sac. Sacs contain alveoli in which diffusion occurs.

The lungs must be protected from external mechanical influences, for this reason there is chest. Chest can also protect other organs such as heart and esophagus, important blood vessels, and nerves. The chest consists of twelve pairs of ribs, sternum, and thoracic spine. For the first 7 pairs of ribs, the cartilage attaches the ribs directly to the sternum. The other 3 pairs are connected by cartilage with the ribs placed above. The last 2 pairs remain unconnected, these ribs ending between the muscles of the abdominal wall. Together with the sternal vertebrae and sternum, the ribs form the thorax. Sternum is divided into three parts, the manubrium is the most superior region that is connected with the clavicle and the first pair of ribs. Body that is connected with the 3rd − 7th ribs, xiphoid process is the last inferior part.

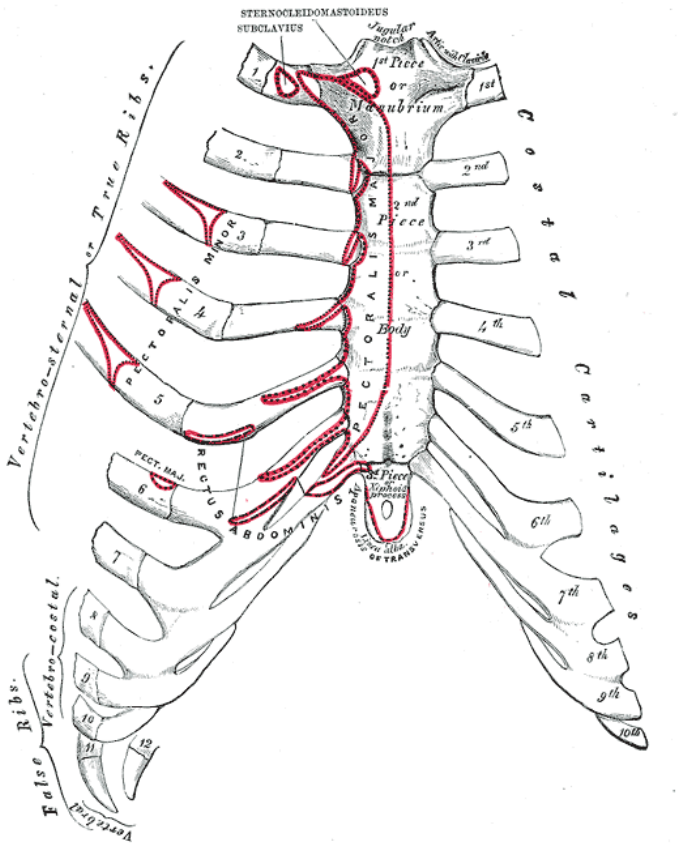

Figure 3: Anatomy of thorax anterior look [4]

1.2. Ventilation

This section was sourced from [6−8].

Each breathing cycle consists of inspiration and expiration phases. These phases alternate periodically to guarantee a sufficiently high partial pressure of oxygen and, conversely, a sufficiently low partial pressure of CO_2 in the alveoli. Maintaining these partial pressures is absolutely vital for the effective exchange of respiratory gases with the alveolocapillary membrane. Only with the optimal course of the respiratory cycle is sufficient extraction of CO_2 from the blood ensured and its saturation with oxygen.

1.2.1. Lung volume and capacity

Volume values are divided into two static classes. One is static volumes consist of four values. And the second one is the static capacity consisting of four values.

Static volumes:

- **Tidal volume (TV) –** volume that is inhaled during a normal breath. The physiological volume of an adult is approximately 10% of the volume of the lungs.
- **Inspiratory Reserve Volume (IRV) –** volume that will be forcibly inhaled after a normal breath (TV). The physiological volume of an adult is approximately 1900−3300 ml.
- **Expiratory Reserve Volume (ERV) –** volume that will be forcibly exhaled after a normal breath (TV). The physiological volume of an adult is approximately 700−1500 ml.

- **Residual Volume (RV) –** the rest of the volume after maximal exhalation. The physiological volume of an adult is approximately 1500 ml. This volume prevents the lungs from collapsing.

Static capacities:

- **Total Lung Capacity(TLC) –** is the total amount of air that the lungs may contain, it is calculated by the sum of TV, ERV, RV, and IRV. The physiological volume of an adult is approximately 6000 ml.
- **Inspiratory capacity (IC) –** maximum amount of air that can be inhaled after a normal exhale, it is calculated by the sum of TV and IRV.
- **Vital Capacity (VC) –** maximum amount of air that can be exhaled after a maximal breath, it is calculated by the sum of TV, ERV, and IRV.
- **Function Residual Capacity(FRC) –** amount of air that remains in the lungs after a normal exhale, it is calculated by the sum of TV and ERV.

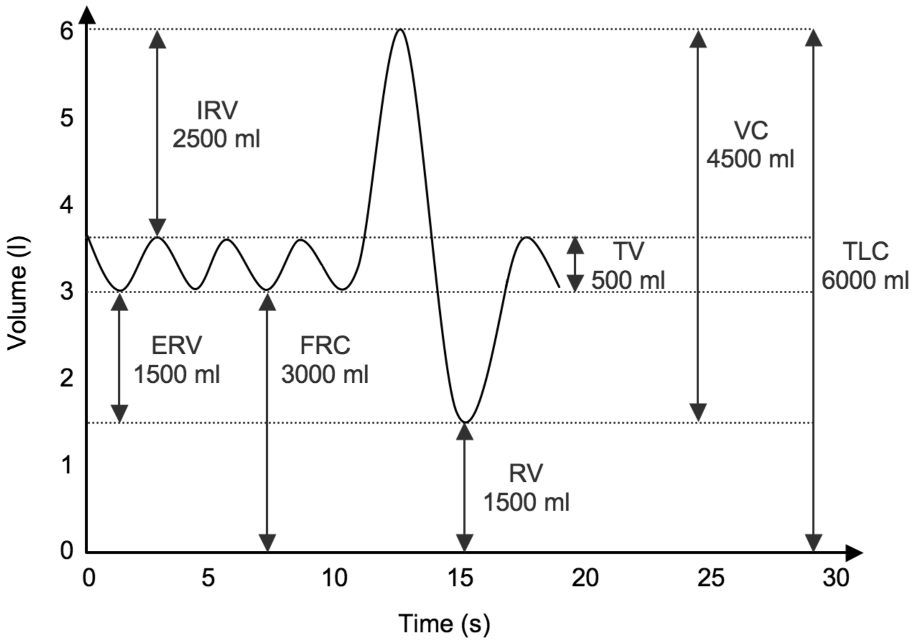

Figure 4: Lung volume and capacity with approximate values [6]

1.2.2. Mechanics of ventilation

Furthermore, called external or pulmonary respiration is the movement of air between the lungs and the external surroundings. The air moves to the lungs due to pressure changes inside of lungs. These changes are provided by contraction of the thoracic muscles and diaphragm. The process by which air travels to the lungs is called inspiration or inhalation. During inspiration inside of the lungs the pressure is lower than the atmospheric pressure due to expansion of the lungs. External ventilation involves atmospheric pressure, intrapulmonary pressure and intrapleural pressure. Atmospheric pressure is the pressure around us. Intrapulmonary the pressure is pressure inside on alveoli. Intrapleural pressure is the pressure between the lungs and chest, which holds the shape of the lungs.

"Inspiration (inhalation) is the process of taking air into the lungs. It is the active phase of ventilation because it is the result of muscle contraction. During inspiration, the diaphragm contracts

and the thoracic cavity increases in volume. This decreases the interalveolar pressure so that air flows into the lungs. Inspiration draws air into the lungs.

Expiration (exhalation) is the process of letting air out of the lungs during the breathing cycle. During expiration, the relaxation of the diaphragm and elastic recoil of tissue decreases the thoracic volume and increases the interalveolar pressure. Expiration pushes air out of the lungs." [8]

1.3. Pathology of pleural cavity

This section was sourced from [9].

Typical disease of the pleural cavity is called pleurisy, also pleuritis. A typical sign of this disease is stabbing pain in the chest area while breathing. Other symptoms may include shortness of breath, cough, fever, or weight loss, depending on the underlying cause. Pleurisy is manifested by inflammation in the pleural cavity. According to the findings in the pleural cavity, the pleurisy is divided into pleuritis sicca and pleuritis humida. Pleuritis sicca is without the presence of fluid in the pleural cavity and signs of this form are stabbing pain and shortness of breath. Pleuritis humida is with the fluid inside of the pleural cavity. The course of this form is more difficult for patients. To cure this form, it is necessary to perform a puncture in the area of the 7th to 9th ribs. The cause of both of these forms is mostly viral infection, but also bacterial infections, pneumonia, pulmonary embolism, autoimmune disorders, lung cancer, subsequent heart surgery, pancreatitis and asbestosis. The most related problems will be pneumothorax, hemothorax, or pleural effusion. The most common treatment for the pleural cavity is pneumothorax

1.4. Physiology of the pleural space [10]

Between 4-7 weeks of embryonic development, a pleural cavity is formed which is lined with splanchnopleure and somatopleure. Both pleura have two layers and have different anatomical properties. Between the underlying connective tissue layer and the pleural space is a layer of superficial mesothelial cells. In the cavity there is a relationship. For proper pleural membrane function, there is a relationship between the maintenance of the pleural fluid and the local inflammatory response. The fluid works like a transmitter of transpleural forces caused by breathing. The fluid moves from the costal pleura to the mediastinal.

The cavity is made up of stretchable mesothelial cells as has been said and thus provides enough space for organ expansion. The lungs maintain their shape only due to the mechanical connection between the chest wall and the lungs. Resistance, rich enzymes and organelles is a property of activated mesothelial unlike normal mesothelial cells which are very fragile in air. The endothelium acts as a major barrier to the free movement of fluids and electrolytes through normal mesothelial cells (Starling's law). In the lower part of the mediastinum there are a preformed stoma by which proteins and cells are removed. And due to respiratory movements, the pleural fluid is removed by the preformed stoma. Lymphatic vessels, central capillaries, lymphoreticular and activated mesothelial cells are conglomerates called Kampmeier's foci.

The air in the pleural cavity and sac is called pneumothorax. Pneumothorax occurs in lung or chest disorders in lung diseases and occurs when the lungs are injured near the pleural cavity, when inhaled air escapes into the cavity. Pneumothorax can have several possible complications. Tension pneumothorax can cause mediastinal movement, which is caused by ball valve leak. Compromise of the pulmonary circulation can also be fatal. If the lungs do not expand after pneumothorax and the leak heals within a few weeks, irreversible scarring of the lungs may occur and thus the lungs will not expand to their original size again. During lengthy treatment, the lungs and cavity become prone to infection. Once a person suffers from pneumothorax, there is a greater chance that pneumothorax will recur because the predisposing condition remains.

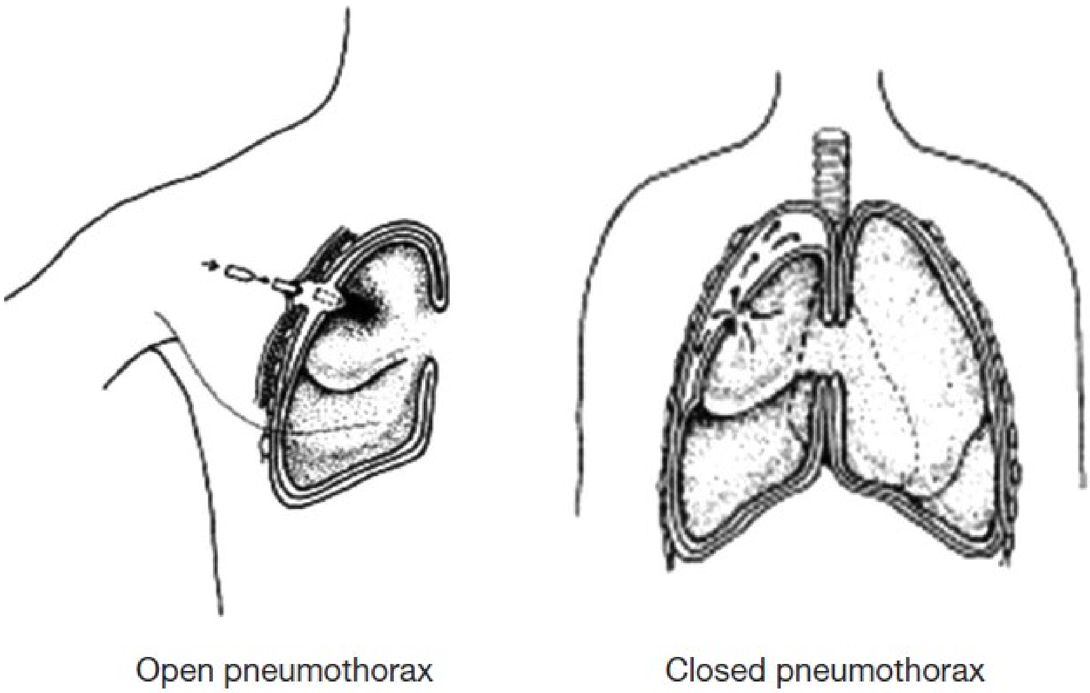

Figure 5: Types of pneumothorax [10]

2. Review

2. This chapter focuses on recent publication focused on pleural space from the view of anatomy and methods for measurement.

2.1. Evarts Ambrose Graham, Empyema, and the Dawn of Clinical Understanding of Negative Intrapleural Pressure [11]

2.1.1. Introduction

Understanding of negative intrapleural pressure is new. The first definition of mechanical breathing was in 1923 by Wirz. Empyema disease was known since antique during the time of Hippocrates. Most of the empyema cases were often successfully cured per open drainage, because it did not result in pneumothorax. During the epidemy in 1917−1918, there was a lot of cases with empyema and it was the catalyst for the renewed study of empyema. To cure the epidemy was used opening drainage, it resulted in a high mortality rate, likely because it causes pneumothorax. Due to the high mortality rate, U.S. Army let doctors study and try to understand the disease. During this period was created the Empyema Commission, one of the founders is Evarts Graham.

Few people who meet a patient with a chest tube connected to underwater seal drainage perceive how recent is our understanding of the dynamics of the pleural space and how much we owe to the work of the Empyema Commission.

2.1.2. Methodology

In 1674, John Mayow was the first who developed a functional model of breathing. Model consist of a balloon A, that is inserted to bigger balloon B. Balloon A has an opening that is open to outside. Balloon B is transparent. When balloon B is expanding, passive expansion acts on balloon A and through the opening of balloon A starts flowing air.

The first who measure intrapleural pressure was Ludwig in 1847 by using a balloon filled with water, balloon was in pleural space, which was connected to mercury manometer. Later in 1900, Aron made a measurement of intrapleural pressure on a healthy human. Meanwhile, clinical surgeons still cannot operate patients, because if they open the chest immediately the adhesion between the lung and thoracic is lost, it means pneumothorax.

The problem with immediate pneumothorax was solved by Sauerbuch and Mikulicz in 1904, which built low-pressure chambers, where the head of the patient and anesthetist are outside of the chamber and the body of patient and surgeons are inside of the chamber. By using the chamber during the operation, surgeons can operate on the esophagus, the lungs, and even the heart. (the chamber was replaced by endotracheal intubation and positive pressure ventilation).

Despite the fact that Graham started working with Empyema Commission in 1918 and described the negative intrapleural pressure and Wirz made the first definition of mechanical breathing in 1923, clinicians still did not understand the pressure completely.

Empyema disease was known since antique during the time of Hippocrates. Hippocrates created a method of open drainage almost 2000 years ago and nobody found a better way how to cure this disease approximately 1500 years after. Few people such as Roe, Stokes, Hewitt, or Bulau improved the method, but every step was created by Hippocrates´s open drainage.

2.1.3. Findings of the Empyema commission

Empyema commission found out the main reason of the empyema disease is hemolytic streptococcus. The Commission issued questionnaires to 32 US Army camps and found out that in most of the camps there is a mortality rate approximately 30%, but in some other army camps there was a mortality rate higher than 90%. Graham guesses it is because of the insufficient knowledge of the doctors about respiratory physiology.

The main reason that affects on pneumothorax during operation is what is the reason of the disease, if it is streptococcal or pneumococcal pneumonia. During pneumococcal pneumonia is usually formed fibrinous adhesion very early and it means there is less pus in the pleural space and open drainage does not cause pneumothorax. During streptococcal pneumonia pus made very late, approximately after 2 weeks, it means if the open drainage was made before the 14th day it causes pneumothorax.

Graham made principle of negative intrapleural pressure is "*counterplay of two forces*". It means there are two forces that interact with each other. One force is the tendency of the lung to pull away from the chest wall, and the second force is a very strong adhesion between the lung and chest wall. During inspiration, the intrapleural pressure becomes more negative, so it causes the lungs to expand. This means that during opening the chest intrapleural pressure raises and it causes lung collapse.

In 1906 L. Mayer said that opening the chest caused a difference pressure between the two pleural cavities: *"On the healthy side negative pressure of 7 mm of mercury, on the other side atmospheric pressure"* [11].

Meanwhile, in Europe there were two opponents, Pierre Duval and Sir Berkeley Moynihan, that disagreed with the results about negative intrapleural pressure, because they made successful removing shell fragments from the chest without any special technique and it did not cause pneumothorax, as Graham said. This expression could cause a lot of dangerous operations, because somebody could open the chest without any special technique, and it can cause pneumothorax.

Graham acknowledged that these problematics are very special, because there are some cases when the patient after surgical pneumothorax survives and can breathe with one lung. Mortality rate depends on the patients ability of breathing and their health condition.

Graham made experiments on dogs and found that the mediastinum did not isolate the pressure between lungs. "Graham drew 2 critical conclusions that paved the way for more ambitious forms of thoracic surgery. The first was that the normal thorax could be considered 1 cavity, because the mediastinum offers negligible resistance to pressure changes; the second was that the size of the pleural opening compatible with life was directly proportional to one's vital capacity, unless the mediastinum is fixed in position." [11]

2.1.4. Conclusion

Graham is recognized for his studies in the medical area, for example the discovery and explanation of intrapleural pressure. Graham was awarded by Samuel D. Gross Prize of Philadelphia. He became the second full-time professor of surgery in US. Graham was the first who made a successful pneumonectomy for lung cancer in 1933 on a 48-years-old gynecologist.

"What Graham is best remembered for is his ability to translate physiological understanding of respiratory mechanics into rational treatment for empyema." [11]

2.2. Real-Time Noninvasive Estimation of Intrapleural Pressure in Mechanically Ventilated Patients: a Feasibility Study [12]

2.2.1. Introduction

Monitoring of intrapleural pressure P_{pl} can provide Pressure-Time Product (PT product), Work of Breathing (WOB), or transpulmonary pressure, which is essential for choosing the strategy of ventilation and protect patients from overdistention of lung. For direct measure P_{pl} must be used an invasive method (pleural manometry), which can be dangerous for the patient because it can cause infection or other complications. That is why this method is not very typical and the method is replaced by the measure esophagus pressure (P_{es}). This technique is not very favorite because it is hard to use it correctly. There is a lot of artifacts and errors, if the operator did not work properly. For patients, this method is uncomfortable, because they must swallow the balloon with a catheter. These all disadvantages limit the use of this method in practice. Noninvasive real-time measurement is needed. Authors of this article [12] propose an estimated P_{pl} by using first-order lung mechanics model (FLM) and modified Recursive Least Squares (RLS). RLS and FLM used with exponential forgetting (EF) and vector-type forgetting factor (VFF-RLS) were applied for online calculation of lung parameters of human and animals.

2.2.2. Methodology

2.2.2.1. The Lung Mechanics Model

In the past, there was a few designed models with simple first-order resistance compliance model and higher-order resistance compliance that was made because of the inhomogeneity of lung. High-order model provided not satisfactory results because when there are more components, online algorithm sharply deteriorates as the number of parameters increases. To avoid this problem is better to use a simple first-order single-compartment model, which was chosen for this study [12].

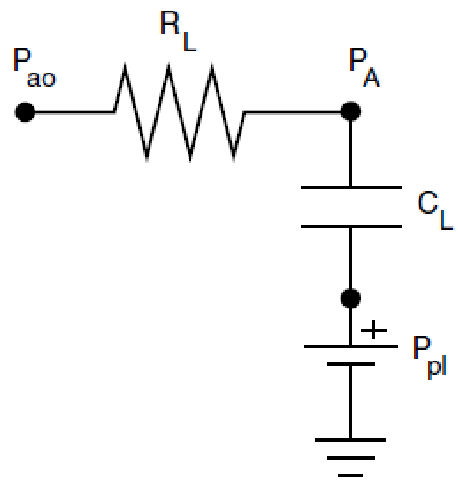

Figure 6: „Electrical analog of the single-compartment lung mechanics model. P_{ao}, airway pressure; R_L, lung resistance; P_A, alveolar pressure; C_L, lung compliance; P_{pl}, intrapleural pressure.“ [12]

Resistive components represent:

- conductive airways and the viscosity of the lung tissue (R_L)
- elastic properties of the lungs (C_L),
- pleural pressure (P_{pl})
- alveolar resistance (P_A)
- pressure at the airway opening (P_{ao})

Where P_{ao} depends on the balance between conductive airways and the viscosity of the lung tissue (R_L) and pleural pressure (P_{pl}).

$$P_{ao}(t) = R_L(t)\dot{V}(t) + \frac{1}{C_L(t)}V(t) + P_{pl}(t) + P_0 \qquad (1.)$$

Equation describing "equation of motion of the lung". Where $\dot{V}$ is the air flow, V is the lung volume, and P_0 is a constant of the functional residual capacity (FRC).

2.2.2.2. The Parameter Estimation Algorithm

Basic form of equation for this algorithm (2.2.2.2) is $P_{tp}= P_{ao}–P_{pl}$, where P_{pt} is transpulmonary pressure. The equation is transformed to a standard linear regression problem:

$$y(t) = P_{tp}(t) = \underbrace{\left[R_L(t) \frac{1}{C_L(t)} P_0\right]}_{\theta^T(t)} \underbrace{\begin{bmatrix}\dot{V}(t) \\ V(t) \\ 1\end{bmatrix}}_{x(t)} \qquad (2.)$$

where x(t) is the input variables vector, y(t) is output and θ^T is unknown parameters vector.

Authors of this article [12] propose to use equation (1.) with RLS technique. $P_{pl}(t)$ must be estimated from $R_L(t)$ and $C_L(t)$. More difficult thing is P_0 substituted by a time–varying term $P_0*(t)$:

$$y(t) = P_{ao}(t) = \underbrace{\left[R_L(t) \frac{1}{C_L(t)} P_0 * (t)\right]}_{\theta^T(t)} \underbrace{\begin{bmatrix}\dot{V}(t) \\ V(t) \\ 1\end{bmatrix}}_{x(t)} \qquad (3.)$$

by evaluating (1.) we can get offset term and by estimating $P_0*(t)$ we are actually estimating $P_{pl}(t)$. When estimating P_0 and substituting P_0 with $P_0*(t)$ leads to:

$$P_{pl}(t) – P_{pl}(t_{EE}) = P_0 * (t) - PEEP \qquad (4.)$$

where PEEP is the positive end–expiratory pressure value and t_{EE} is the end–expiratory time constant. By knowing PEEP and estimating $P_0*(t)$, we get only an estimate of the P_{pl} variation with respect to its base value.

2.2.2.3. Animal Experiment

The proposed technique was tested on 30 kg pig. Pig was anaesthetized, intubated, and connected to an ventilator. Pressure was measured on Y–piece. Esophageal pressure was measured by an esophageal balloon. Measured data was collected by a real−time dedicated system. The test took approximately 7 hours and during the time was used different ventilator modes and maneuvers.

2.2.3. Conclusion

The results of this article show the basic first-order lung mechanics model by using RLS technique is sufficient in ventilated patients for the estimation of intrapleural pressure, lung resistance, and compliance if airway pressure and flow are known. During mechanical ventilation, airway pressure and flow are commonly controlled. It means that this method is very useful to estimate intrapleural pressure during ventilation, because using other techniques is not necessary.

The best results had VFF−RLS algorithm. All measurements were done on one animal, it results to make a new study and try to make measurements on more animals or people because the data of one subject for credibility of the article is not enough.

In the new study, authors of the article [12] have to test more subjects, use more ventilation settings, control all ventilation parameters in more detail, and watch all changes of algorithm.

2.3. Improved technique for estimating pleural pressure from esophageal balloons [13]

2.3.1. Introduction

The most used method to measure pleural pressure is measure pressure from the esophagus. Measuring the pressure is done by a latex balloon putted in the esophagus, the balloon is connected with a catheter, and catheter leads to a manometer. Esophagus pressure would be the same like pleural pressure, if the pressure difference between all intervening structures is zero.

During measurement, a small part of the pressure is absorbed by the balloon. However, when the balloon is inserted into the esophagus, the volume of the balloon is increased by the effects of the esophageal wall and surrounding structures and the measured pressure grows.

Known fact is that esophageal pressure is more positive than pleural pressure. During the measurement, we cannot get the exact pleural pressure, but we can record the changes of pressure. It is assumed that the pleural pressure does not change when the lung volume changes. This article disproves this fact. Balloon volume is essential for measuring the pressure because it affects the measurement. When the balloon is bigger, it makes distortions on curves. To measure pleural pressure is better to use the smaller shape of balloons and the volume that is near to zero.

2.3.2. Methodology

Test was made on one man in an upright posture, lung volume was measured by a 9 liter Collins spirometer. Balloon is made from rubber and the dimensions are 30x50 cm and the wall thickness is ca. 0,06 mm. The balloon is connected to a polyethylene catheter of length 100 cm. When the balloon was inserted, the balloon was filled with 0,2 to 5 ml of air. Movement of balloon caused by breathing results in small pressure changes. Record of measurements was made after 3 full inspirations and then the subject holds breath for 2−4 seconds.

2.3.3. Result

With constant lung volume, the esophageal pressure is linear with balloon volume. Change in esophageal pressure was recognized when the volume of the balloon was changed, but these changes were seen only in extremes of vital capacity.

In the five other subjects, the relationship between esophageal pressure and balloon volume was also linear. The relationship was not linear when the volume of the balloon was less than 2 ml. Best result has subjects with the highest lung and residual volume.

2.4. Measurement of intrapleural pressure in patients with spontaneous pneumothorax: a pilot study [14]

2.4.1. Introduction

Recognition of spontaneous pneumothorax is complicated. Computed tomography or chest radiography are not able to recognize air leak. These techniques are able to show only a static image. Recognition of pneumothorax is able to interventional drainage with a chest tube and drainage connected to measure system is able to measure intrapleural pressure. Overall it is very problematic to recognize an air leak on the patient without drainage.

Authors of the article [14] develop a system that can measure air leak on a patient with pneumothorax and measure intrapleural pressure. This is system was tested on a handmade model of the thoracic cavity. They made a recording of the measurement and they get a periodical curve when they change the pressure from 0 to −20 cmH_2O. Model with pneumothorax was made by making small holes on model. Verifying of the model that is able to measure intrapleural pressure was made on the pig model.

The main aim of this article is the developed system is able to recognize the air leak on patient.

2.4.2. Methodology

Patient was chosen according to the type of pneumothorax. Pulse oximetry was used to measure oxygen saturation. By using chest radiography, they decide the degree of lung collapse according to the guideline. Definition for using chest drainage is persistent air leak. Permanent air leak is defined by drainage is used for more than 7 days. After measuring intrapleural pressure, the treatment was performed by conventional methods.

2.4.2.1. Needle puncture and measurement of intrapleural pressure

Measuring was made with the patient in the lateral position. Puncture was made on the site that was recognized on CT or radiography with a 16−gauge needle. To the needle was connected manometer. Measuring takes 30 seconds. Authors [14] made a device for measuring this pressure and they are waiting for patent. The device can measure air pressure with high sample speed (10 ms), 0,5% precision, and the range is from −4000 Pa to 4000 Pa. Output from the device is a continual curve.

2.4.2.2. Clinical course after measurement of intrapleural pressure

Although this study didn’t using any special methods for treatment pneumothorax, the treatment was started after measuring intrapleural pressure and the treatment follows the reason of pneumothorax. Treatment follows conventional methods such as observation, aspiration, and chest drainage in the outpatient clinic.

2.4.2.3. Data acquisition and statistical analysis

The time of measurement was 30 seconds with periodical breathing. Data during coughing was deleted. End−expiration and end−inspiration data were recorded prospectively. Anamnesis of patients were statistically evaluated for better understanding. “*The continuous data were analyzed using the*

Student's t−test and the categorical data using the chi−squared test. A p−value < 0.05 was considered statistically significant." [14]

2.4.3. Result

In this study [14] was measured eleven patients (3 women, 8 men, average age 46,6). Seven patients had secondary spontaneous pneumothorax and four patients had primary spontaneous pneumothorax. Four of the patients had pneumothorax for the first time. Two cases showed severe collapse of the lung on chest radiography and nine showed moderate collapse. Eight patients needed drainage for treatment, one of them needed evacuation of air with needle aspiration, and two of them were treated by oxygenation. All patients were measured for intrapleural pressure. Periodical curve was measured for all patients and in Figure 7 are shown the 3th, 4th, and 5th patients.

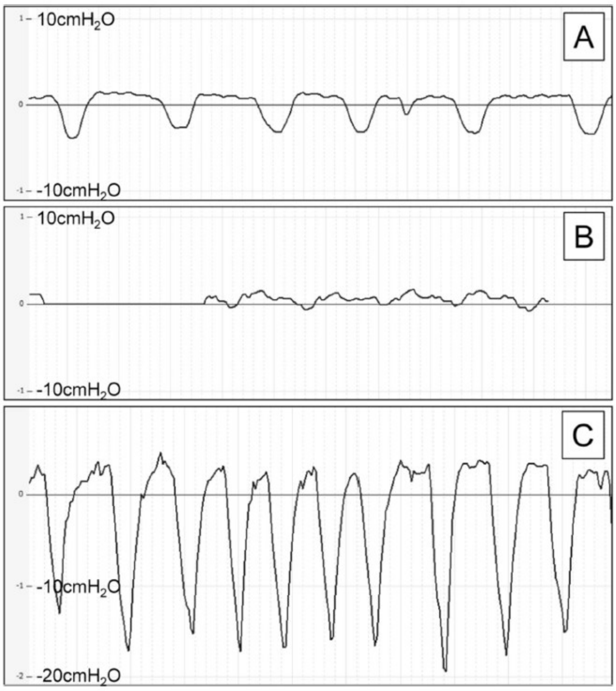

Figure 7: Intrapleural pressure of 3th, 4th, and 5th patient [14]

These data show the variation of the state of pneumothorax. Intrapleural pressure values were recorded at end−expiration and end−inspiration for each patient, these data are shown in Figure 8.

Case	Intrapleural pressure (cmH_2O)			Treatment and clinical outcome
	End-inspiration	End-expiration	Mean of end-inspiration and end-expiration pressure	
1	−4.18	−1.12	−2.65	Evacuation of 2200 ml of air full expansion
2	−3.16	0.71	−1.23	Drainage for 4 days
3	−3.37	1.43	−0.97	Drainage for 7 days
4	−0.82	2.04	0.61	Drainage for 7 days
5	−19.78	4.79	−7.50	Observation with oxygenation
6	0.10	2.75	1.43	Drainage for 11 days followed by surgery
7	0.00	5.81	2.91	Drainage for 8 days followed by surgery
8	2.65	6.02	4.34	Drainage for 10 days
9	−1.02	0.82	−0.10	Drainage for 1 days
10	−3.26	0.71	−1.28	Drainage for 4 days
11	−12.24	−6.22	−9.23	Observation

Figure 8: Intrapleural pressure values [14]

Intrapleural pressure was negative on end−inspiration and positive on end−expiration in six cases, permanently negative in two cases, and permanently positive in three cases. *"Figure 9 shows the changes in intrapleural pressure on treatment of aspiration in one of the patients (case 1), in whom the pressure in the thoracic cavity gradually decreased in proportion to the volume of air evacuated.*

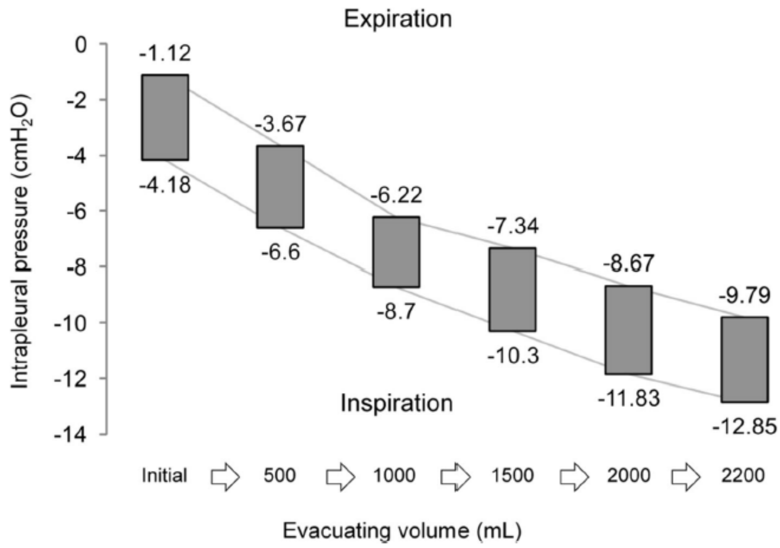

Figure 9:Changes in intrapleural pressure during evacuation of air in case 1 [14]

The number of mean intrapleural pressure values at end−inspiration and end−expiration in patients with persistent air leak, defined by a need for more than 7 days of chest drainage, was significantly lower than those in patients without persistent air leak (p = 0.020). The number of negative mean pressure recordings in end−inspiration and end−expiration was significantly lower in patients with persistent air leak than in those without persistent air leak (p = 0.0060)." [14].

3. Methodology

Intrapleural pressure is measured according to a measuring chain described in Figure 10. The main part is measuring balloon and pressure sensor. Signals from the sensor are acquired by PowerLab 4/26 and processed in software LabChart 7.

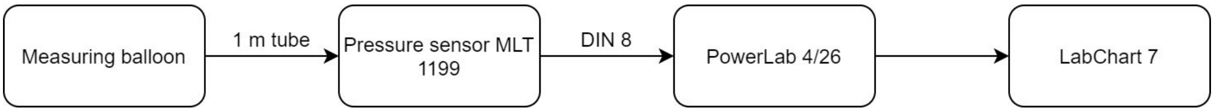

Figure 10: Measuring chain

3.1. The pressure sensor

The pressure sensor MLT1199 BP Transducer/Cable Kit as shown is used for pressure measurements. The sensor is dedicated for precise measurements in biomedical applications, with the sensitivity 5 µV/V/mmHg. The operating range is –50 to +300 mmHg.

Figure 11: MLT1199 BP Transducer/Cable Kit.

3.1.1. Sensor specifications

- *“Operating range: –50 to +300 mmHg*
- *Excitation voltage: 2 to 10 V DC*
- *Sensitivity (full range): 5 µV/V/mmHg*
- *Overpressure protection: –400 to +4000 mmHg*
- *Non−linearity and hysteresis: ±2 % of reading or ±1 mmHg (whichever is greater)*
- *Output impedance: ≤400 Ω*
- *Input impedance: 350 Ω ±10%*
- *Operating temperature: +15° C to 40° C*
- *Storage temperature: –25° C to +70° C*
- *Operating life: >500 hours*
- *Cable length: 1.2 m (3.9')*
- *Weight (including cable): 256 g*
- *Connector: Spacelabs plug MLAC06*
- *Adaptor Cable: 8 pin DIN to Spacelabs plug”* [15]

3.2. Measuring balloons

A measuring balloon is connected to the sensor described above. The connections I made by 1 meter long tube (made from polyvinyl chloride (PVC), business name “Hadice Luer Lock 36"”). In accordance with the aim of this work was designed and tested a set of different measuring ballons. Measuring ballons should be made by 3D printers, so the shape and material has to be discussed. There were designed 4 basic shapes and tested two different 3D printing methods- FDM (Fused Deposition Modeling) and SLA (Stereolithography) 3D printers, because printing hollow and sizable shapes are very complicated. Other aspect to consider was choosing the correct material.

3.2.1. Shape

When choosing the shape of the measuring balloon, it was considered the manufacturing process, because the measuring balloon has a cavity. Based on experiments, the vertical position of the measuring balloon in the 3D printer was chosen (Figure 12).

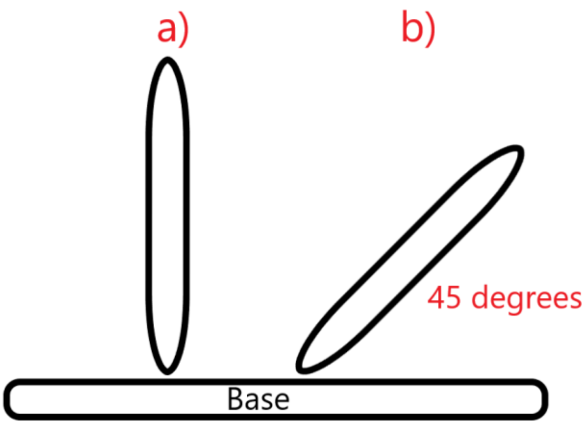

Figure 12: Shape orientation

It was also required to use a standard connector between the measuring balloon and the pressure sensos. The Luer Lock connector was chosen. Each measuring balloon have also the handling bore. (Figure 13).

Figure 13: Description of small triangle measuring balloon

Based on review, the anatomy and 3D printers options it was designed 4 different shapes of the measuring balloons (Figure 14). The easiest shape to print was the triangle, that is why the wall of the measuring balloon is thicker than other shapes. Dimensions are described in Table 1. The volumes are according to maximum height given to the contracting authority. The precise technical documentation could be found in in Appendice A: Dimensions of the measuring balloons.

Table 1: Dimension of the measuring balloons

Shape	Volume	Wall thickness	Measuring balloon width	Measuring balloon height
Circle	39,2 cm^3	0,12 cm	0,5 cm	10,9 cm
Square	50 cm^3	0,12 cm	0,5 cm	10,3 cm
Triangel	21,6 cm^3	0,06 cm	0,5 cm	8,7 cm
Small triangle	5,4 cm^3	0,06 cm	0,5 cm	4,5 cm

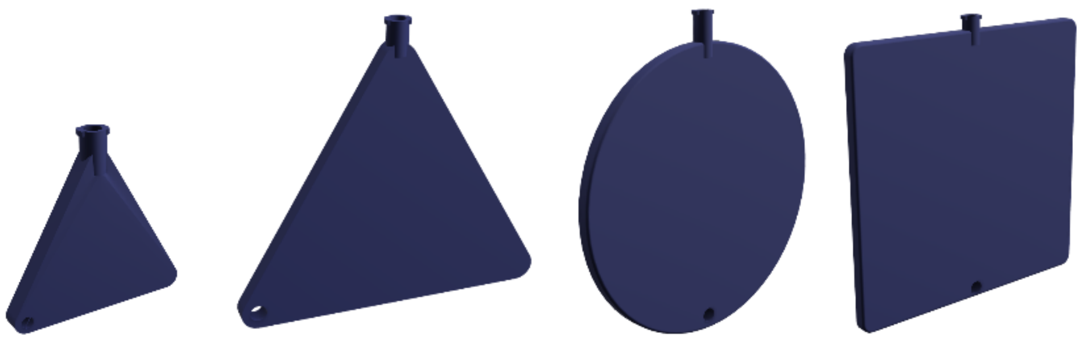

Figure 14: Small triangle measuring balloon, triangle measuring balloon, circle measuring balloon, square measuring balloon

3.2.2. Material

Materials that can be used for producing measuring balloons must be biocompatible or not harmless to health and flexible. Materials for 3D FDM printing are called filaments and for SLA 3D printing are called resins. Hardness of flexible filaments are described by a scale called Shore scale (Table 2). If the filament hardness is 95A, it means it is a flexible material like a pencil eraser.

Table 2: Shore scale [16]

Shore scale	Soft	Medium soft	Medium hard	Hard	Extra hard
Shore A	10 to 20	25 to 35	40 to 70	75 to 85	90 to 100
Flexible materials like	Gummies	Gel	Rubber		Eraser
Shore D	–	6 to 7	8 to 22	25 to 33	39 to 58
Semiflexible materials		Tire	Shoe heel	Shopping cart wheel	

Tested Measuring balloons are made of 7 different materials, 5 for FDM printer, and 2 for SLA printer. All materials are described in Table 3

Table 3: Chosen materials

Material	**Marking**	**Shore**	**Business name**
FDM printer			
Thermoplastic polyurethane	TPU	92A	Ultimaker TPU 95A
Thermoplastic elastomer	TPE	95A	Gembird TPE flexible
Polypropylene	PP	32D	Ultimaker PP 32D
Polylactic acid	PLA	rigid	Prusament PLA
Polyethylene terephthalate glycol	PETG	rigid	Prusament PETG
SLA printer			
Photopolymer resin based on Thermoplastic polyurethane	TPU resin	85 - 90 A	eSUN LCD UV 405nm TPU-Like Resin
Photopolymer resin	-	rigid	ANYCUBIC 405nm UV Sensitive Resin

A total of 28 measuring balloons of various shapes and materials were realized, which were further subjected to testing of their properties.

4. Measurement

This chapter describes the testing procedures of realized measuring balloons. The frequency response, sensitivity to pressure change, and quality of controlled respiration recording with an artificial lung and physical model was tested. Top rated measuring balloons will be used for further testing on laboratory animals.

4.1. Frequency response tests

To be able to test the frequency response of the sensory measuring balloon, test equipment was designed and implemented. It consists of a tube 5 cm wide and 70 cm long. The tested sensory measuring balloon was placed under the test device. The test was performed by lowering a roll-shaped weight of 500 g from a height of 50 cm onto a sensory measuring balloon (Figure 15).

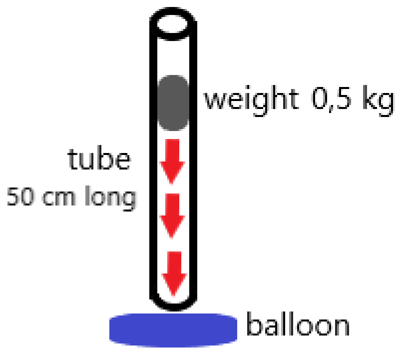

Figure 15: Example of measuring

After the impact, the weight bounces off the measuring balloon and after the bounce the weight is stopped, so it does not fall on the measuring balloon again, which creates a delta function(Figure 16). In the test was measured the time of leading edge (T_r) as you can see in Figure 16, marked orange, which were measured manually.

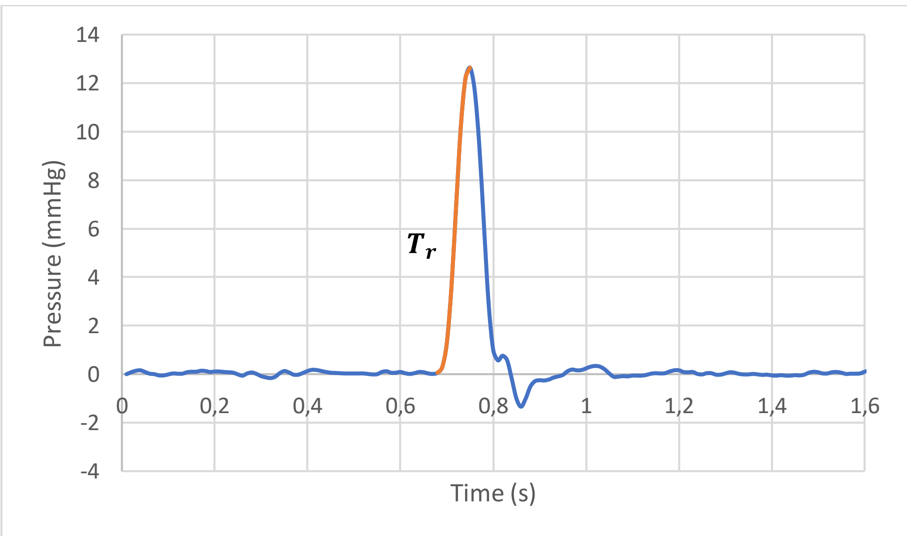

Figure 16: Delta function

Each measuring balloon was tested 10 times. To calculate the frequency response of the measuring balloon, a calculation according to the formula(5.) was done. It corresponds to first-order transfer function. Calculation of this value was made by measuring the time of the leading edge (Figure 16- T_r). From T_r calculated 63%, after that, this value was multiplied by 2π, then was calculated value ω_0 and 1 was divided by ω_0.

$$F_R = \frac{1}{2 \cdot \pi \cdot (\frac{T_r}{100} \cdot 63)} \tag{5.}$$

From the calculated F_R for each of the performed experiments, an average value was calculated, which represents the frequency response of the measuring balloon - i.e. the highest possible detectable frequency change by a given measuring balloon.

4.1.1. Analysis of results

The aim of this test is to find out if measuring balloons with different shape and made from different materials are able to measure every single hale and exhale. Normal respiration rate is around 0,15 Hz to 0,35 Hz. Measured values (see Table 4) are higher. It means each of designed measuring balloon is sufficient for measurement intrapleural pressure and there is not necessary to discard some of measuring balloons.

Table 4: Averaged value of frequency response of all measuring balloon shapes and materials (Hz)

	PETG	**PLA**	**PP**	**Rigid resin**	**TPE 95A**	**TPU 92A**	**TPU resin**
Triangle	2,3	3,2	6,2	4,3	26,6	60,6	36,2
Small triangle	2,3	3,1	3,0	3,7	24,1	42,2	31,3
Square	2,8	2,4	5,0	4,2	28,8	39,8	47,2
Circle	2,2	2,6	3,6	4,5	27,9	44,0	47,2

Best frequency response had measuring balloons made from flexible materials, TPU 92A, which shows the best results, followed by TPU resin and TPE 95A as it is shown in Figure 17-23 and in Appendice B: Frequency response. Semiflexible material PP has a much smaller frequency response, but it is still enough to measure high frequency respiration. The smallest frequency responses have the remaining rigid materials, but it is also still enough to measure high frequency respiratory rate such as baby tachypnea (2 Hz), the normal respiratory rate is around 0,15 Hz to 0,35 Hz. [17]

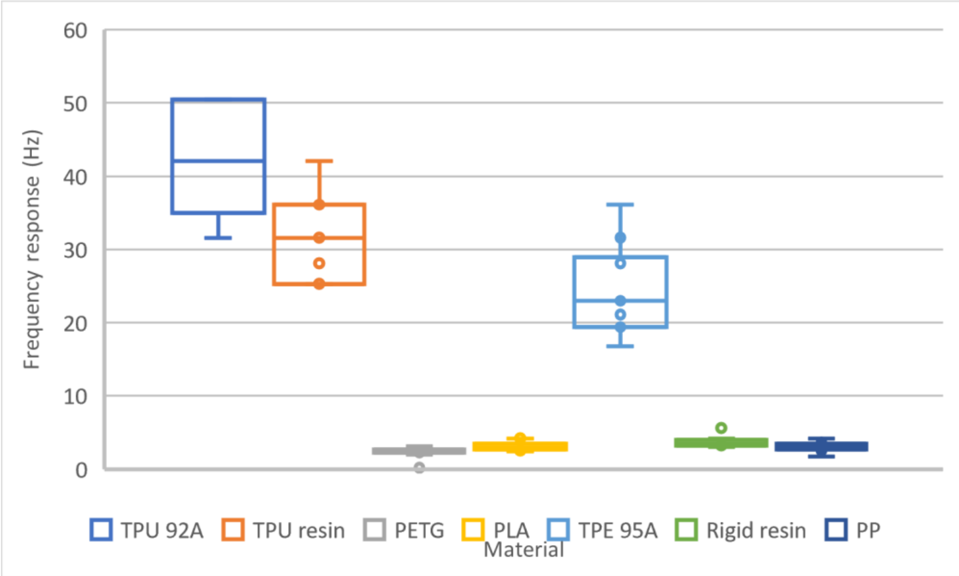

Figure 17: Frequency response of a small triangle measuring balloon shown by a boxplot

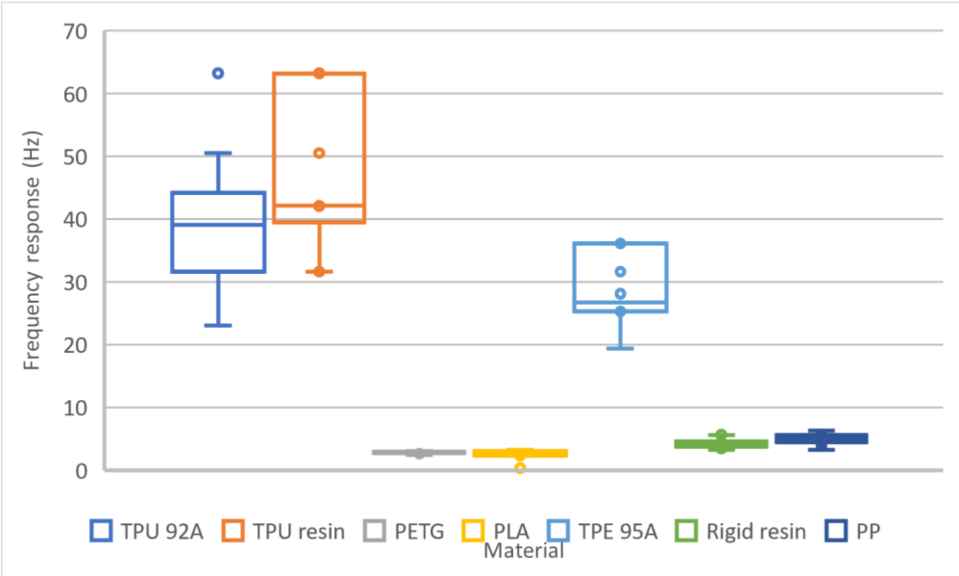

Figure 18: Frequency response of a square measuring balloon shown by a boxplot

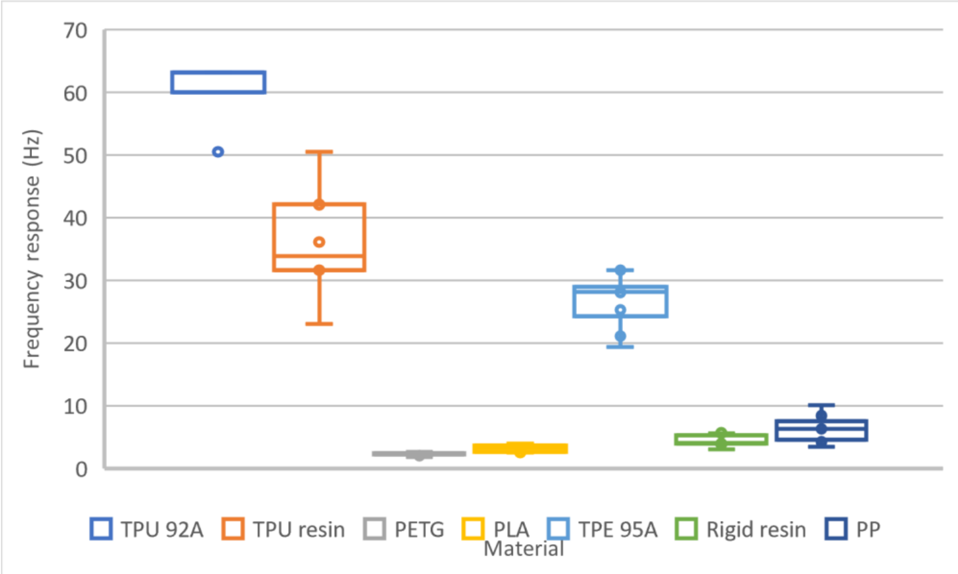

Figure 19: Frequency response of a triangle measuring balloon shown by a boxplot

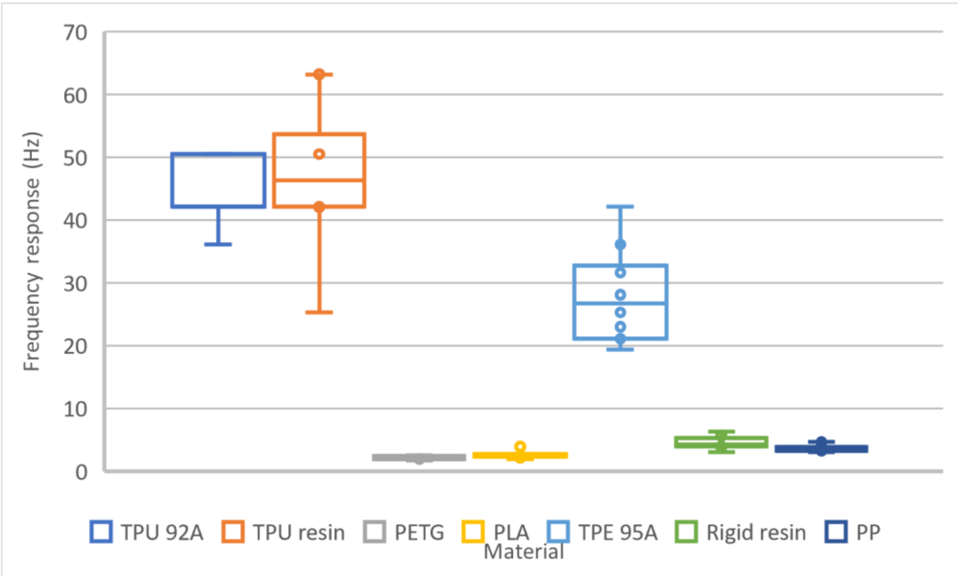

Figure 20: Frequency response of a circle measuring balloon shown by a boxplot

All frequencies are recorded in the tables in Appendice B: Frequency response.

4.2. Measuring balloon dive

In this test was measured pressure change when the depth is changed. Measurement was made in 7 different depths 0, 15, 30, 45, 60, 75, and 105 centimeters. The test was performed in a graduated cylinder as u can see in Figure 21, 12 cm wide and 120 cm long. Cylinder is filled with water. The depths were checked by a string to which the measuring balloon was tied, with the string was also attached a weight, which ensured the measuring balloon remained at one depth. There were marks on the string according to which the measuring balloon was immersed. In every depth the measuring was made for 15 seconds. There was performed measurements on all measuring balloons which were 28 measurements. During 15 seconds was measured approximately 10 000 samples.

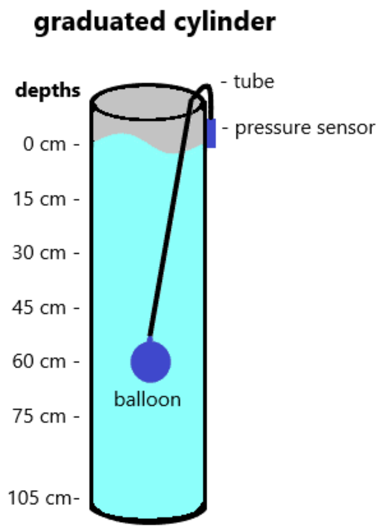

Figure 21: Example of measuring in depth 60 cm

The dive of a 15 cm measuring balloon in water corresponds to a pressure change of 10 mmHg, which is the proof is this equation

$$p = h \cdot g \cdot \rho \qquad (6.)$$

where p is the pressure (Pa), h is the depth (m), g is the gravitational constant (N/kg), and ρ is the fluid density (kg/m^3)

$$h = 0{,}15\ m \qquad g \sim 10\frac{N}{kg} \qquad \rho \sim 1000\ kg/m^3$$

$$p = 0{,}15 \cdot 10 \cdot 1000 \rightarrow 1500\ Pa$$

$$constant\ 10\ mmHg = 1333\ Pa$$

$$10\ mmHg \sim 15\ cm$$

this leads to the fact that if we immerse the measuring balloon to a depth of 15 cm, it will be exposed to a pressure of approximately 10 mmHg, that is 1333 Pa. Every measurement is computed with this approximation of pressure.

The process of one test is shown in Figure 22, where outliers were removed from the 20-second interval, the intervals were averaged (Figure 22, intervals marked orange) and recorded in a table in mV (Table 3). Output values are recorded in mV, in upcoming tests this experiment will be used as a unit conversion to mmHg. All data were recorded in the tables in Appendice C: Measuring balloon diving.

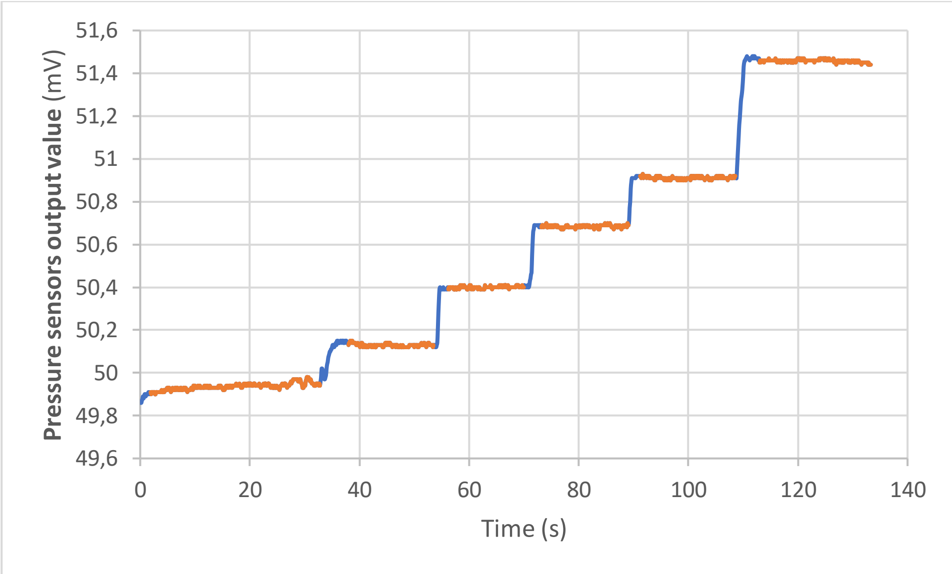

Figure 22: Water pressure recorded by circle measuring balloon made from TPU 92A

First pressure that was measured was set as offset. Pearson correlation coefficient was calculated, which calculate linearity. Also was calculated P-value which shows if the value is statistically significant, it means we do not confirm the null hypothesis, so the correlation will not be zero, and 95% confidence interval, which tell us with 95% probability the correlation coefficient will be in the calculated interval. All these operation was calculated in Rstudio and recorded to table (Table 6). Also for all 28 measurements were made graphs of dependence of water pressure and the measured measuring balloon pressure (Figure 23).

Table 5: Example of static characterization

Pressure sensors output value (mV)	**Height (cm)**	**Pressure sensors output value with offset (mV)**	**Water pressure (mmHg)**
8,93	0	0	0
9,22	15	0,29	10
9,46	30	0,53	20
9,637	45	0,707	30
9,85	60	0,92	40
10,11	75	1,18	50
10,61	105	1,68	70

Table 6: Pearson correlation coefficient, 95% confidence interval and P-value of all measuring balloon shapes and materials

	small triangle	triangle	square	circle
PLA	0,974 (0,826; 0,997) < 0,001 (n = 7)	0,993 (0,950; 0,999) < 0,001 (n = 7)	0,991 (0,936; 0,999) < 0,001 (n = 7)	0,993 (0,948; 0,999) < 0,001 (n = 7)
TPU resin	0,995 (0,967; 1,000) < 0,001 (n = 7)	1,000 (0,997; 1,000) < 0,001 (n = 7)	0,996 (0,974; 1,000) < 0,001 (n = 7)	0,995 (0,965; 1,000) < 0,001 (n = 7)
PETG	0,992 (0,945; 0,999) < 0,001 (n = 7)	0,973 (0,821; 0,997) < 0,001 (n = 7)	0,987 (0,911; 0,999) < 0,001 (n = 7)	0,993 (0,952; 0,999) < 0,001 (n = 7)
PP	0,993 (0,950; 0,999) < 0,001 (n = 7)	1,000 (0,996; 1,000) < 0,001 (n = 7)	0,969 (0,800; 0,996) < 0,001 (n = 7)	0,997 (0,981; 1,000) < 0,001 (n = 7)
rigid resin	0,918 (0,533; 0,988) 0,004 (n = 7)	0,993 (0,950; 0,999) < 0,001 (n = 7)	0,987 (0,911; 0,999) < 0,001 (n = 7)	0,976 (0,841; 0,997) < 0,001 (n = 7)
TPE 95A	0,962 (0,758; 0,995) 0,001 (n = 7)	0,984 (0,893; 0,998) < 0,001 (n = 7)	0,986 (0,901; 0,998) < 0,001 (n = 7)	0,971 (0,810; 0,996) < 0,001 (n = 7)
TPU 92A	0,999 (0,991; 1,000) < 0,001 (n = 7)	0,999 (0,990; 1,000) < 0,001 (n = 7)	0,999 (0,995; 1,000) < 0,001 (n = 7)	0,994 (0,956; 1,000) < 0,001 (n = 7)

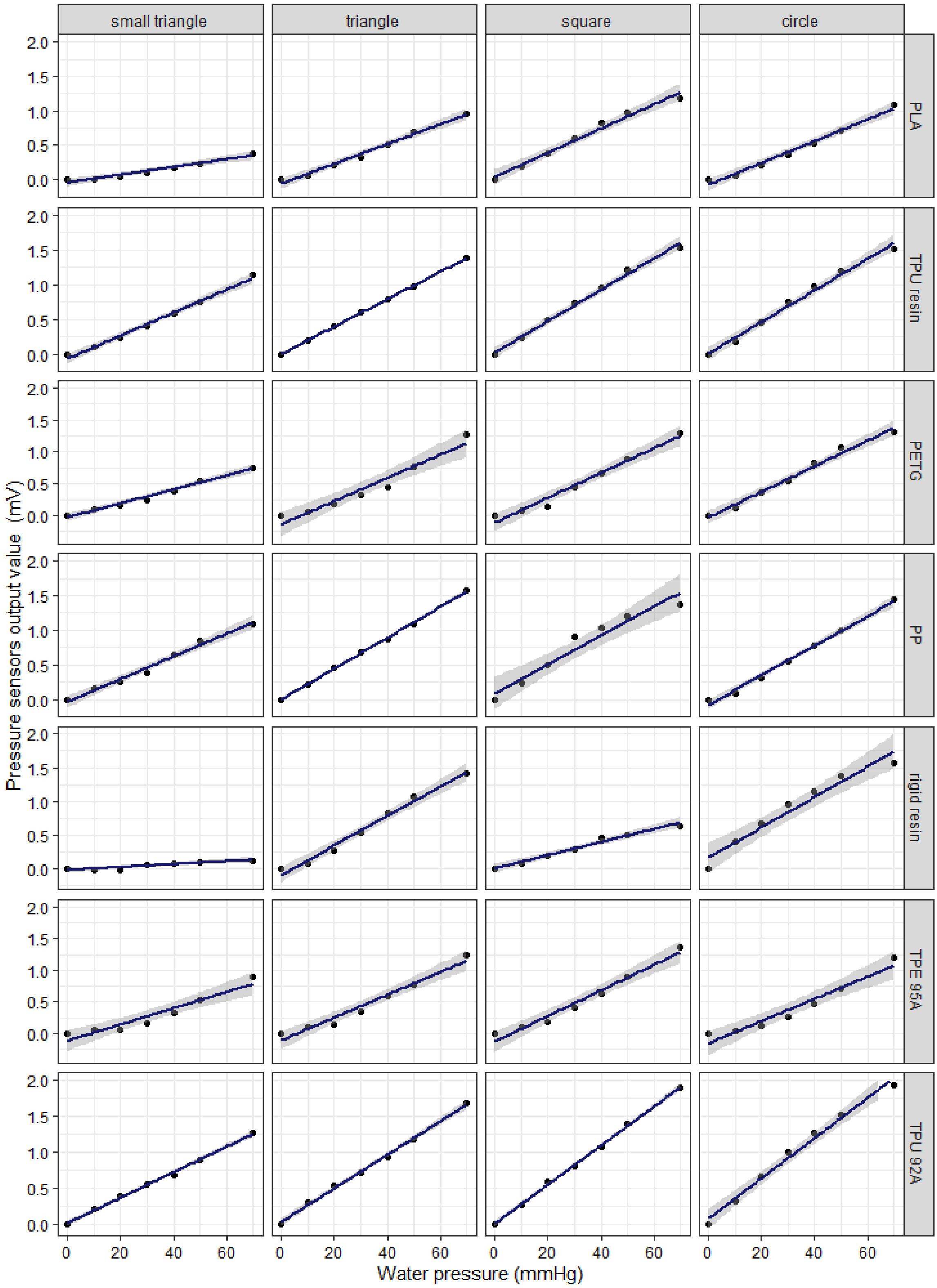

Figure 23: Static characterization of all measuring balloon shapes and materials

4.2.1. Analysis of results

Static characterization shows that the TPU 92A material has a smoother linear curve and the largest range as you can see in Figure 23 than other measuring balloons. This also shows Pearson correlation coefficient in Table 6, which shows the linearity of the recorded data. This means they are more consistent during measuring, which means these measuring balloons are more reliable and record pressure changes more smoothly. This is because TPU 92A is more flexible than other materials, which means the material can react better to pressure changes. In addition, this material has good properties for printing. This aspect surely acts on the results because the 3D printer prints these measuring balloons more consistent.

Other measuring balloons that can be used are the triangle measuring balloon made from PP and circle measuring balloon made from TPU resin. These measuring balloons have good linear curve, good sensitivity, and mainly a high correlation coefficient.

For the following tests were chosen all measuring balloons from TPU 92A, triangle measuring balloon made from PP, and circle measuring balloon made from TPU resin. From other materials was chosen measuring balloon with the best range and linear curve; from rigid resin it was a triangle measuring balloon, from PETG and TPE it was a circle measuring balloon, and from PLA it was a square measuring balloon.

4.3. Physical model

Physical model was designed and produced to test and characterize the measuring balloon response to simulated respiration. Physical model consists of two parts. One body simulated lung. Lung is imitated by a rectangle without one side. On the empty side is glued Teflon plate (Polytetrafluoroethylene- PTFE, business name- Aidmer78-021/022 PTFE Sheet/Coil) which is flexible and simulates stretching of lung during respiration (Figure 24 A)−white body). On the bottom is Luer lock for the inflating the measuring balloon (Figure 24 B)).Second body simulate ribs. The ribs are imitated by a plastic plate with strip−shaped holes that resemble the appearance and function of the ribs (Figure 24). Detailed dimensions are shown in Appendice D: Physical model in Figure 54 and Figure 55.

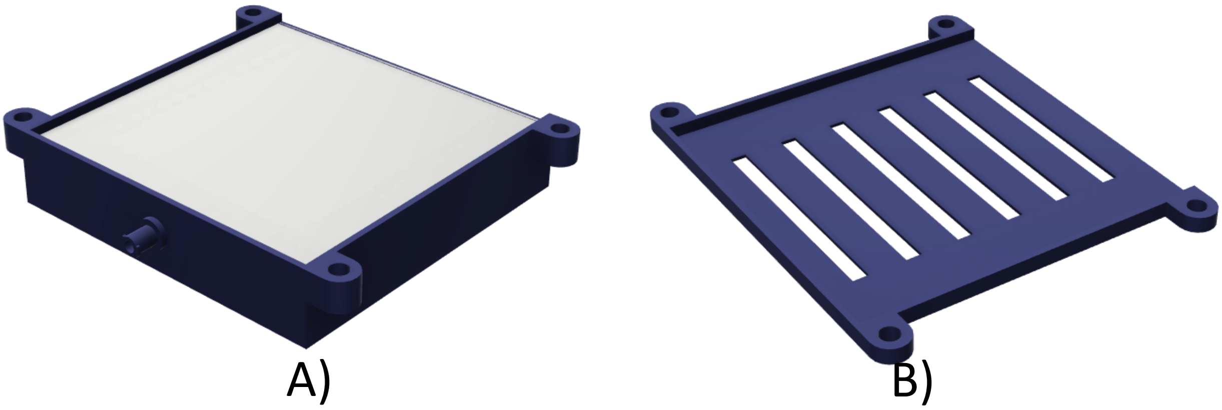

Figure 24: A) lung model, B) Ribs model

On the top of both models is a small opening for the insertion measuring balloon. These two models are fixed together with four screws.

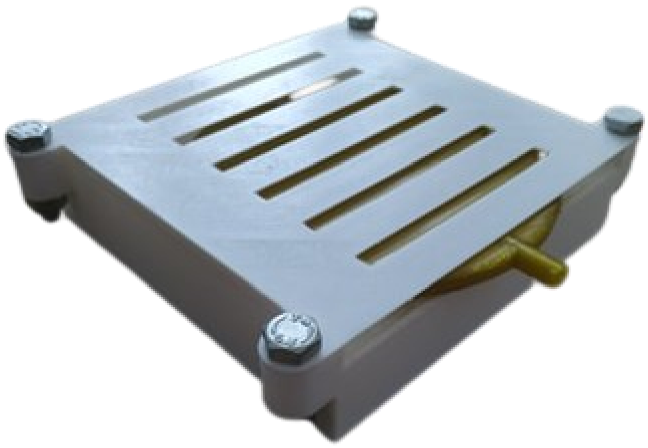

Figure 25: Implemented model of the chest with a measuring measuring balloon

Inflating the lung causes pressure on the measuring balloon, creating conditions similar to those in the intrapleural cavity. Discharge of inflated air is made by small openings made during gluing the Teflon part. It means there is not necessary to make a valve to discharge the air. The measurement was performed by connecting a pressure sensor to the measuring balloon and connecting a second pressure sensor to the tube through which the model is inflated.

From the previous test, Measuring balloon was set unit conversation as you can see in Figure 26. Where data from the first depth was set to 0 mmHg (Figure 26: Part 1) and the last depth was set to 70 mmHg (Figure 26: Part 2). It means the measuring balloons are now calibrated to pressure.

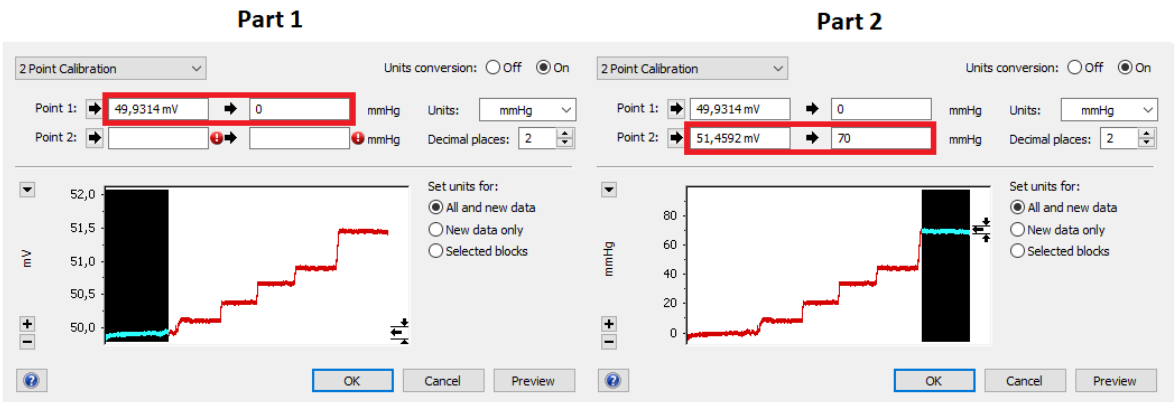

Figure 26: Unit conversion in LabChart 7 (circle measuring balloon made from TPU resin)

This test was performed with measuring balloons that was chosen in chapter Measuring balloon which are: all measuring balloons from TPU 92A, triangle measuring balloon made from PP and rigid resin, circle measuring balloon made from TPU resin, PETG and TPE, squared measuring balloon made from PLA.

4.3.1. Analysis of results

The aim of this part is to confirm right functionality of made physical model, but also to test and characterize measuring balloon response. Recorded curves shows the measuring balloons are able to measure the pressure, but the pumped pressure spread all over the surface and does not transform the force directly to the measuring balloon.

Best results have circle measuring balloon made from TPU resin (Figure 27), and square measuring balloon made from TPU 92A (Figure 28). For unknown reason in some cases isoline with time raises (Figure 28).

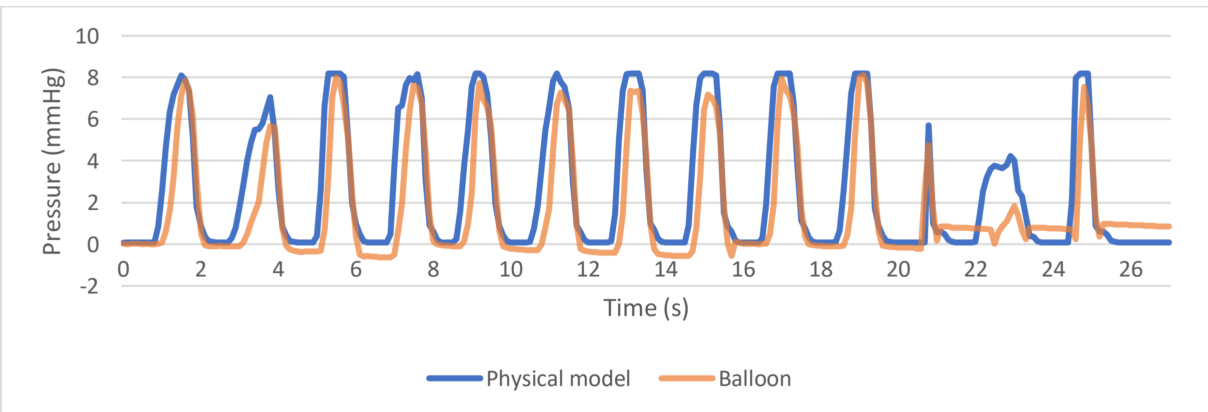

Figure 27: Physical model respiration curve of the circle measuring balloon made from TPU resin

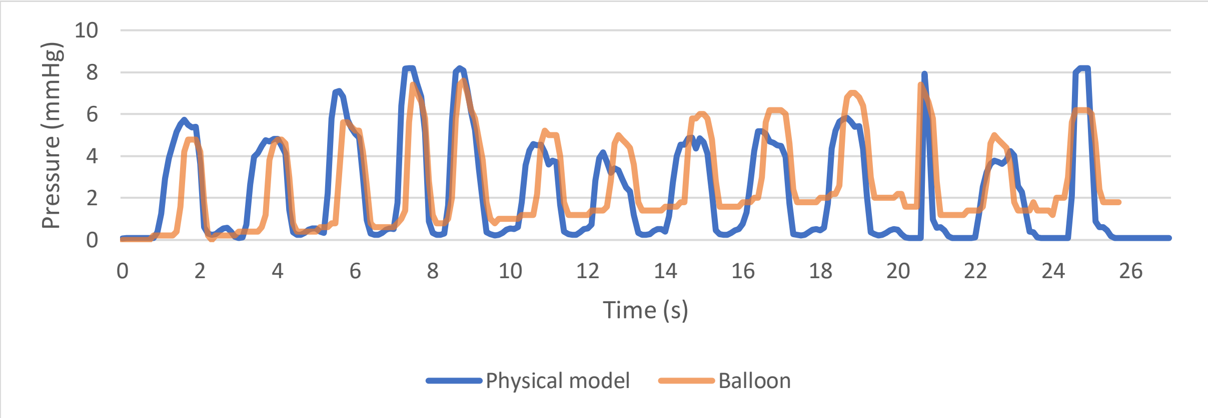

Figure 28: Physical model respiration curve of the square measuring balloon made from TPU 92A

Almost in every measurement when pressure begin to rise recorded curve by the measuring balloon is delayed (Figure 29).

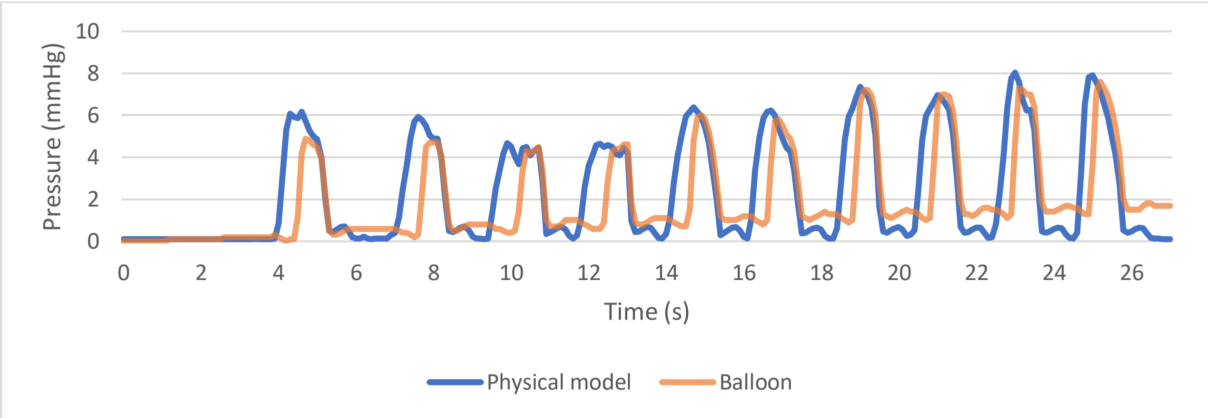

Figure 29: Physical model respiration curve of the circle measuring balloon made from TPU 92A

Overall, the recorded curves are in my opinion sufficient, but the calculated correlation coefficient shows the opposite (Figure 30). Coefficients were calculated from both curves of one measurement in excel using the function "CORREL". The fault is not on the side of the measuring balloon but of the physical model. For the future development of the physical model will be recommended usage same model, but using more flexible material than Teflon which will better act like flexibility of the lung.

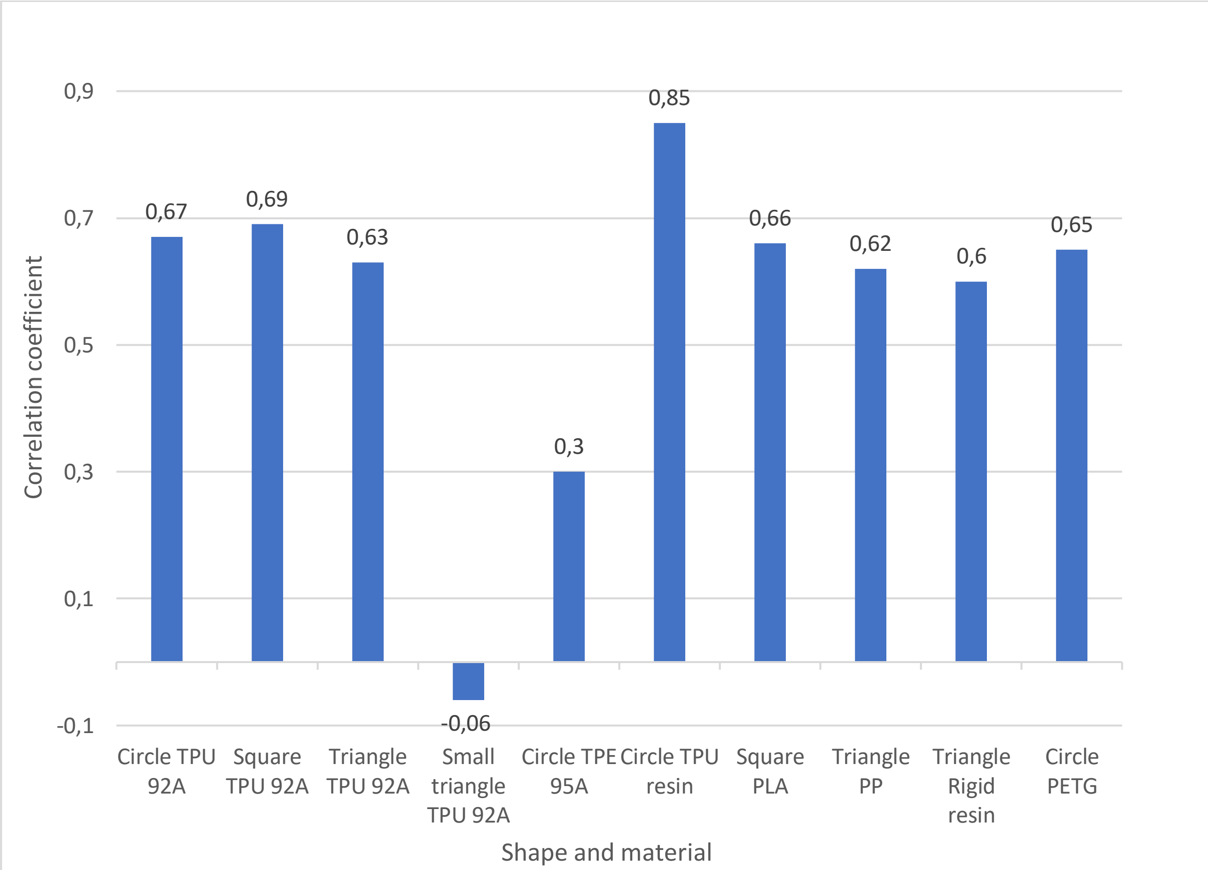

Figure 30: Correlation coefficient of the measuring balloons of physical model respiration

The rest of recorded curves are shown in the Appendice D: Physical model.

4.4. Test with artificial lung

Simulated respiration was made by an artificial lung connected to the hospital ventilator Monnal T50. These measurements are performed to test the measuring chain (Figure 10) to see if it is able to measure intrapleural pressure in practice. Furthermore, this test was performed for characterization of measuring balloon response to simulated respiration. By inserting the measuring balloon into the artificial lung, as you can see in , was measured response of the measuring balloon to the simulated respiration. Controlled respiration was measured by a flow sensor "ML 311", connected to the ventilator tube, for comparing recorded curve of the ventilator and curve of the measuring balloon (Figure 32). This test was performed with measuring balloons that were chosen in chapter 5.2 which are: all measuring balloons made from TPU 92A, triangle measuring balloon made from PP and rigid resin, circle measuring balloon made from TPU resin, PETG and TPE, squared measuring balloon made from PLA. The experiment lasted 60 seconds, the number of breaths which were recorded depended on the set frequency of the ventilator.

Figure 31: Artificial lung with inserted measuring balloon (marked with red arrow)

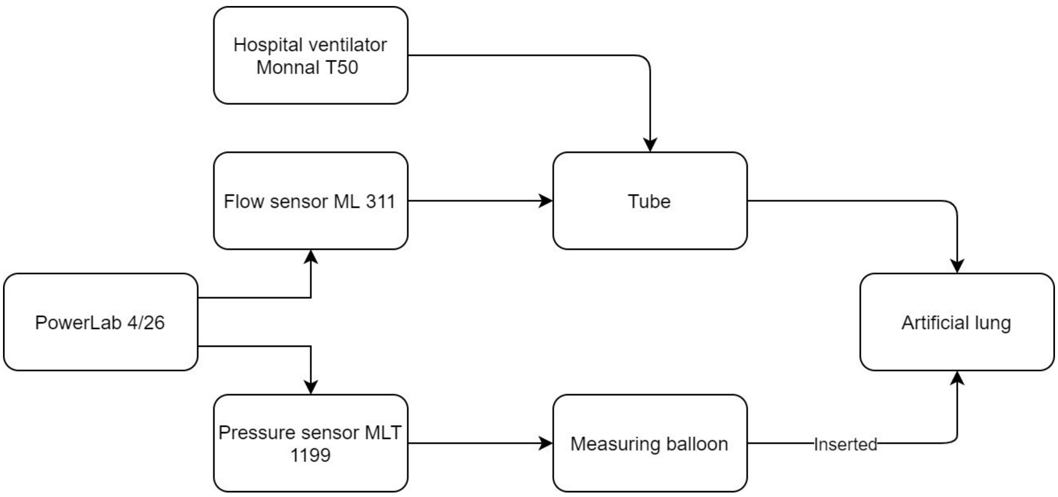

Figure 32: Measuring chain wiring diagram

Respiration frequency of the hospital ventilator was set to ten, twenty, and forty inhales per minute, which is 0,16 Hz, 0,33 Hz and 0,66 Hz. Unit conversion was made in previous measurement and as in the previous point, the data is processed (4.3).

There was calculated correlation coefficient of the curves which shows the similarity between them (Appendice E: Test with artificial lung). Coefficients were calculated from both curves of one measurement in excel using the function "CORREL". The closer the number is to one, the more similar the data are. A graph of recorded curve was made. Using the graph, we can visually compare the two recorded curves.

4.4.1. Analysis of results

The recording accuracy decreases with increasing respiration frequency as is shown in Table 7, Table 8, and Table 9.

In the first experiment with frequency 10 breaths per minute, there were not any measuring balloons that had a coefficient under 0,80. Displayed average difference in each maxima shows the differences are minimal, but in some cases (triangle made from rigid resin and PP, circle made from PETG) the differences are higher (Figure 33).

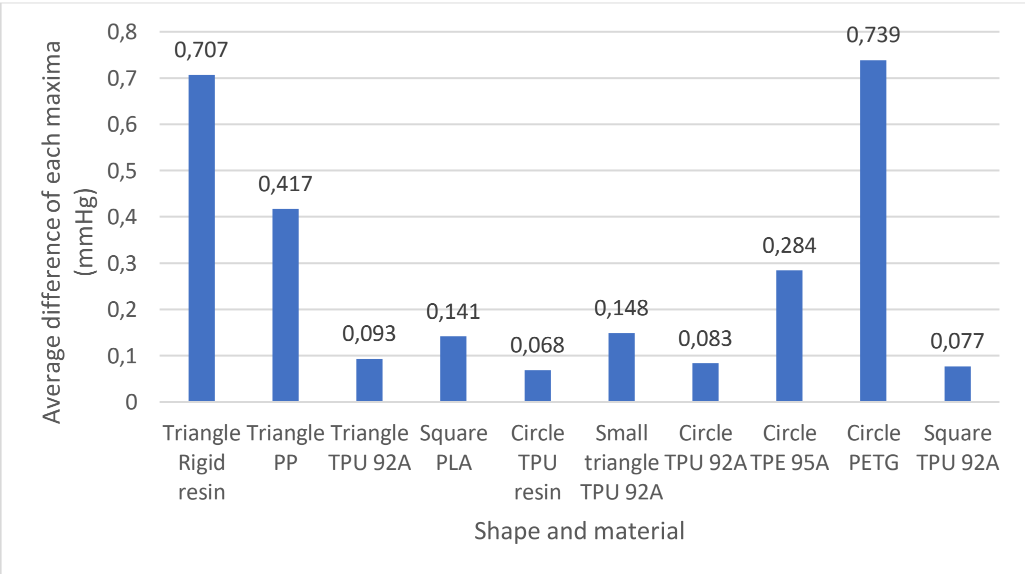

Figure 33: Average difference of each maxima with respiratory frequency 10 breaths per minute

The best measuring balloons with this frequency are circle measuring balloon made from TPU resin (Figure 34), circle and square measuring balloons from TPU 92A (Table 7).

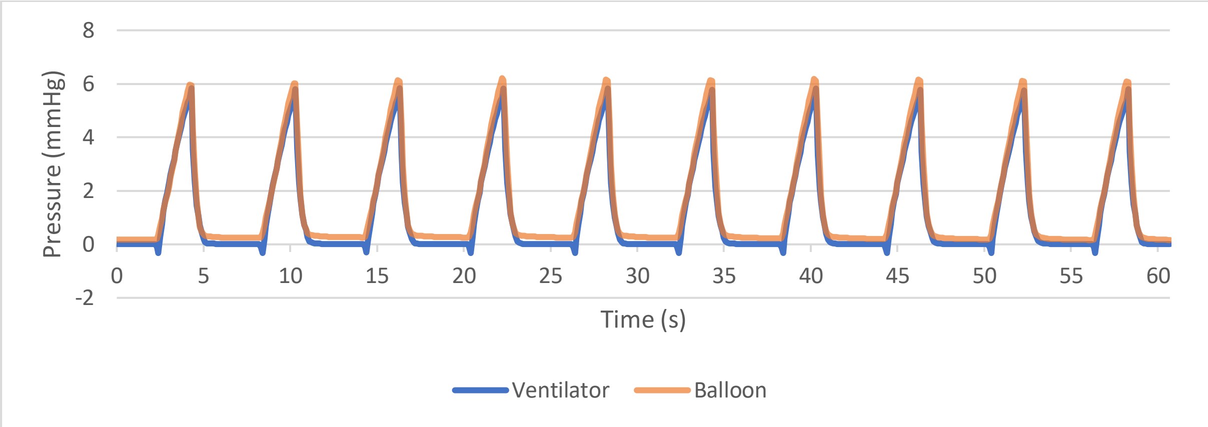

Figure 34: Respiration curve of the circle measuring balloon made from TPU resin (best of frequency 10 breaths per minute)

Table 7: Calculated correlation coefficient of the measuring balloon and ventilator with set respiration frequency to 10 breaths per minute

Correlation coefficient	Material	Shape
0,93	Circle	TPU 92A
0,96	Square	TPU 92A
0,89	Triangle	TPU 92A
0,88	Small triangle	TPU 92A
0,87	Circle	TPE 95A
1,00	Circle	TPU resin
0,87	Square	PLA
0,86	Triangle	PP
0,84	Triangle	Rigid resin
0,86	Circle	PETG

In the second experiment of this test was set 20 breaths per minute and there were few measuring balloons which correlation moves around 0,80 (square measuring balloon made from PLA and TPU 92A, triangle measuring balloons from PP and rigid resin, and circle measuring balloon made from PETG). The best results have, as in the previous experiment, a circle measuring balloon made from TPU resin (Figure 35) and TPU 92A (Table 8).

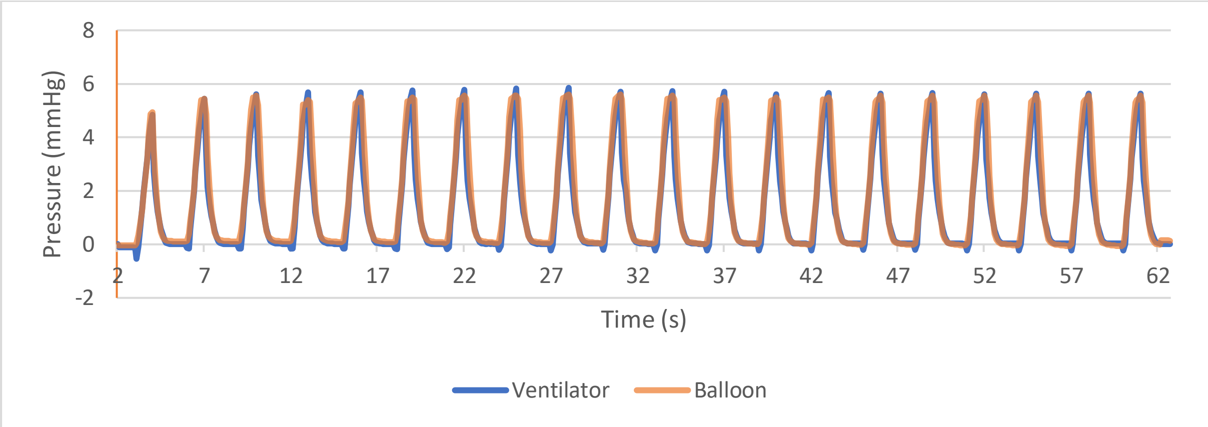

Figure 35: Respiration curve of the circle measuring balloon made from TPU resin (best of frequency 20 breaths per minute)

Table 8: Calculated correlation coefficient of the measuring balloon and ventilator with set respiration frequency to 20 breaths per minute

Correlation coefficient	Material	Shape
0,96	Circle	TPU 92A
0,81	Square	TPU 92A
0,88	Triangle	TPU 92A
0,75	Small triangle	TPU 92A
0,84	Circle	TPE 95A
0,98	Circle	TPU resin
0,81	Square	PLA
0,80	Triangle	PP
0,84	Triangle	Rigid resin
0,84	Circle	PETG

This also confirms average differences in each maxima, the differences are minimal, same like in previous frequency (Figure 36).

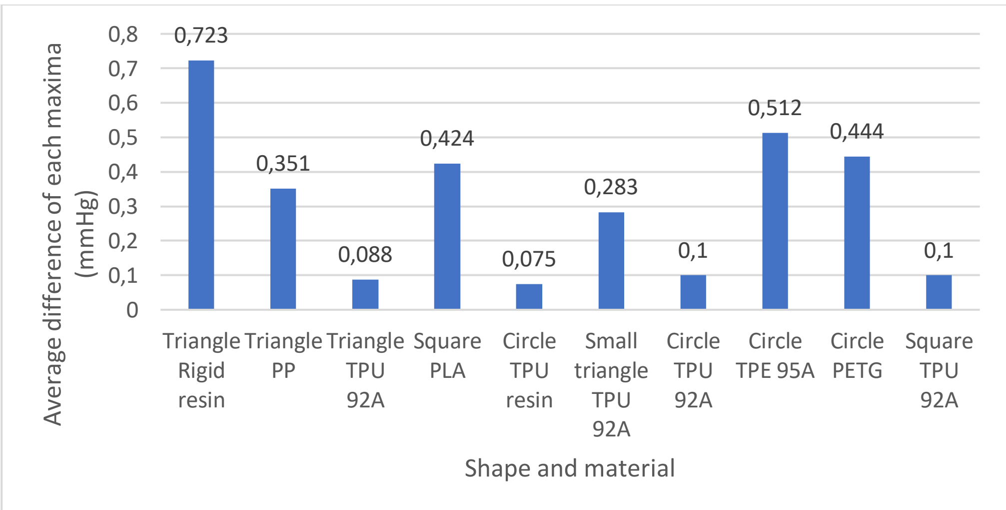

Figure 36: Average difference of each maxima with respiratory frequency 20 breaths per minute

The last experiment was with frequency 40 breaths per minute. Six out of ten measuring balloons have a correlation coefficient much below the limit 0,80. Positive results have only the circle measuring balloon made from TPU resin and all measuring balloons from TPU 92A except the small triangle (Table 9). The best measurement was recorded by a square measuring balloon made from TPU 92A (Figure 37).

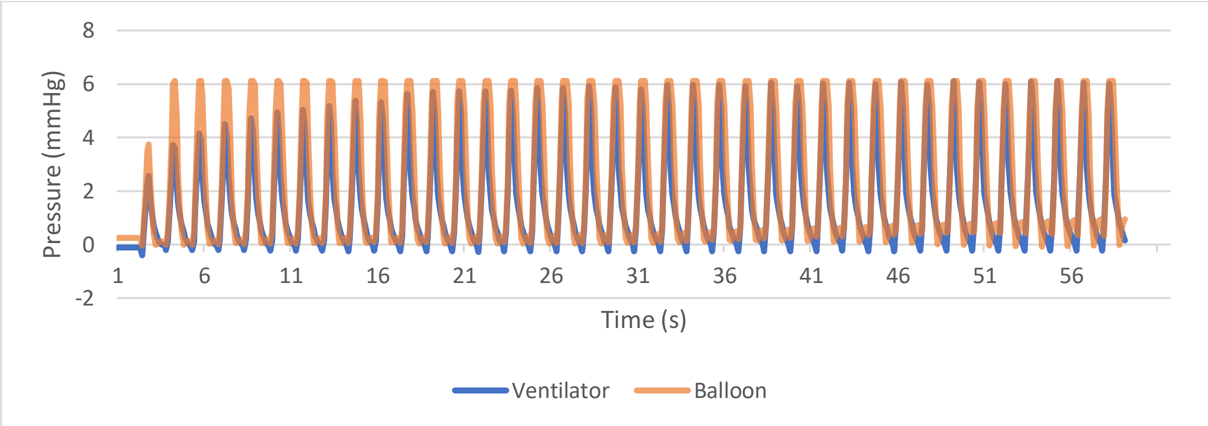

Figure 37: Respiration curve of the square measuring balloon made from TPU (best of frequency 40 breaths per minute)

Table 9: Calculated correlation coefficient of the measuring balloon and ventilator with set respiration frequency to 40 breaths per minute

Correlation coefficient	Material	Shape
0,89	Circle	TPU 92A
0,91	Square	TPU 92A
0,88	Triangle	TPU 92A
0,45	Small triangle	TPU 92A
0,71	Circle	TPE 95A
0,86	Circle	TPU resin
0,75	Square	PLA
0,74	Triangle	PP
0,58	Triangle	Rigid resin
0,68	Circle	PETG

The most consistent result has the triangle measuring balloon made from TPU 92A, because the correlation coefficient in every experiment was 0,88 or 0,89 unlike the circle measuring balloon made from TPU resin. This measuring balloon has significant differences between individual experiments, the correlation coefficients were from 0,86 to 1,0.

In Figure 33, Figure 36, Figure 38 is evident that the measurement of all measuring balloons from TPU 92A except the small triangle, and circle measuring balloon made from TPU resin is constant and the difference of the maxima is minimal.

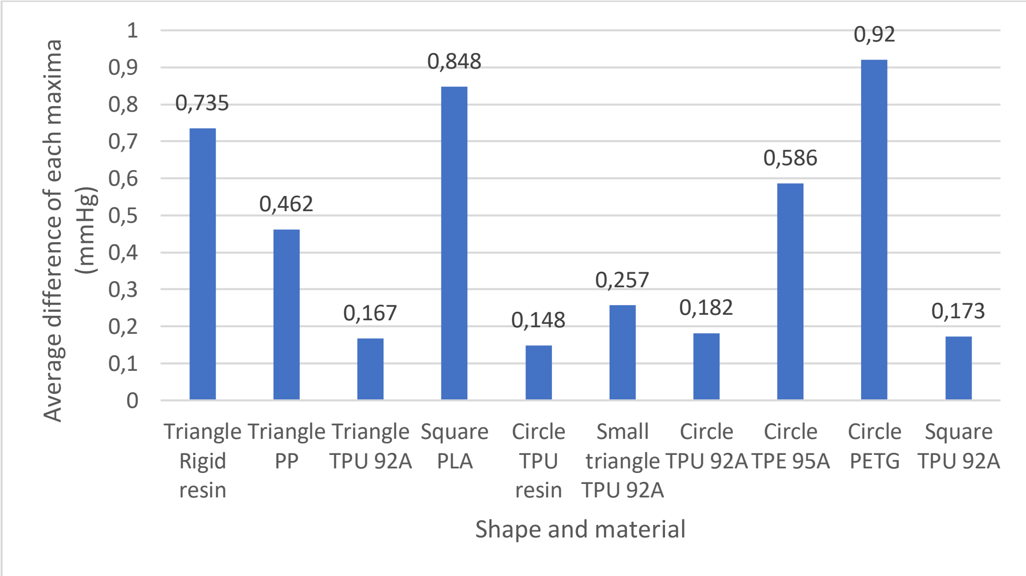

Figure 38: Average difference of each maxima with respiratory frequency 40 breaths per minute

Overall best average results have the circle measuring balloon made from TPU resin and all measuring balloons from TPU 92A except the small triangle, this measuring balloon has the worst results (Figure 39). I suppose it is because of the small volume of the measuring balloon, where the pressure inside of the artificial lung spread out around the measuring balloon.

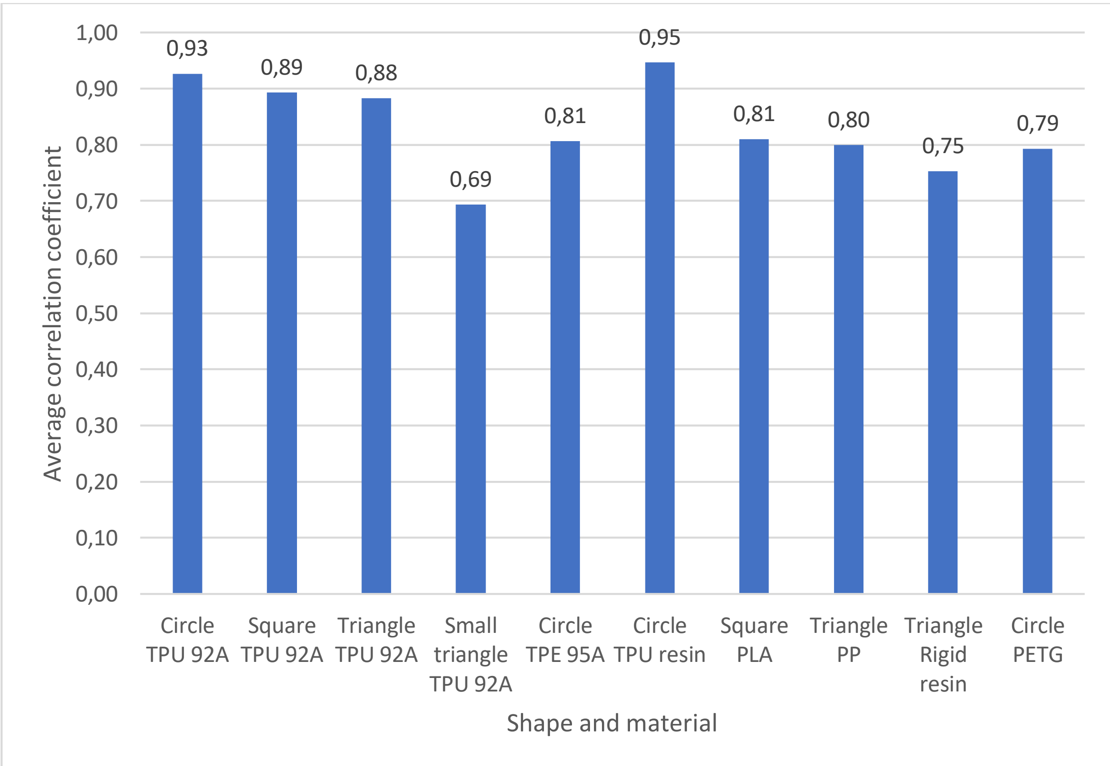

Figure 39: Averaged correlation coefficients of the measuring balloons

The rest of recorded curves are in Appendice E: Test with artificial lung.

5. Conclusion

At the beginning, there was an idea how to measure intrapleural pressure. Widespread method for estimating the pressure is measuring through the esophagus. However, it is only estimating, not measuring.

Difficulty was choosing method, how will be measured the pressure. The best idea was to produce a measuring balloon that will be inserted into the pleura cavity, which will be connected to a widespread pressure sensor.

The biggest difficulty was to choose the right shape and material. The main difficulty was how will be the measuring balloons made. The answer was 3D printing. However, to print large and hollow shapes is very complicated. Another question was which material can be used. Material for this measuring balloon must be flexible and biocompatible or not harmless to health. Chosen was 7 types of material TPU 92A, TPE 95A, PP, TPU resin, and out of curiosity 3 rigid materials; PLA, PETG, and resin. I designed 4 measuring balloons with different shapes, which are described in the Table 1.

Four tests were chosen to evaluate the quality of measuring balloon measurability.

First step was to verify if the measuring balloons are able to measure respiration frequency. The chosen method for verifying the frequency response was calculated using first-order transfer function. This equation was used for the leading edge of a delta function. The delta function was performed by lowering a roll-shaped weight of 500 g from a height of 50 cm onto a sensory measuring balloon. Every test contained 10 created delta functions, which were subsequently averaged. Output of this experiment is the maximum frequency which can the measuring balloon measure. This test shows that all used measuring balloons are able to measure the respiration frequency. Physiology respiration frequency is 0,15 Hz to 0,35 Hz. The lowest frequency response has a circle measuring balloon made from PETG where the average frequency was 2,2 Hz, but the frequency is still enough. Best results had material TPU 92A where the frequency response moves between 39,8 and 60,6 Hz.

To compare the measurement sensitivity of the measuring balloons, there were dived to different depths. Measuring balloon was dived into 7 depths (0 to 105 cm). In every depth, the measuring balloons lasted for 20 seconds. In the intervals were removed outliers and the interval was averaged and recorded in a table in mV. Method for decision making was static characterization but the primary comparison of the calculated Pearson correlation coefficient, P-value, and 95% confidence interval. If Pearson correlation coefficient is higher than 0,80, it means the results are linear. In every case, the coefficient was higher than 0,80, which means the measuring balloons are able to measure pressure changes very accurately. Best results have measuring balloons from TPU 92A and circle measuring balloon made from TPU resin. More measuring balloons had a correlation coefficient near to 1, but the sensitivity range was wider than others. For the following tests were chosen all measuring balloons from TPU 92A, triangle from PP, and circle measuring balloon made from TPU resin. From other materials was chosen the measuring balloon with the best range and linear curve; from rigid resin it was a triangle measuring balloon, from PETG and TPE 95A it was a circle measuring balloon, and from PLA it was a square measuring balloon.

For practical testing of the chosen measuring balloons was used an artificial lung connected to a hospital ventilator Monnal T50. Respiration frequency was set to 10, 20, and 40 breaths per minute, and other settings have not changed. Measured was the reaction of the measuring balloons and the respiration curve by inserting flow sensor into the respiration circle. Recorded curves were compared by the correlation coefficient which was calculated in excel using the function “CORREL”. With rising frequency, the precision of the measurement decreases. In the first experiment with the lowest respiration frequency were not any measuring balloons that had a coefficient under 0,80. The best measuring balloons with this frequency are circle measuring balloon made from TPU resin, circle and square measuring balloons made from TPU 92A. In the second experiment, with respiration frequency 20 breaths per minute, in this test, there were few measuring balloons which correlation moves around 0,80. It was a square measuring balloon made from PLA and TPU 92A, triangle measuring balloon made from PP and rigid resin and circle measuring balloon made from PETG. The best results have, as in the previous experiment, a circle measuring balloon made from TPU resin and TPU 92A. In the last experiment, six out of ten measuring balloons have a correlation coefficient much below the limit 0,80. Positive results have only the circle measuring balloon made from TPU resin and all measuring balloons from TPU 92A except the small triangle. The best measurement was recorded by a square measuring balloon made from TPU 92A. The most consistent result has the triangle measuring balloon made from TPU 92A, because the correlation coefficient in every experiment was 0,88 or 0,89.

As a last experiment was to confirm the right functionality of self-made physical model, but also to test and characterize the measuring balloon response of the respiration made by the model. Physical model consists of two parts where between them was inserted the measuring balloon. Measured was the reaction of the measuring balloons and the respiration curve by inserted a flow sensor into the respiration circle. Recorded curves were compared by correlation coefficient. Recorded curves show the measuring balloons are able to measure the pressure, but the pumped pressure spreads all over the surface and does not transform the force directly to the measuring balloon. Best results have a circle measuring balloon made from TPU resin, and a square measuring balloon made from TPU 92A. For unknown reasons, in some cases the isoline with time raises. Almost in every measurement, when the pressure begins to rise, the recorded curve by the measuring balloon is delayed. Overall, the recorded curves are in my opinion sufficient, but the calculated correlation coefficient shows the opposite. The fault is not on the side of the measuring balloon but on the side of the physical model. For the future development of the physical model will be recommended usage same model, but using more flexible and extensible material than Teflon which will better act like flexibility of the lung.

Based on performed experiments the best measuring balloon suitable for further tests is a triangle measuring balloon made from TPU 92A. This measuring has the most consistent results (60,6 Hz frequency response, 0,88 correlation coefficient for artificial lung). It is also easy to product it at the 3D printers. As a second choice, is recommend a circle shape from TPU 92A or TPU resin. It is preferable to use TPU92A, because TPU resin production is more complicated and also more expensive.

For the future development of the physical model will be recommended usage the same model, but using more flexible and extensible material than Teflon which will better act like flexibility of the lung. I will recommend this physical model to universities and schools because the production is very cheap and simple.

In my opinion, this method of measuring intrapleural pressure is groundbreaking, because nowadays there is not any method which measures intrapleural pressure, only estimating.

6. References

[1] Upper Respiratory Tract: What is the Upper Respiratory Tract. In: The Respiratory system: Upper Respiratory Tract [online]. The Respiratory system, 2017 [cit. 2020−10−29]. Available from: https://www.therespiratorysystem.com/category/upper−respiratory−tract/

[2] Lower Respiratory Tract: What is the Lower Respiratory Tract. In: The Respiratory system: Lower Respiratory Tract [online]. The Respiratory system, 2017 [cit. 2020−10−29]. Available from: https://www.therespiratorysystem.com/category/lower−respiratory−tract/

[3] Romer, Alfred Sherwood; Parsons, Thomas S. The Vertebrate Body. Philadelphia, PA: Holt−Saunders International, 1977. ISBN 0−03−910284−X. S. 170–173.

[4] ČIHÁK, Radomír. Anatomie 1. 2. vyd. Praha: Grada Publishing, 2001. ISBN 978−80−7169−970−5.

[5] VIGUÉ, Jordi a Emilio MARTÍN ORTE. Atlas lidského těla. Dobřejovice: Rebo, 2005. ISBN 80−7234−408−0.

[6] Cross, M., & Plunkett, E. (2014). Lung volumes. In Physics, Pharmacology and Physiology for Anaesthetists: Key Concepts for the FRCA (pp. 203-204). Cambridge: Cambridge University Press. doi:10.1017/CBO9781107326200.083

[7] MAIOLO, C., E. I. MOHAMED a M. G. CARBONELLI. Body composition and respiratory function. Acta Diabetologica [online]. 2003, 40, s32-s38 [cit. 2020-11-10]. ISSN 0940-5429. Available from: doi:10.1007/s00592-003-0023-0

[8] Mechanics of Ventilation. National Cancer Institute - SEER Training Modules [online]. Rockville Pike: USA.gov, 2016 [cit. 2020-11-10]. Available from: https://training.seer.cancer.gov/anatomy/respiratory/mechanics.html

[9] LENFANT, Claude. Pleural Disease. 2nd ed. New York: Taylor & Francis, 2004. ISBN 9781420077384.

[10] Charalampidis C, Youroukou A, Lazaridis G, Baka S, Mpoukovinas I, Karavasilis V, Kioumis I, Pitsiou G, Papaiwannou A, Karavergou A, Tsakiridis K, Katsikogiannis N, Sarika E, Kapanidis K, Sakkas L, Korantzis I, Lampaki S, Zarogoulidis K, Zarogoulidis P. Physiology of the pleural space. J Thorac Dis 2015;7(S1):S33-S37. doi: 10.3978/j.issn.2072-1439.2014.12.48

[11] ABOUD, Fionnuala Cormack a Abraham C. VERGHESE. Evarts Ambrose Graham, Empyema, and the Dawn of Clinical Understanding of Negative Intrapleural Pressure. *Clinical Infectious Diseases* [online]. 2002, **34**(2), 198−203 [cit. 2020−03−18]. DOI: 10.1086/338148. ISSN 1058−4838. Available from: https://academic.oup.com/cid/article−lookup/doi/10.1086/338148

[12] ALBANESE, Antonio, Nikolaos KARAMOLEGKOS, Syed W. HAIDER, Adam SEIVER a Nicolas W. CHBAT. Real−time noninvasive estimation of intrapleural pressure in mechanically ventilated patients: A feasibility study. In: 2013 35th Annual International Conference of the IEEE Engineering in Medicine and Biology Society (EMBC) [online]. IEEE, 2013, 2013, s. 5211−5215 [cit. 2020−03−24]. DOI: 10.1109/EMBC.2013.6610723. ISBN 978−1−4577−0216−7. Available from:http://ieeexplore.ieee.org/document/6610723/

[13] MILIC−EMILI, J., J. MEAD, J. M. TURNER a E. M. GLAUSER. Improved technique for estimating pleural pressure from esophageal measuring balloons. Journal of Applied Physiology [online]. 1964, 19(2), 207−211 [cit. 2020−03−30]. DOI: 10.1152/jappl.1964.19.2.207. ISSN 8750−7587. Available from:https://www.physiology.org/doi/10.1152/jappl.1964.19.2.207

[14] KANEDA, Hiroyuki, Takahito NAKANO a Tomohiro MURAKAWA. Measurement of intrapleural pressure in patients with spontaneous pneumothorax: a pilot study. BMC Pulmonary Medicine [online]. 2019, 19(1) [cit. 2020−03−31]. DOI: D10.1186/s12890−019−1038−9. ISSN 1471−2466. Available from: https://bmcpulmmed.biomedcentral.com/articles/10.1186/s12890−019−1038−9

[15]ADInstruments [online]. Sydney, Australia: ADInstruments, 1988 [cit. 2020−06−15]. Available from: https://www.adinstruments.com/products/bp−transducercable−kit#data−cards
[16]Mereni tvrdosti. Mereni tvrdosti [online]. Ostrava: Mereni tvrdosti, 2005 [cit. 2020−06−15]. Available from: http://www.merenitvrdosti.cz/piblina−pevodni−tabulka−pro−durometry−shore.html
[17]BRODSKY, Dara a Mary QUINN. *A Parent's Guide to the Late Preterm Infant*. Lulu, 2017. ISBN 9781312343924.

List of appendice

List of tables in appendice

List of figures in appendice

Appendice A: Dimensions of the measuring balloons

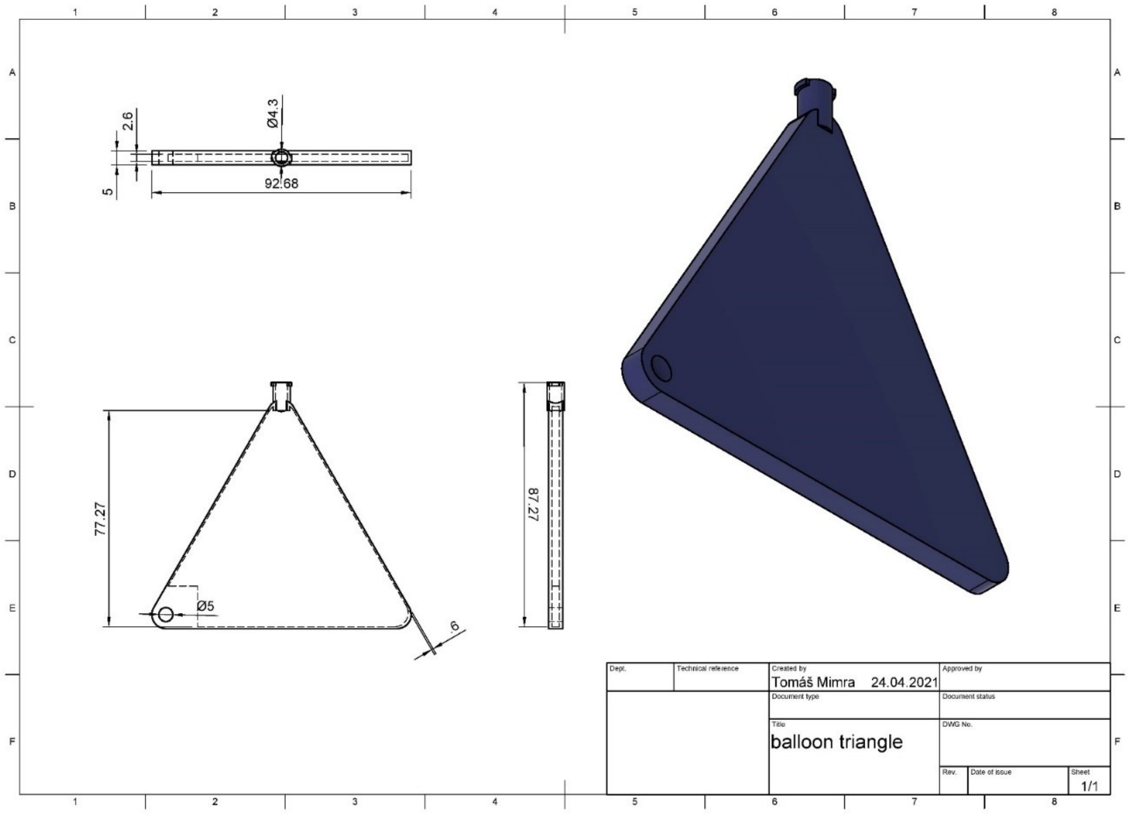

Figure 40: Technical drawing of a triangle measuring balloon

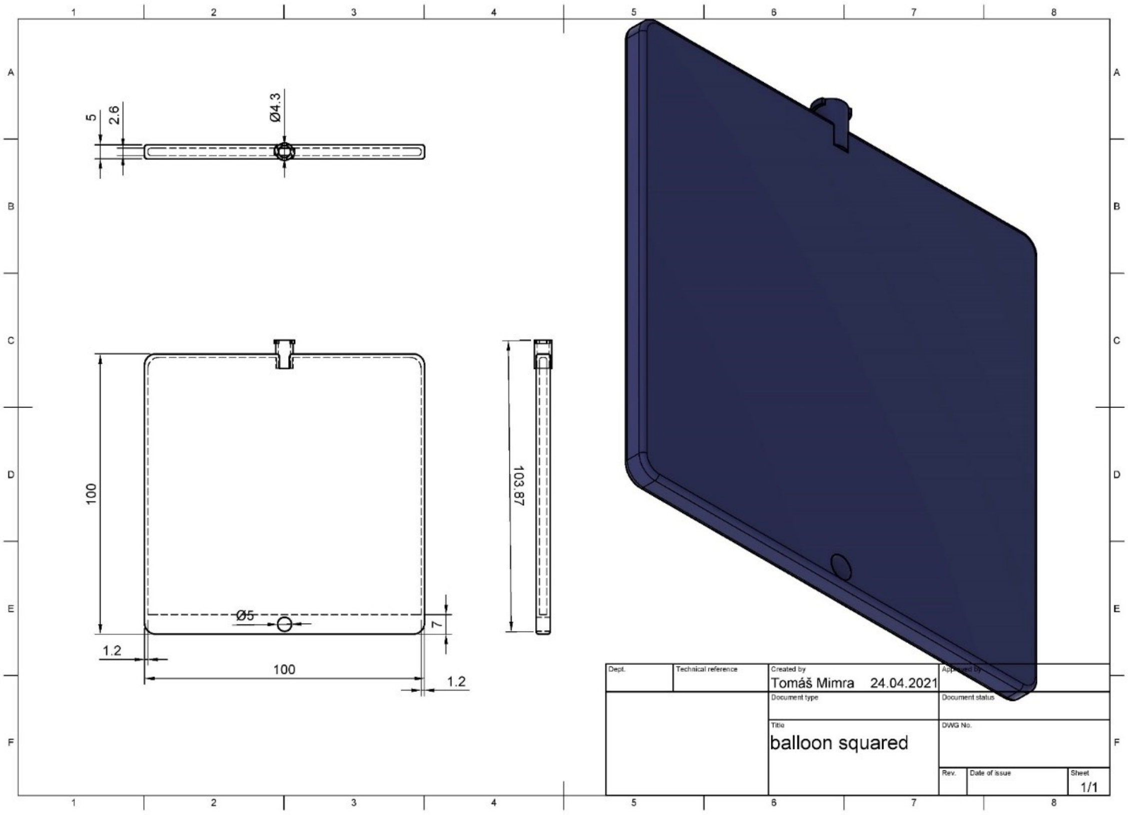

Figure 41: Technical drawing of a square measuring balloon

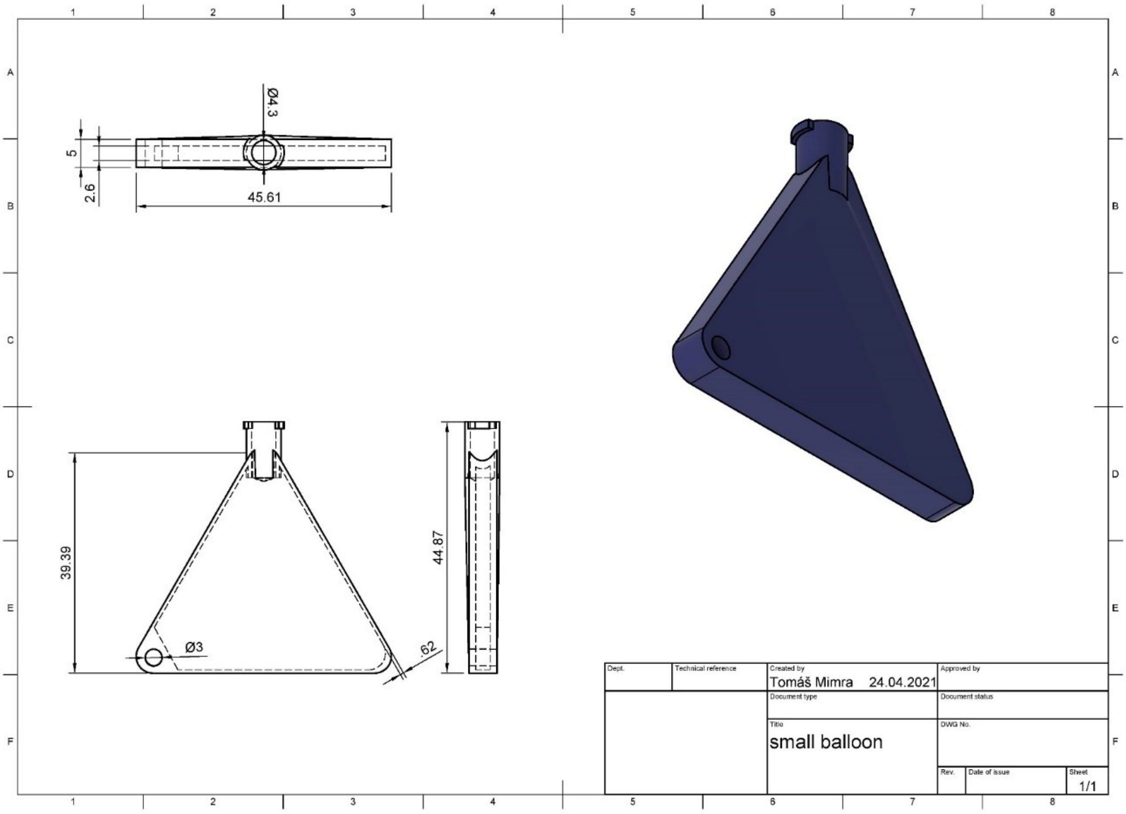

Figure 42: Technical drawing of a small triangle measuring balloon

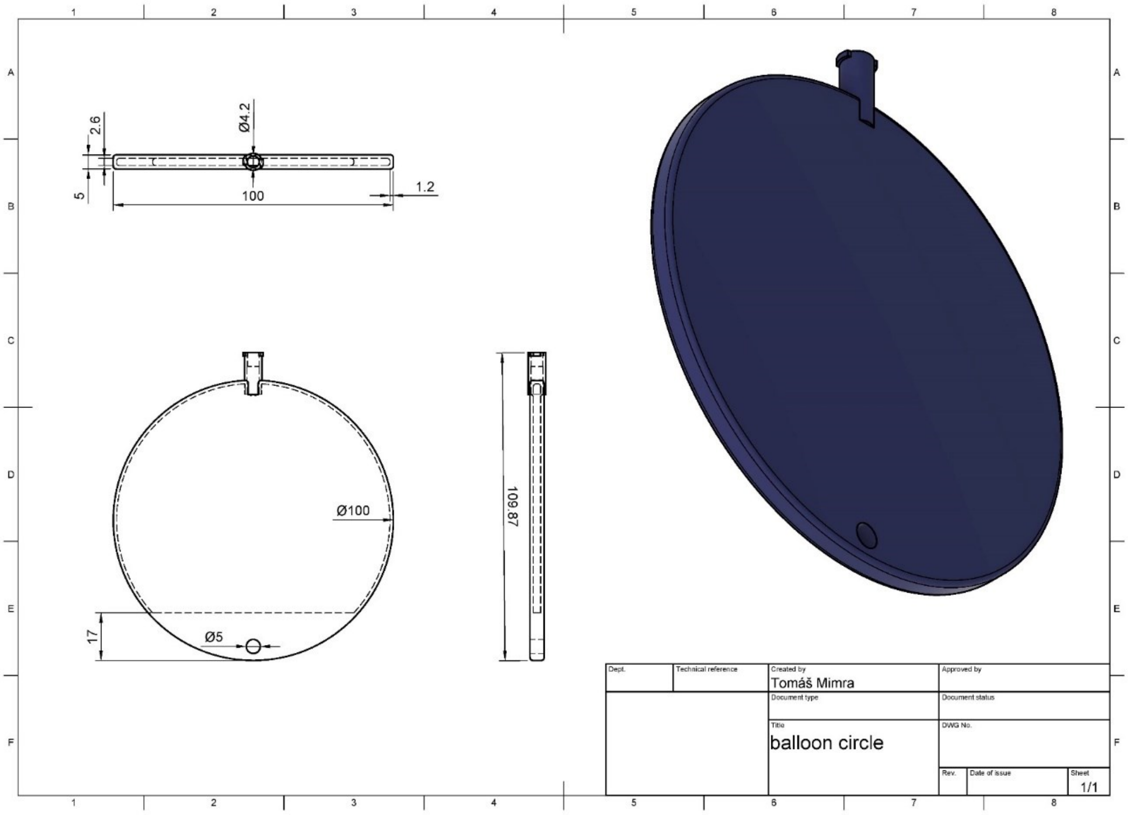

Figure 43: Technical drawing of a circle measuring balloon

Appendice B: Frequency response

Table 10: Frequency response of measuring balloons from TPU 92A, TPU resin, PETG

Small triangle measuring balloon		Square measuring balloon		Triangle measuring balloon		Circle measuring balloon	
	Frequency (Hz)		**Frequency (Hz)**		**Frequency (Hz)**		**Frequency (Hz)**
TPU 92A							
1.	50,5	**1.**	31,6	**1.**	63,2	**1.**	36,1
2.	50,5	**2.**	23,0	**2.**	50,5	**2.**	42,1
3.	31,6	**3.**	42,1	**3.**	50,5	**3.**	42,1
4.	50,5	**4.**	42,1	**4.**	63,2	**4.**	42,1
5.	50,5	**5.**	36,1	**5.**	63,2	**5.**	50,5
6.	31,6	**6.**	63,2	**6.**	63,2	**6.**	42,1
7.	36,1	**7.**	31,6	**7.**	63,2	**7.**	50,5
8.	36,1	**8.**	50,5	**8.**	63,2	**8.**	50,5
9.	42,1	**9.**	36,1	**9.**	63,2	**9.**	42,1
10.	42,1	**10.**	42,1	**10.**	63,2	**10.**	42,1
AVG	**42,2**	AVG	**39,8**	AVG	**60,6**	AVG	**44,0**
TPU resin							
1.	25,3	**1.**	63,2	**1.**	31,6	**1.**	42,1
2.	42,1	**2.**	50,5	**2.**	23,0	**2.**	50,5
3.	31,6	**3.**	63,2	**3.**	42,1	**3.**	50,5
4.	25,3	**4.**	42,1	**4.**	42,1	**4.**	42,1
5.	31,6	**5.**	42,1	**5.**	31,6	**5.**	42,1
6.	36,1	**6.**	42,1	**6.**	31,6	**6.**	63,2
7.	36,1	**7.**	31,6	**7.**	31,6	**7.**	50,5
8.	31,6	**8.**	31,6	**8.**	50,5	**8.**	63,2
9.	28,1	**9.**	63,2	**9.**	36,1	**9.**	42,1
10.	25,3	**10.**	42,1	**10.**	42,1	**10.**	25,3
AVG	**31,3**	AVG	**47,2**	AVG	**36,2**	AVG	**47,2**
PETG							
1.	2,0	**1.**	2,7	**1.**	2,9	**1.**	2,5
2.	0,2	**2.**	2,8	**2.**	1,8	**2.**	1,9
3.	2,3	**3.**	2,9	**3.**	2,3	**3.**	2,4
4.	2,6	**4.**	2,9	**4.**	2,4	**4.**	1,7
5.	2,3	**5.**	2,6	**5.**	2,2	**5.**	1,9
6.	2,8	**6.**	3,0	**6.**	2,0	**6.**	1,9
7.	2,4	**7.**	2,4	**7.**	2,6	**7.**	2,2
8.	2,4	**8.**	2,7	**8.**	2,2	**8.**	2,4
9.	2,6	**9.**	2,8	**9.**	2,4	**9.**	2,3
10.	3,1	**10.**	3,0	**10.**	2,3	**10.**	2,1
AVG	**2,3**	AVG	**2,8**	AVG	**2,3**	AVG	**2,1**

Table 11: Frequency response of measuring balloons from PLA, TPE 95A, rigid resin

Small triangle measuring balloon		Square measuring balloon		Triangle measuring balloon		Circle measuring balloon	
Frequency (Hz)		Frequency (Hz)		Frequency (Hz)		Frequency (Hz)	
PLA							
1.	2,7	**1.**	2,3	**1.**	3,2	**1.**	2,7
2.	3,2	**2.**	3,2	**2.**	2,5	**2.**	3,9
3.	4,2	**3.**	2,3	**3.**	2,7	**3.**	2,5
4.	2,7	**4.**	0,3	**4.**	3,2	**4.**	2,7
5.	2,7	**5.**	2,4	**5.**	2,5	**5.**	2,7
6.	2,5	**6.**	3,2	**6.**	3,0	**6.**	2,5
7.	3,2	**7.**	2,7	**7.**	3,6	**7.**	2,4
8.	4,2	**8.**	2,7	**8.**	3,6	**8.**	2,1
9.	2,4	**9.**	2,4	**9.**	3,4	**9.**	2,4
10.	3,2	**10.**	3,0	**10.**	3,9	**10.**	1,9
AVG	**3,1**	**AVG**	**2,4**	**AVG**	**3,1**	**AVG**	**2,6**
TPE 95A							
1.	28,1	**1.**	25,3	**1.**	21,1	**1.**	31,6
2.	36,1	**2.**	25,3	**2.**	28,1	**2.**	21,1
3.	23,0	**3.**	28,1	**3.**	28,1	**3.**	19,4
4.	23,0	**4.**	19,4	**4.**	31,6	**4.**	25,3
5.	21,1	**5.**	25,3	**5.**	28,1	**5.**	31,6
6.	16,8	**6.**	36,1	**6.**	25,3	**6.**	42,1
7.	23,0	**7.**	36,1	**7.**	31,6	**7.**	21,1
8.	19,4	**8.**	36,1	**8.**	25,3	**8.**	36,1
9.	19,4	**9.**	25,3	**9.**	28,1	**9.**	28,1
10.	31,6	**10.**	31,6	**10.**	19,4	**10.**	23,0
AVG	**24,1**	**AVG**	**28,8**	**AVG**	**26,6**	**AVG**	**27,9**
Rigid resin							
1.	3,2	**1.**	3,2	**1.**	5,6	**1.**	3,9
2.	3,2	**2.**	4,2	**2.**	5,6	**2.**	4,2
3.	3,9	**3.**	3,9	**3.**	3,9	**3.**	4,6
4.	3,6	**4.**	5,6	**4.**	3,9	**4.**	6,3
5.	3,2	**5.**	5,6	**5.**	4,2	**5.**	5,6
6.	4,2	**6.**	3,9	**6.**	5,1	**6.**	3,9
7.	3,9	**7.**	3,9	**7.**	3,0	**7.**	3,9
8.	5,6	**8.**	4,2	**8.**	3,9	**8.**	4,2
9.	3,0	**9.**	3,9	**9.**	3,9	**9.**	5,1
10.	3,4	**10.**	3,4	**10.**	4,2	**10.**	3,0
AVG	**3,7**	**AVG**	**4,2**	**AVG**	**4,3**	**AVG**	**4,5**

Table 12: Frequency response of measuring balloons from PP

Small triangle measuring balloon		Square measuring balloon		Triangle measuring balloon		Circle measuring balloon	
Frequency (Hz)		Frequency (Hz)		Frequency (Hz)		Frequency (Hz)	
PP							
1.	2,5	**1.**	3,9	**1.**	4,6	**1.**	4,6
2.	4,2	**2.**	6,3	**2.**	3,4	**2.**	4,6
3.	3,2	**3.**	5,6	**3.**	6,3	**3.**	3,2
4.	1,7	**4.**	5,6	**4.**	7,2	**4.**	3,2
5.	3,0	**5.**	4,6	**5.**	4,2	**5.**	3,4
6.	3,4	**6.**	3,2	**6.**	5,1	**6.**	3,4
7.	3,6	**7.**	5,1	**7.**	6,3	**7.**	3,4
8.	3,2	**8.**	4,6	**8.**	6,3	**8.**	3,4
9.	2,8	**9.**	5,1	**9.**	8,4	**9.**	3,6
10.	2,7	**10.**	5,6	**10.**	10,1	**10.**	3,0
AVG	**3,0**	**AVG**	**4,9**	**AVG**	**6,2**	**AVG**	**3,6**

Appendice C: Measuring balloon diving

Table 13: Values of static characterization of all measuring balloon shapes and materials

Pressure (mV)	Height (cm)	Pressure with offset (mV)	Water pressure (mmHg)	Shape	Material
49,74	0	0	0	small triangle	PLA
49,74	15	0	10	small triangle	PLA
49,77	30	0,03	20	small triangle	PLA
49,83	45	0,09	30	small triangle	PLA
49,90	60	0,16	40	small triangle	PLA
49,96	75	0,22	50	small triangle	PLA
50,12	105	0,38	70	small triangle	PLA
49,70	0	0	0	triangle	PLA
49,75	15	0,05	10	triangle	PLA
49,90	30	0,2	20	triangle	PLA
50,01	45	0,31	30	triangle	PLA
50,20	60	0,5	40	triangle	PLA
50,39	75	0,69	50	triangle	PLA
50,66	105	0,96	70	triangle	PLA
49,66	0	0	0	square	PLA
49,84	15	0,18	10	square	PLA
50,03	30	0,37	20	square	PLA
50,25	45	0,59	30	square	PLA
50,48	60	0,82	40	square	PLA
50,63	75	0,97	50	square	PLA
50,84	105	1,18	70	square	PLA
49,63	0	0	0	circle	PLA
49,68	15	0,05	10	circle	PLA
49,84	30	0,21	20	circle	PLA
49,98	45	0,35	30	circle	PLA
50,16	60	0,53	40	circle	PLA
50,34	75	0,71	50	circle	PLA
50,71	105	1,08	70	circle	PLA
49,56	0	0	0	small triangle	TPU resin
49,67	15	0,11	10	small triangle	TPU resin
49,79	30	0,23	20	small triangle	TPU resin
49,96	45	0,4	30	small triangle	TPU resin
50,14	60	0,58	40	small triangle	TPU resin
50,32	75	0,76	50	small triangle	TPU resin
50,70	105	1,14	70	small triangle	TPU resin
50,76	0	0	0	triangle	TPU resin
50,97	15	0,21	10	triangle	TPU resin
51,17	30	0,41	20	triangle	TPU resin

Pressure (mV)	Height (cm)	Pressure with offset (mV)	Water pressure (mmHg)	Shape	Material
51,36	45	0,6	30	triangle	TPU resin
51,56	60	0,8	40	triangle	TPU resin
51,73	75	0,97	50	triangle	TPU resin
52,15	105	1,39	70	triangle	TPU resin
49,87	0	0	0	square	TPU resin
50,10	15	0,23	10	square	TPU resin
50,36	30	0,49	20	square	TPU resin
50,61	45	0,74	30	square	TPU resin
50,82	60	0,95	40	square	TPU resin
51,09	75	1,22	50	square	TPU resin
51,40	105	1,53	70	square	TPU resin
49,93	0	0	0	circle	TPU resin
50,12	15	0,19	10	circle	TPU resin
50,39	30	0,46	20	circle	TPU resin
50,68	45	0,75	30	circle	TPU resin
50,91	60	0,98	40	circle	TPU resin
51,12	75	1,19	50	circle	TPU resin
51,45	105	1,52	70	circle	TPU resin
50,41	0	0	0	small triangle	PETG
50,52	15	0,11	10	small triangle	PETG
50,57	30	0,16	20	small triangle	PETG
50,66	45	0,25	30	small triangle	PETG
50,80	60	0,39	40	small triangle	PETG
50,96	75	0,55	50	small triangle	PETG
51,16	105	0,75	70	small triangle	PETG
50,42	0	0	0	triangle	PETG
50,48	15	0,06	10	triangle	PETG
50,60	30	0,18	20	triangle	PETG
50,75	45	0,33	30	triangle	PETG
50,87	60	0,45	40	triangle	PETG
51,18	75	0,76	50	triangle	PETG
51,69	105	1,27	70	triangle	PETG
50,51	0	0	0	square	PETG
50,60	15	0,09	10	square	PETG
50,65	30	0,14	20	square	PETG
50,95	45	0,44	30	square	PETG
51,18	60	0,67	40	square	PETG
51,40	75	0,89	50	square	PETG
51,80	105	1,29	70	square	PETG
50,35	0	0	0	circle	PETG
50,48	15	0,13	10	circle	PETG
50,71	30	0,36	20	circle	PETG

Pressure (mV)	Height (cm)	Pressure with offset (mV)	Water pressure (mmHg)	Shape	Material
50,89	45	0,54	30	circle	PETG
51,17	60	0,82	40	circle	PETG
51,42	75	1,07	50	circle	PETG
51,66	105	1,31	70	circle	PETG
49,51	0	0	0	small triangle	PP
49,67	15	0,16	10	small triangle	PP
49,76	30	0,25	20	small triangle	PP
49,90	45	0,39	30	small triangle	PP
50,16	60	0,65	40	small triangle	PP
50,36	75	0,85	50	small triangle	PP
50,61	105	1,1	70	small triangle	PP
50,22	0	0	0	triangle	PP
50,45	15	0,23	10	triangle	PP
50,69	30	0,47	20	triangle	PP
50,90	45	0,68	30	triangle	PP
51,09	60	0,87	40	triangle	PP
51,32	75	1,1	50	triangle	PP
51,80	105	1,58	70	triangle	PP
50,14	0	0	0	square	PP
50,38	15	0,24	10	square	PP
50,63	30	0,49	20	square	PP
51,04	45	0,9	30	square	PP
51,18	60	1,04	40	square	PP
51,34	75	1,2	50	square	PP
51,51	105	1,37	70	square	PP
50,06	0	0	0	circle	PP
50,16	15	0,1	10	circle	PP
50,38	30	0,32	20	circle	PP
50,62	45	0,56	30	circle	PP
50,83	60	0,77	40	circle	PP
51,06	75	1	50	circle	PP
51,50	105	1,44	70	circle	PP
50,14	0	0	0	small triangle	rigid resin
50,13	15	-0,01	10	small triangle	rigid resin
50,13	30	-0,01	20	small triangle	rigid resin
50,21	45	0,07	30	small triangle	rigid resin
50,23	60	0,09	40	small triangle	rigid resin
50,24	75	0,1	50	small triangle	rigid resin
50,26	105	0,12	70	small triangle	rigid resin
50,10	0	0	0	triangle	rigid resin
50,19	15	0,09	10	triangle	rigid resin
50,37	30	0,27	20	triangle	rigid resin

Pressure (mV)	Height (cm)	Pressure with offset (mV)	Water pressure (mmHg)	Shape	Material
50,63	45	0,53	30	triangle	rigid resin
50,92	60	0,82	40	triangle	rigid resin
51,17	75	1,07	50	triangle	rigid resin
51,51	105	1,41	70	triangle	rigid resin
49,93	0	0	0	square	rigid resin
50,01	15	0,08	10	square	rigid resin
50,13	30	0,2	20	square	rigid resin
50,23	45	0,3	30	square	rigid resin
50,40	60	0,47	40	square	rigid resin
50,44	75	0,51	50	square	rigid resin
50,57	105	0,64	70	square	rigid resin
49,85	0	0	0	circle	rigid resin
50,25	15	0,4	10	circle	rigid resin
50,52	30	0,67	20	circle	rigid resin
50,81	45	0,96	30	circle	rigid resin
51,00	60	1,15	40	circle	rigid resin
51,22	75	1,37	50	circle	rigid resin
51,42	105	1,57	70	circle	rigid resin
46,82	0	0,00	0	small triangle	TPE 95A
46,87	15	0,05	10	small triangle	TPE 95A
46,89	30	0,07	20	small triangle	TPE 95A
46,99	45	0,17	30	small triangle	TPE 95A
47,14	60	0,32	40	small triangle	TPE 95A
47,34	75	0,53	50	small triangle	TPE 95A
47,71	105	0,89	70	small triangle	TPE 95A
46,78	0	0,00	0	triangle	TPE 95A
46,89	15	0,11	10	triangle	TPE 95A
46,94	30	0,15	20	triangle	TPE 95A
47,14	45	0,35	30	triangle	TPE 95A
47,38	60	0,59	40	triangle	TPE 95A
47,57	75	0,78	50	triangle	TPE 95A
48,02	105	1,23	70	triangle	TPE 95A
47,33	0	0,00	0	square	TPE 95A
47,43	15	0,09	10	square	TPE 95A
47,51	30	0,18	20	square	TPE 95A
47,74	45	0,41	30	square	TPE 95A
47,96	60	0,63	40	square	TPE 95A
48,23	75	0,90	50	square	TPE 95A
48,70	105	1,37	70	square	TPE 95A
47,22	0	0,00	0	circle	TPE 95A
47,26	15	0,04	10	circle	TPE 95A
47,34	30	0,12	20	circle	TPE 95A

Pressure (mV)	Height (cm)	Pressure with offset (mV)	Water pressure (mmHg)	Shape	Material
47,49	45	0,26	30	circle	TPE 95A
47,69	60	0,47	40	circle	TPE 95A
47,93	75	0,71	50	circle	TPE 95A
48,42	105	1,20	70	circle	TPE 95A
7,77	0	0,00	0	small triangle	TPU 92A
7,97	15	0,20	10	small triangle	TPU 92A
8,15	30	0,38	20	small triangle	TPU 92A
8,32	45	0,55	30	small triangle	TPU 92A
8,45	60	0,68	40	small triangle	TPU 92A
8,65	75	0,88	50	small triangle	TPU 92A
9,04	105	1,27	70	small triangle	TPU 92A
8,93	0	0,00	0	triangle	TPU 92A
9,22	15	0,29	10	triangle	TPU 92A
9,46	30	0,53	20	triangle	TPU 92A
9,64	45	0,71	30	triangle	TPU 92A
9,85	60	0,92	40	triangle	TPU 92A
10,11	75	1,18	50	triangle	TPU 92A
10,61	105	1,68	70	triangle	TPU 92A
8,05	0	0,00	0	square	TPU 92A
8,31	15	0,26	10	square	TPU 92A
8,63	30	0,57	20	square	TPU 92A
8,85	45	0,80	30	square	TPU 92A
9,11	60	1,06	40	square	TPU 92A
9,44	75	1,39	50	square	TPU 92A
9,94	105	1,89	70	square	TPU 92A
9,29	0	0,00	0	circle	TPU 92A
9,60	15	0,31	10	circle	TPU 92A
9,95	30	0,66	20	circle	TPU 92A
10,28	45	0,99	30	circle	TPU 92A
10,56	60	1,27	40	circle	TPU 92A
10,80	75	1,51	50	circle	TPU 92A
11,21	105	1,92	70	circle	TPU 92A

Appendice D: Physical model

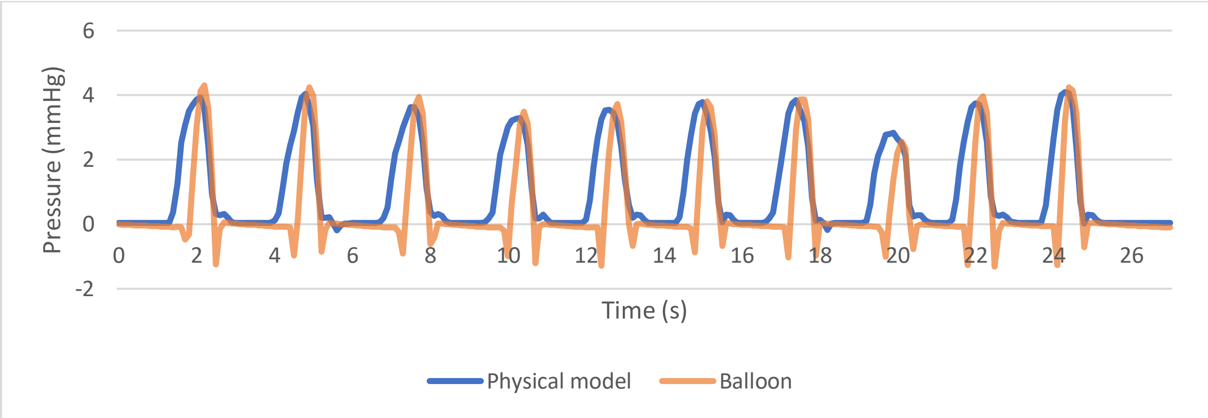

Figure 44: Physical model respiration curve of the triangle measuring balloon made from TPU 92A

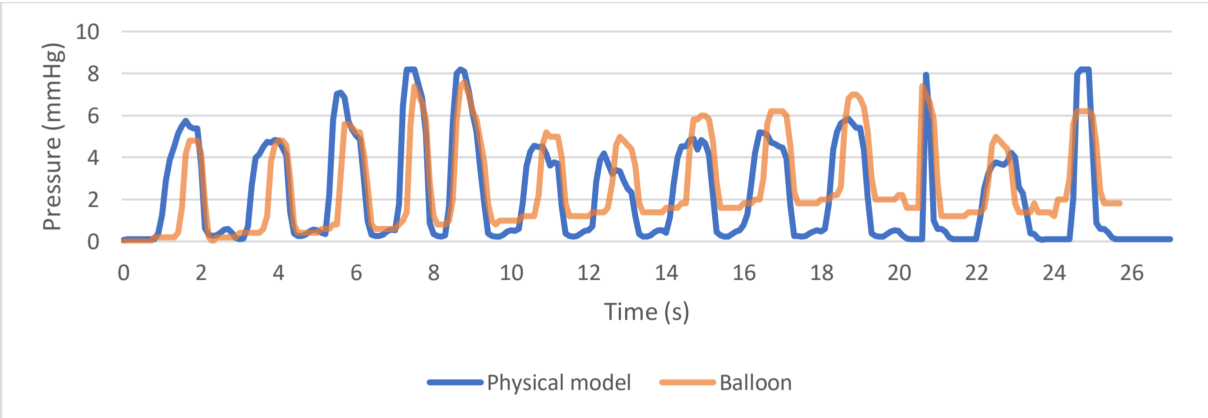

Figure 45: Physical model respiration curve of the square measuring balloon made from TPU 92A

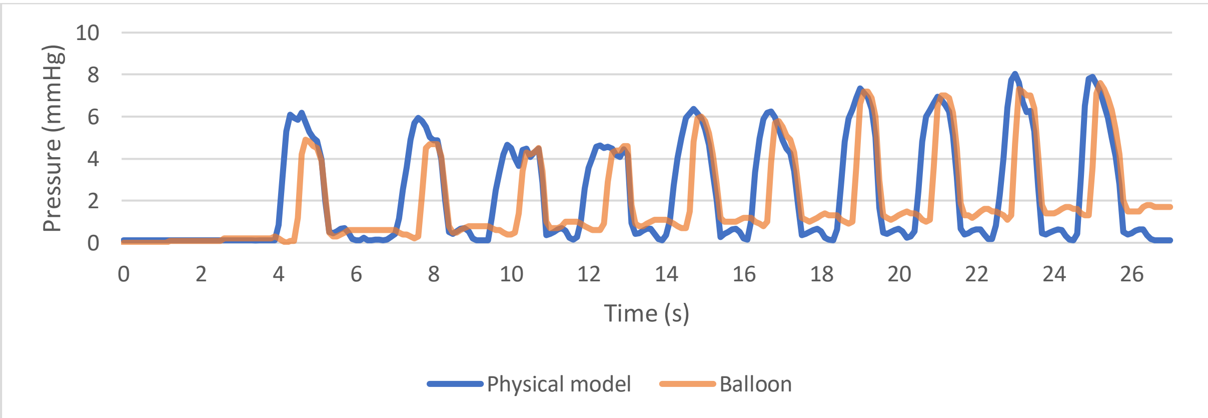

Figure 46: Physical model respiration curve of the circle measuring balloon made from TPU 92A

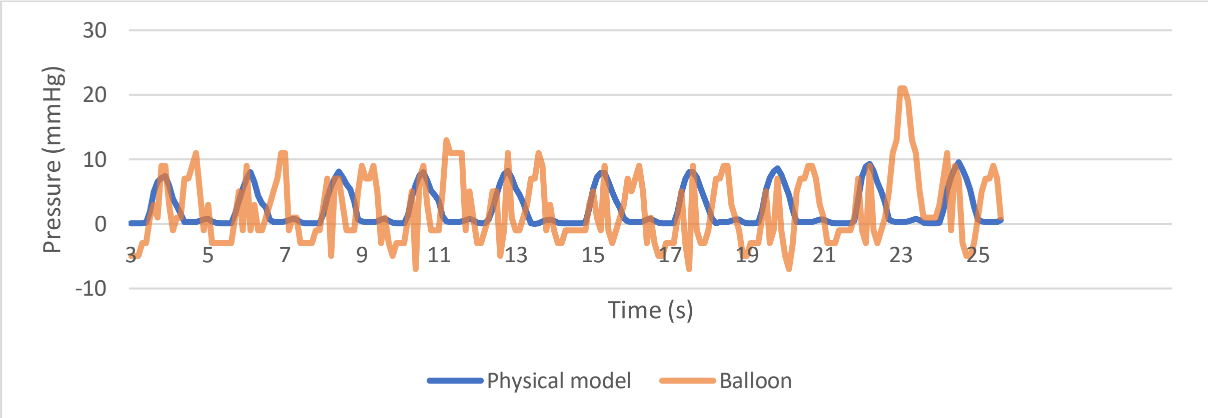

Figure 47: Physical model respiration curve of the small triangle measuring balloon made from TPU 92A

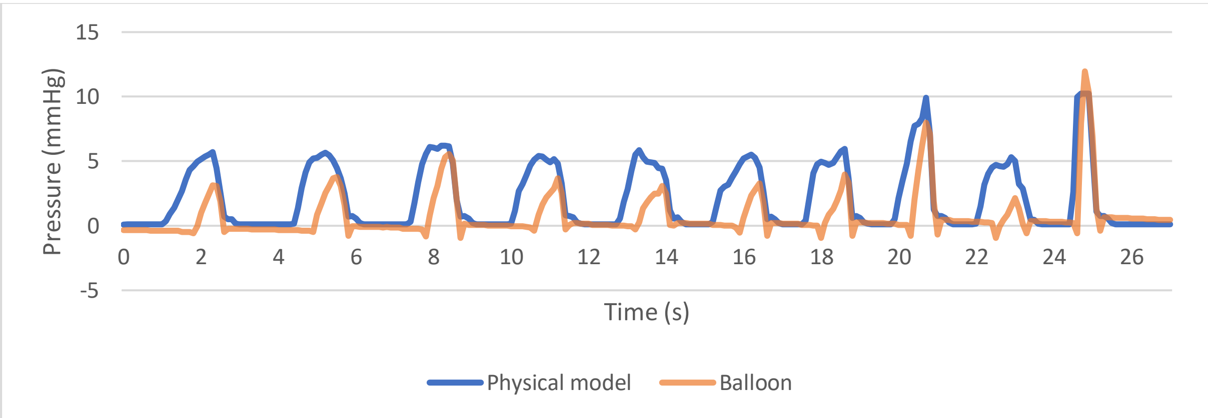

Figure 48: Physical model respiration curve of the circle measuring balloon made from PETG

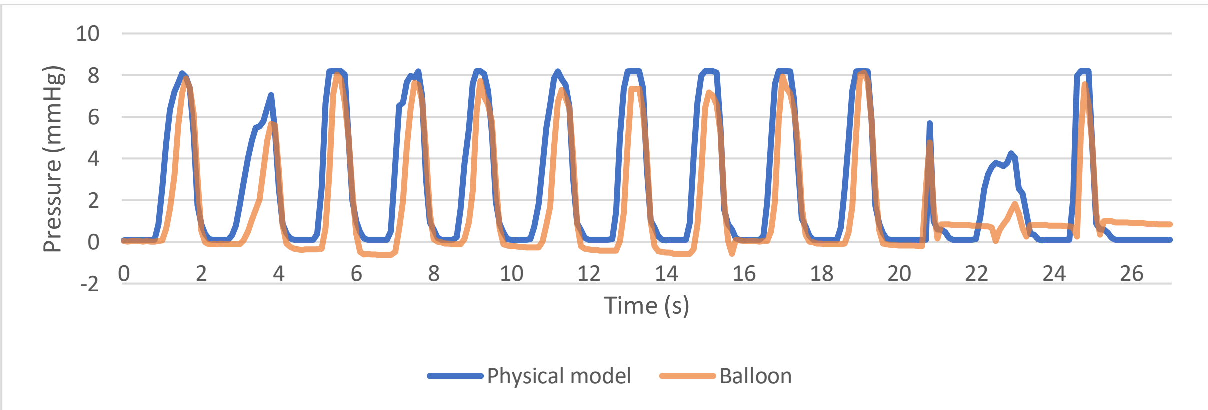

Figure 49: Physical model respiration curve of the circle measuring balloon made from TPU resin

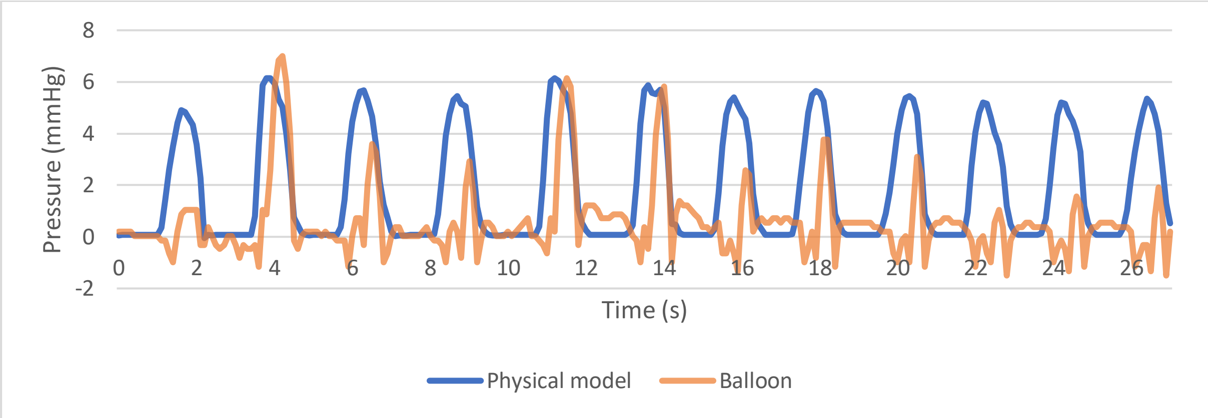

Figure 50: Physical model respiration curve of the circle measuring balloon made from TPE 95A

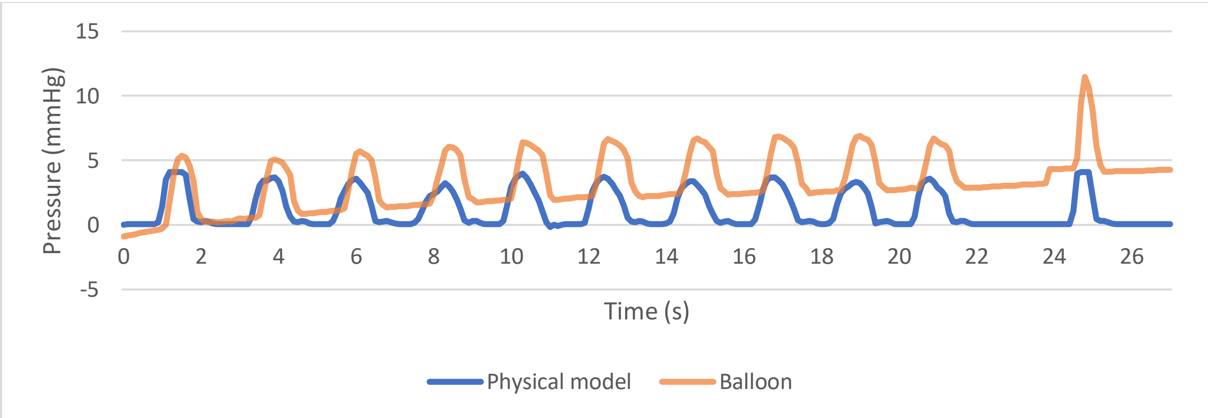

Figure 51: Physical model respiration curve of the triangle measuring balloon made from rigid resin

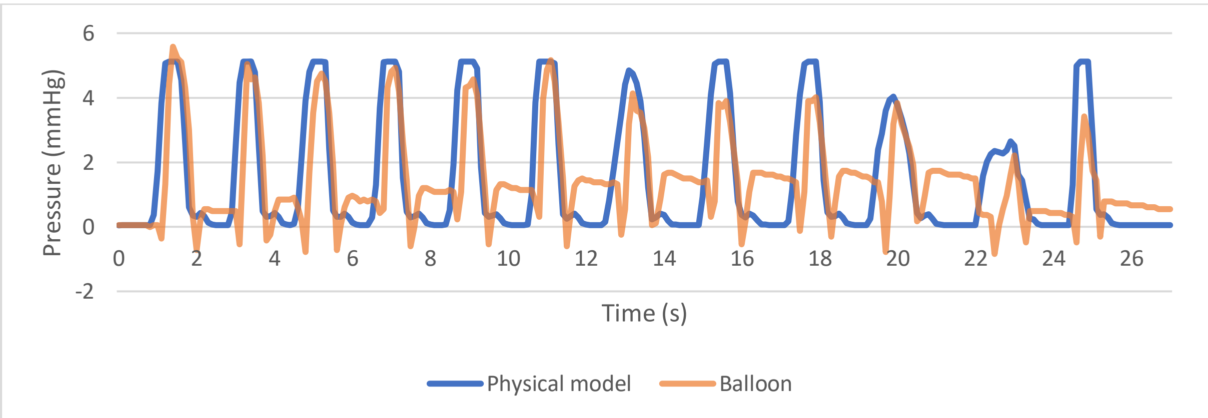

Figure 52: Physical model respiration curve of the triangle measuring balloon made from PP

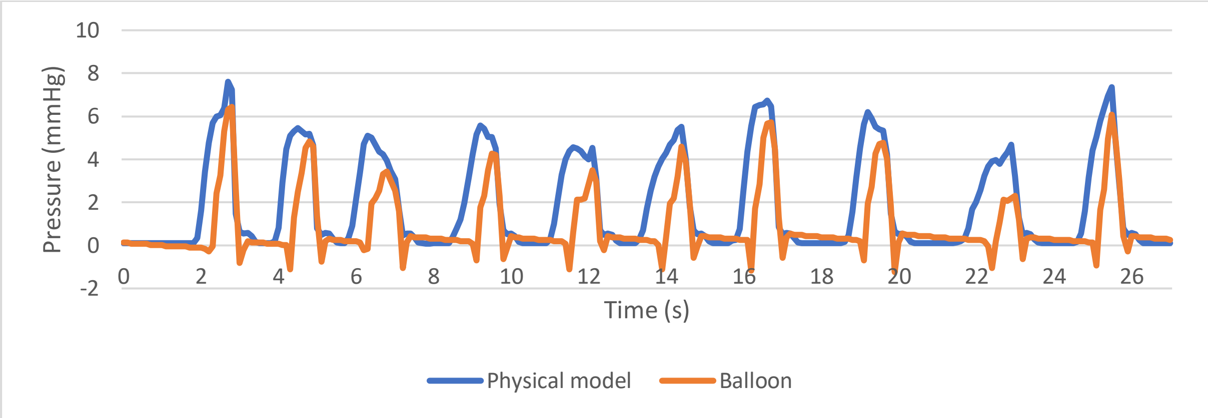

Figure 53: Physical model respiration curve of the square measuring balloon made from PLA

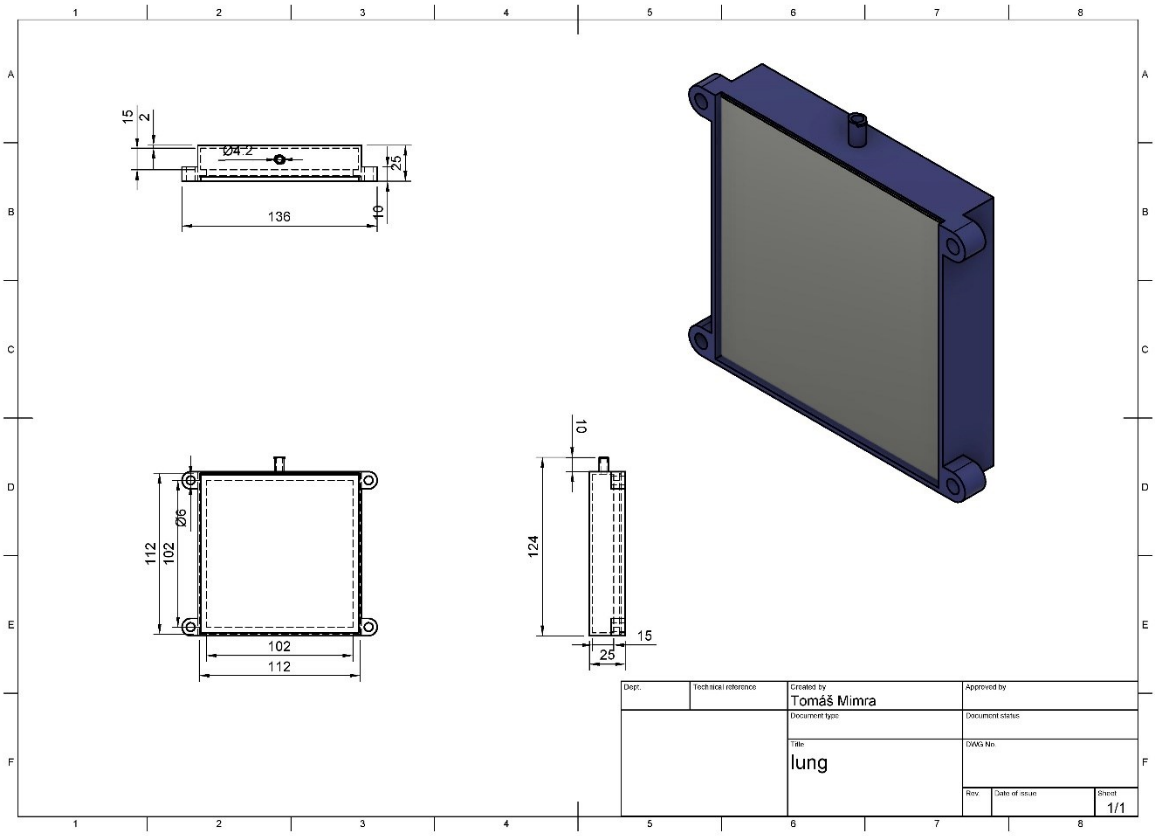

Figure 54: Technical drawing of a self-made lung

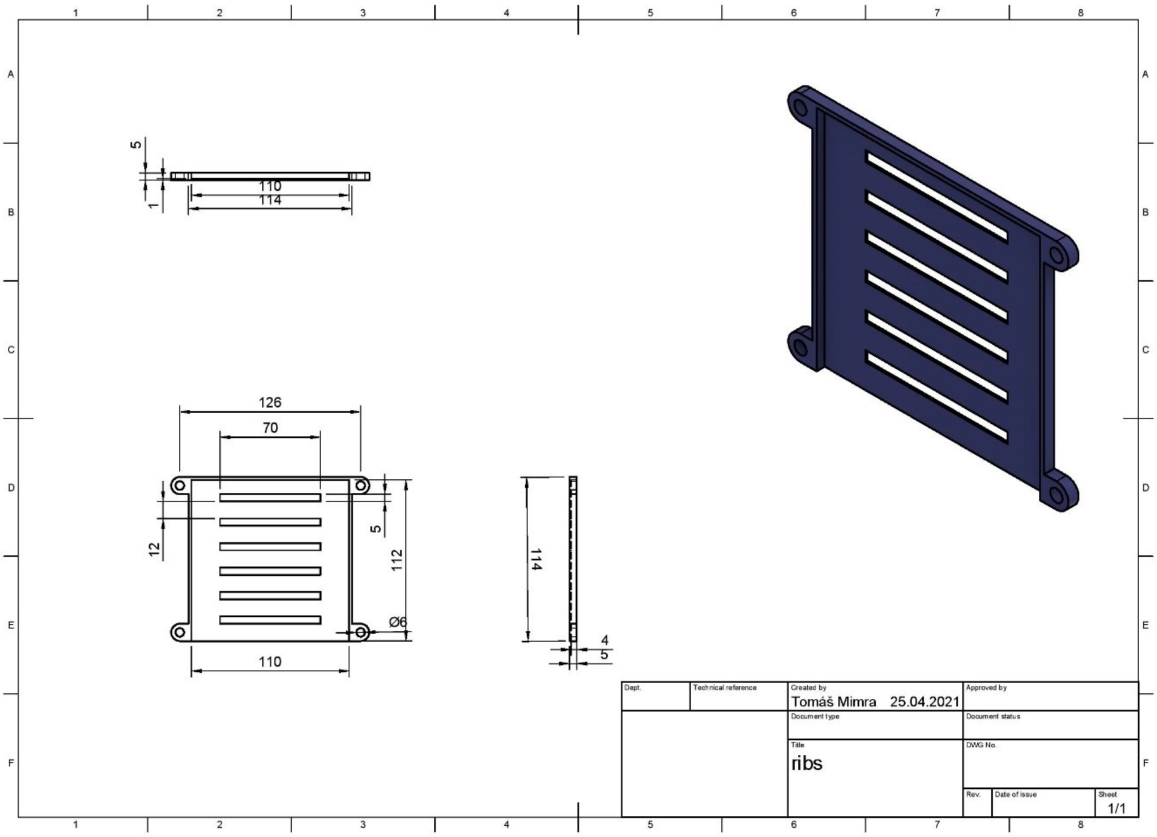

Figure 55: Technical drawing of a self-made ribs

Appendice E: Test with artificial lung

Frequency set to 10 breaths per a minute

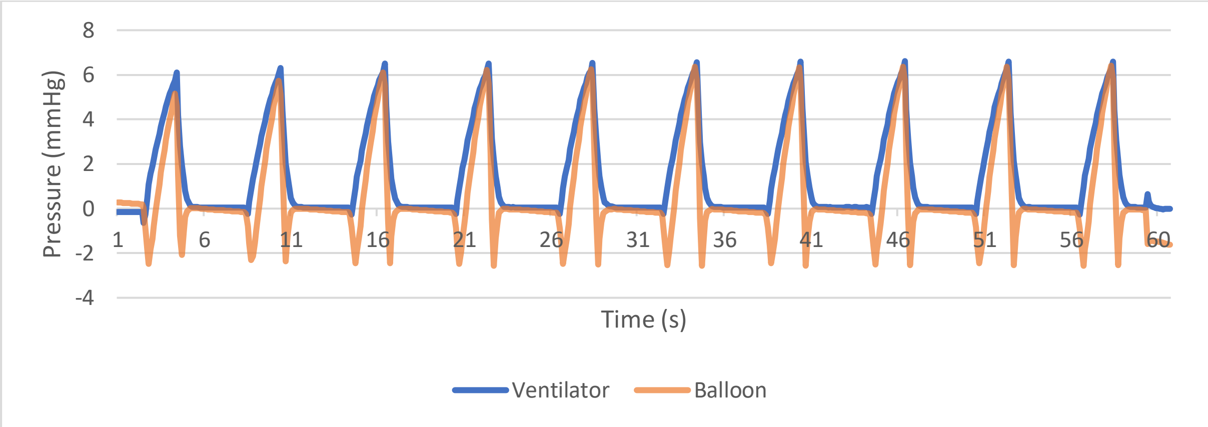

Figure 56: Respiration curve of the triangle measuring balloon made from TPU 92A

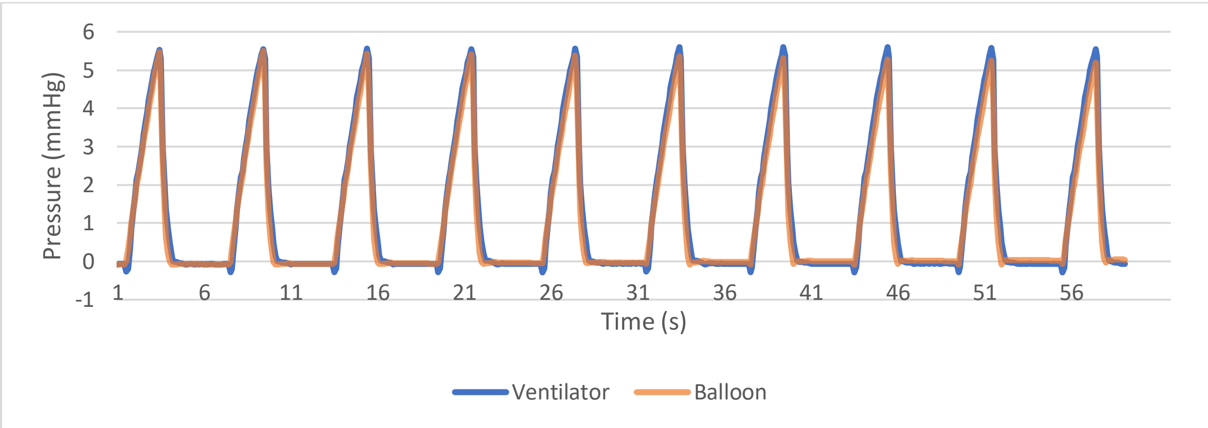

Figure 57: Respiration curve of the square measuring balloon made from TPU 92A

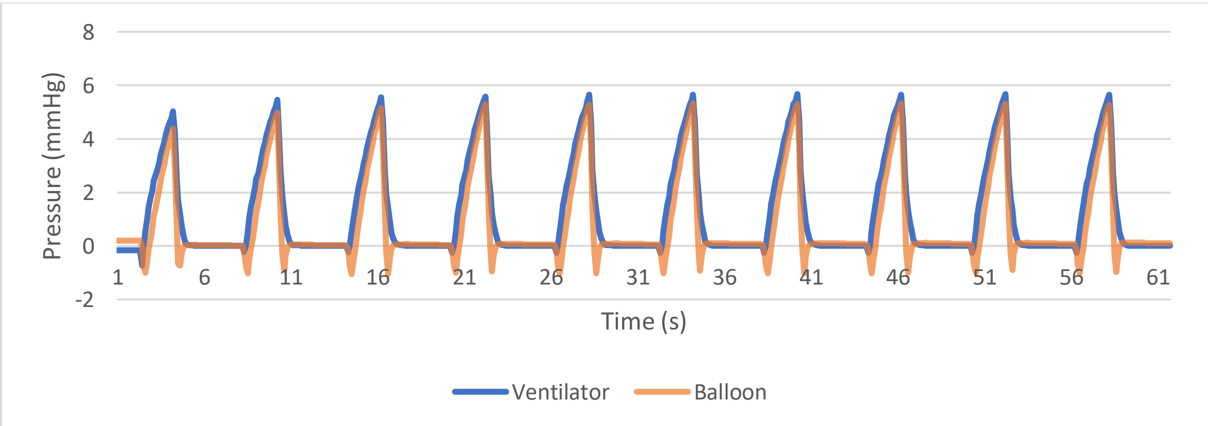

Figure 58: Respiration curve of the circle measuring balloon made from TPU 92A

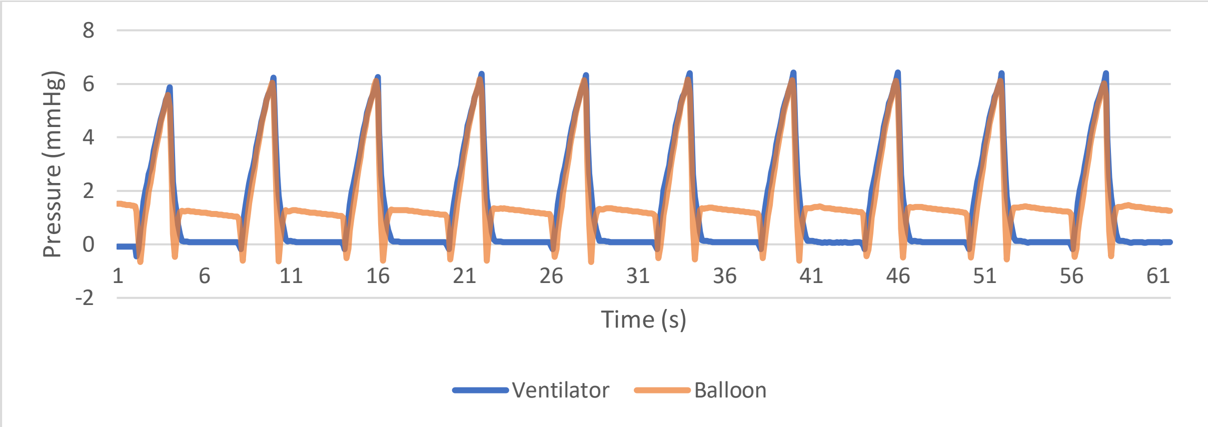

Figure 59: Respiration curve of the small triangle measuring balloon made from TPU 92A

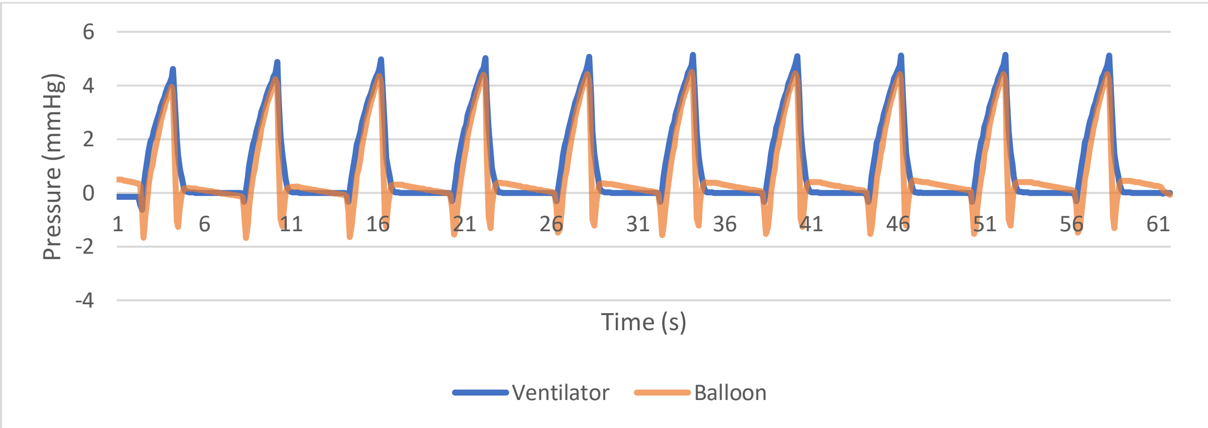

Figure 60: Respiration curve of the circle measuring balloon made from PETG

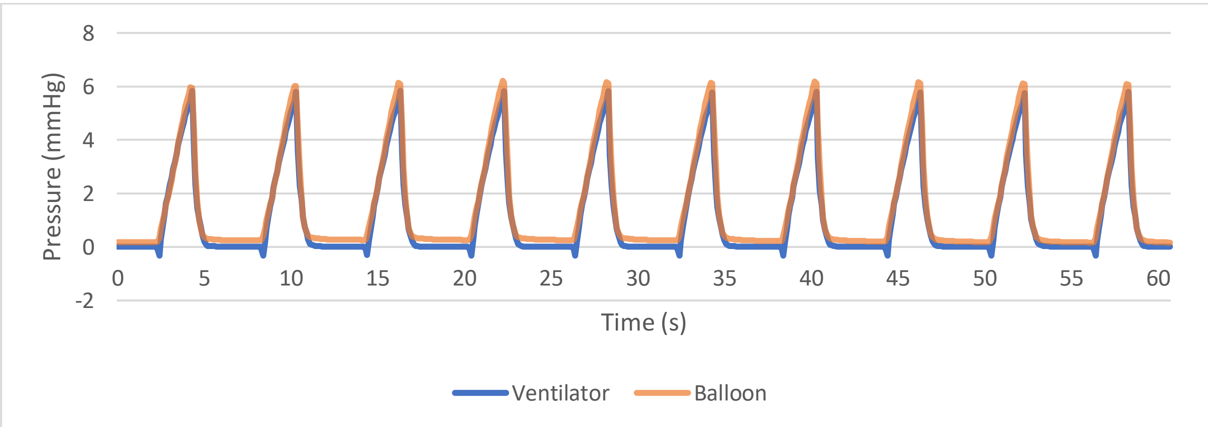

Figure 61: Respiration curve of the circle measuring balloon made from TPU resin

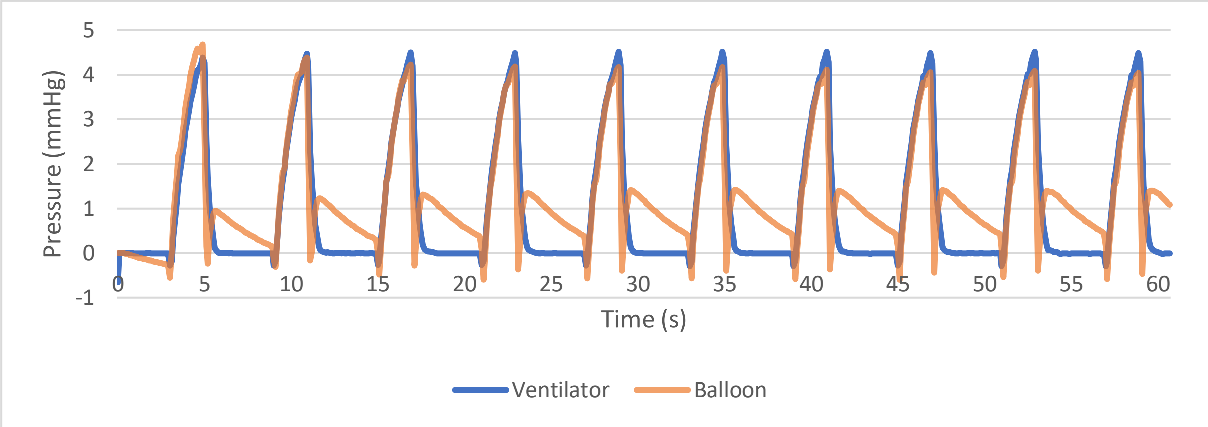

Figure 62: Respiration curve of the circle measuring balloon made from TPE 95A

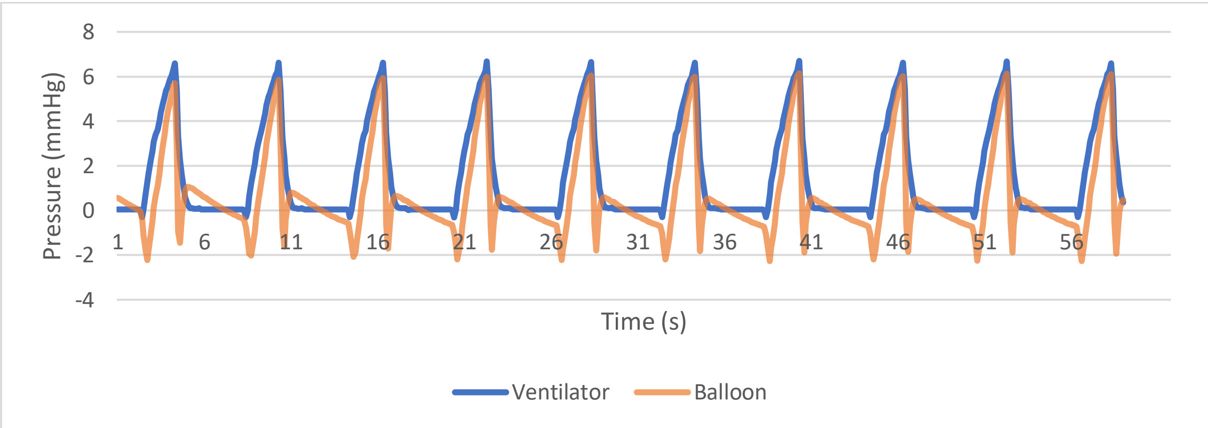

Figure 63: Respiration curve of the triangle measuring balloon made from rigid resin

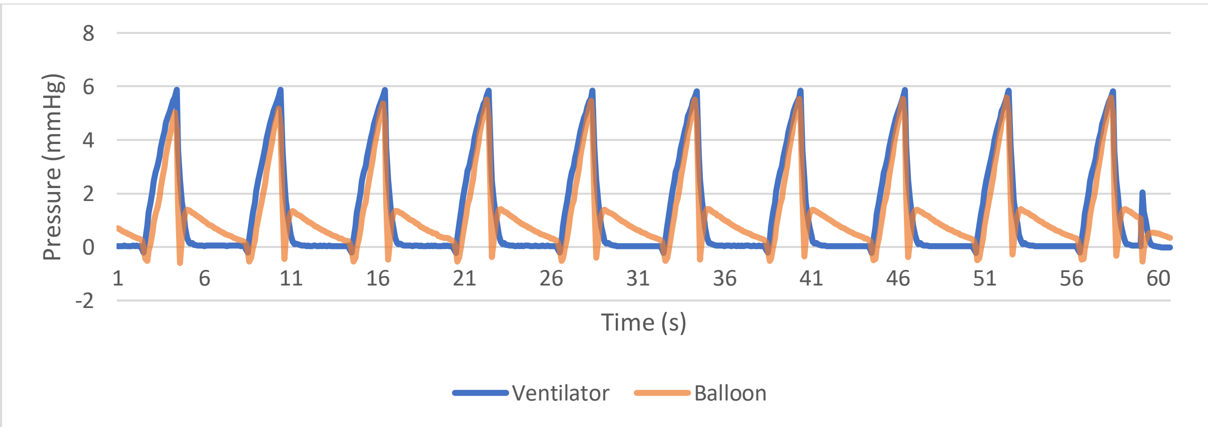

Figure 64: Respiration curve of the triangle measuring balloon made from PP

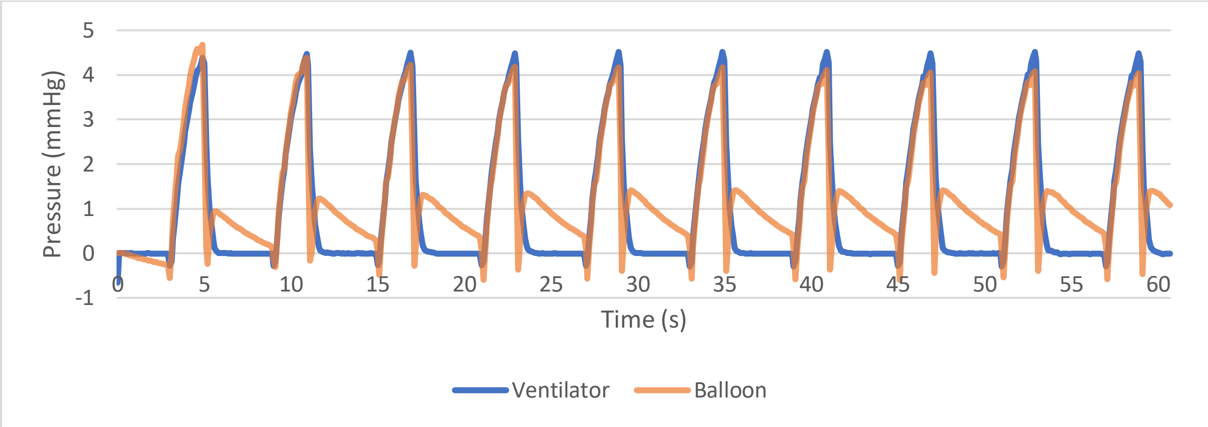

Figure 65: Respiration curve of the square measuring balloon made from PLA

Frequency set to 20 breaths per a minute

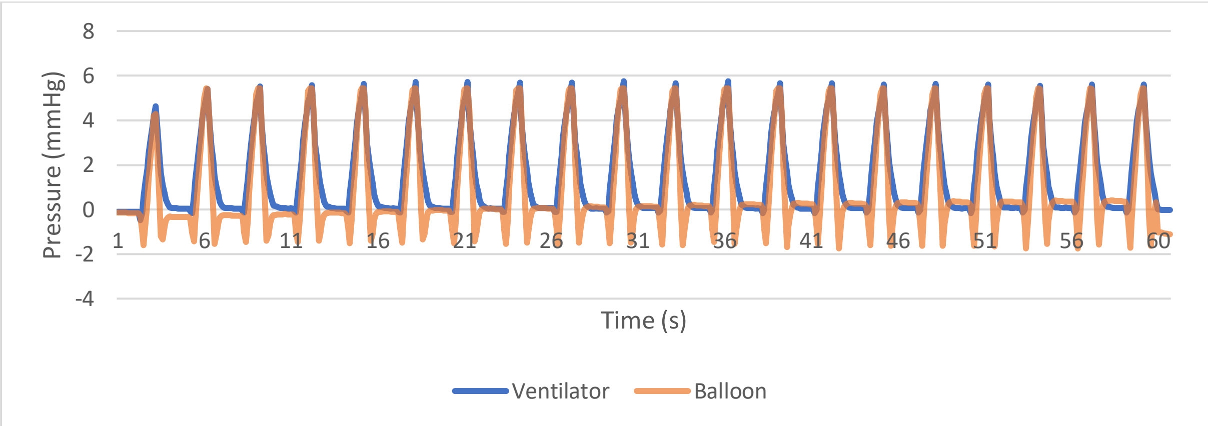

Figure 66: Respiration curve of the triangle measuring balloon made from TPU 92A

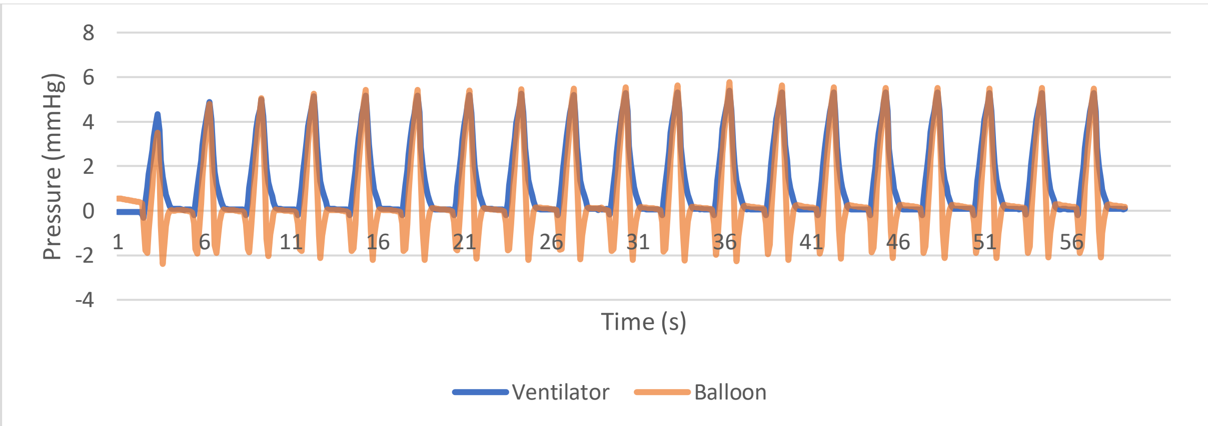

Figure 67: Respiration curve of the square measuring balloon made from TPU 92A

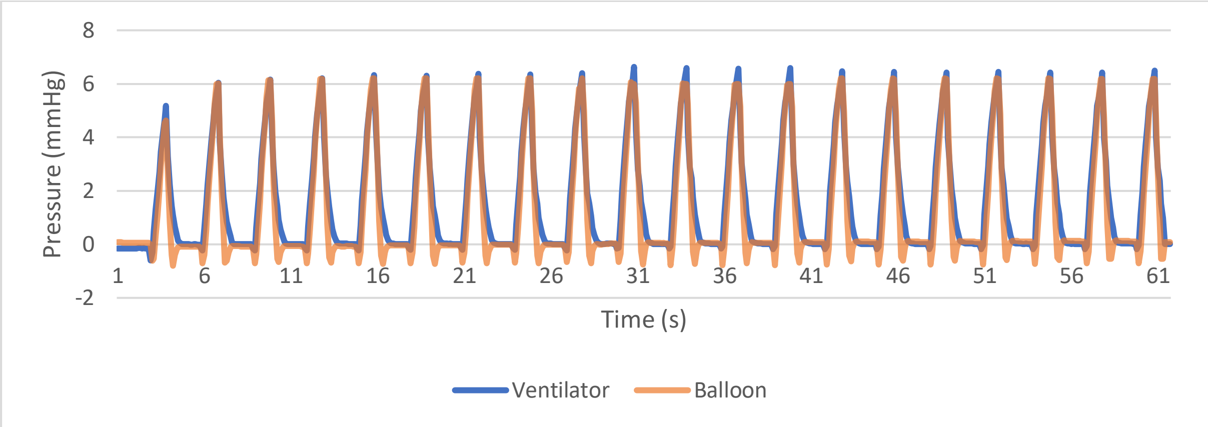

Figure 68: Respiration curve of the circle measuring balloon made from TPU 92A

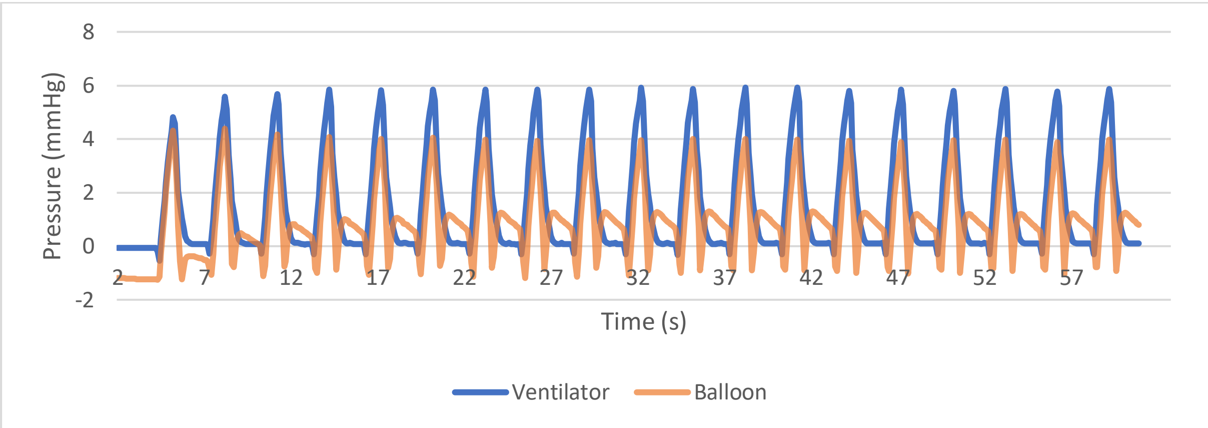

Figure 69: Respiration curve of the small triangle measuring balloon made from TPU 92A

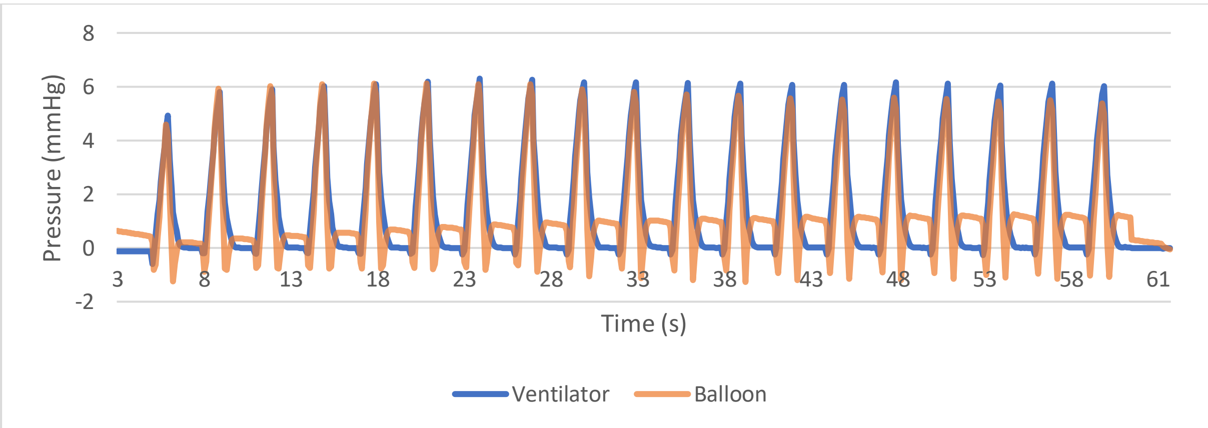

Figure 70: Respiration curve of the circle measuring balloon made from PETG

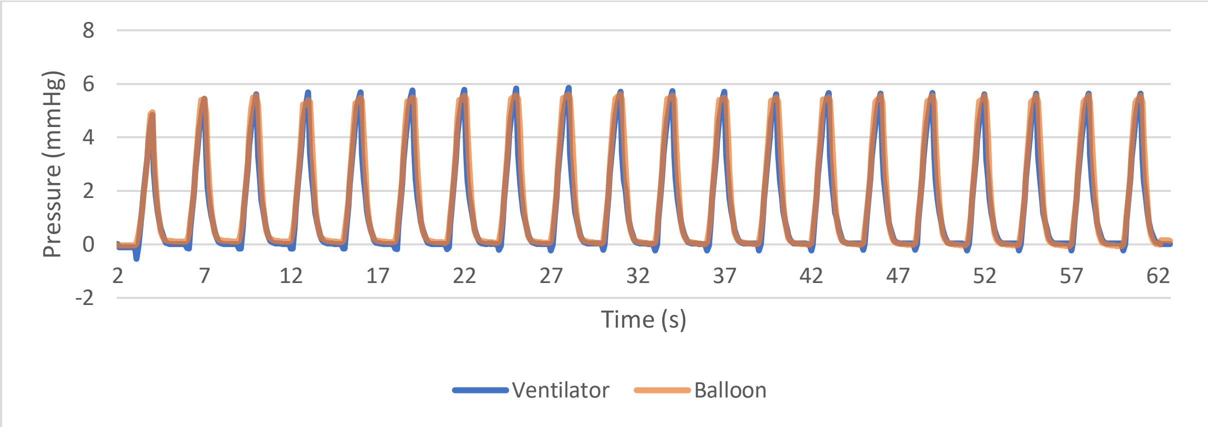

Figure 71: Respiration curve of the circle measuring balloon made from TPU resin

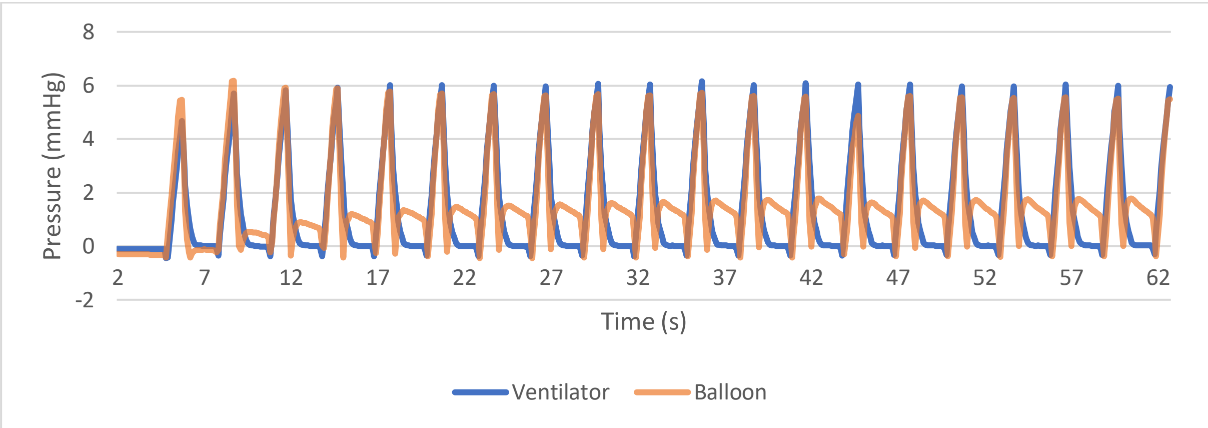

Figure 72: Respiration curve of the circle measuring balloon made from TPE 95A

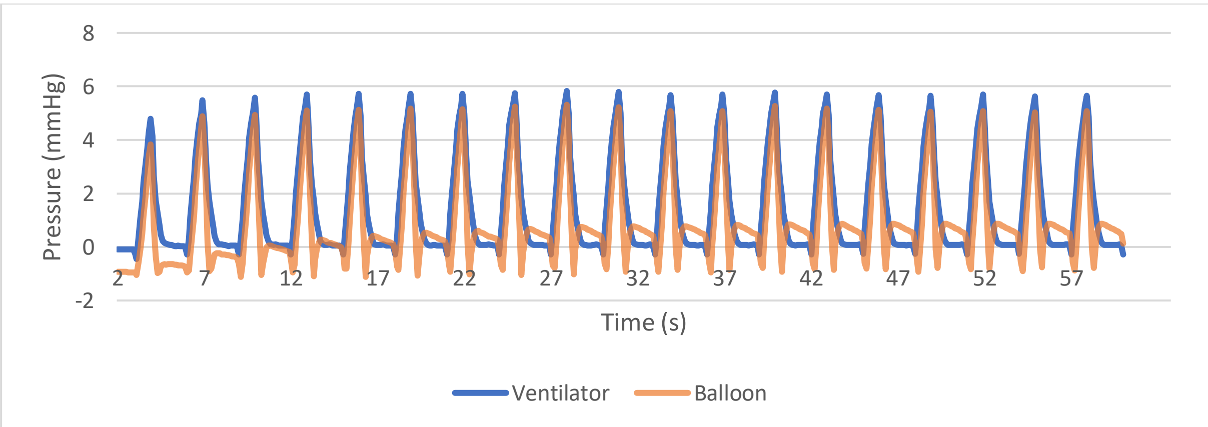

Figure 73: Respiration curve of the triangle measuring balloon made from rigid resin

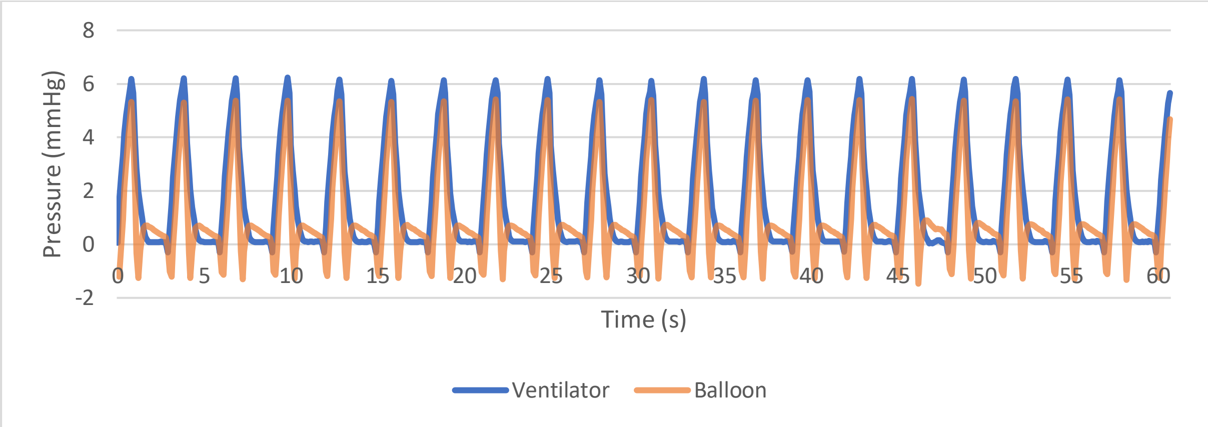

Figure 74: Respiration curve of the triangle measuring balloon made from PP

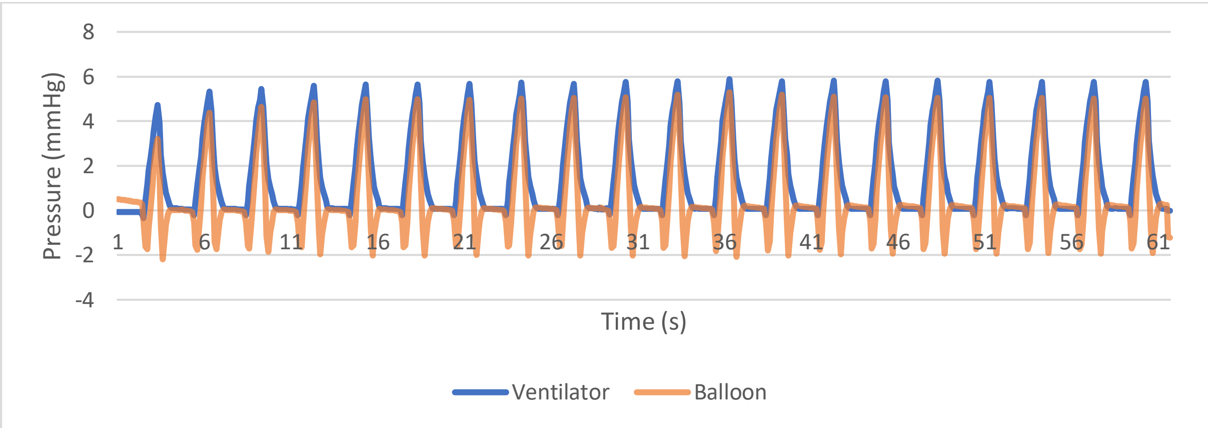

Figure 75: Respiration curve of the square measuring balloon made from PLA

Frequency set to 40 breaths per a minute

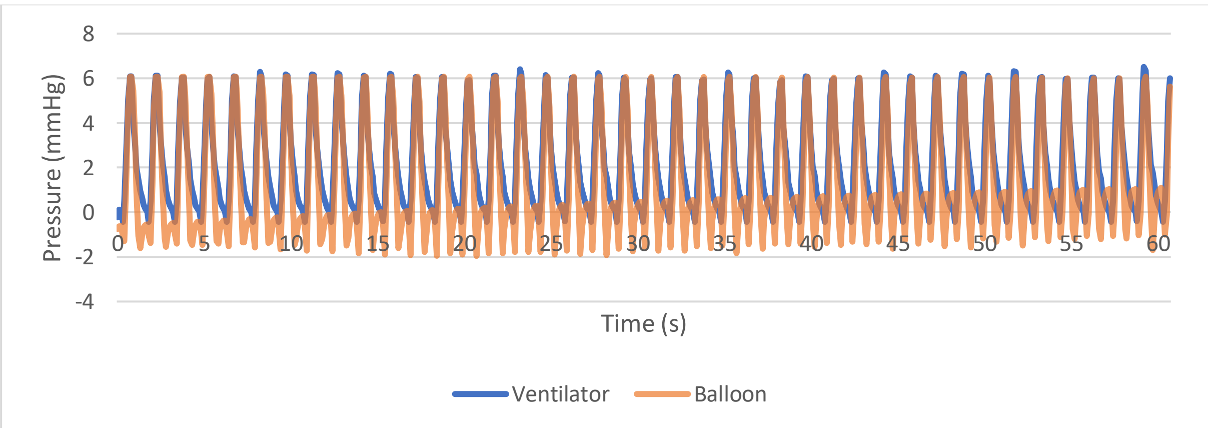

Figure 76: Respiration curve of the triangle measuring balloon made from TPU 92A

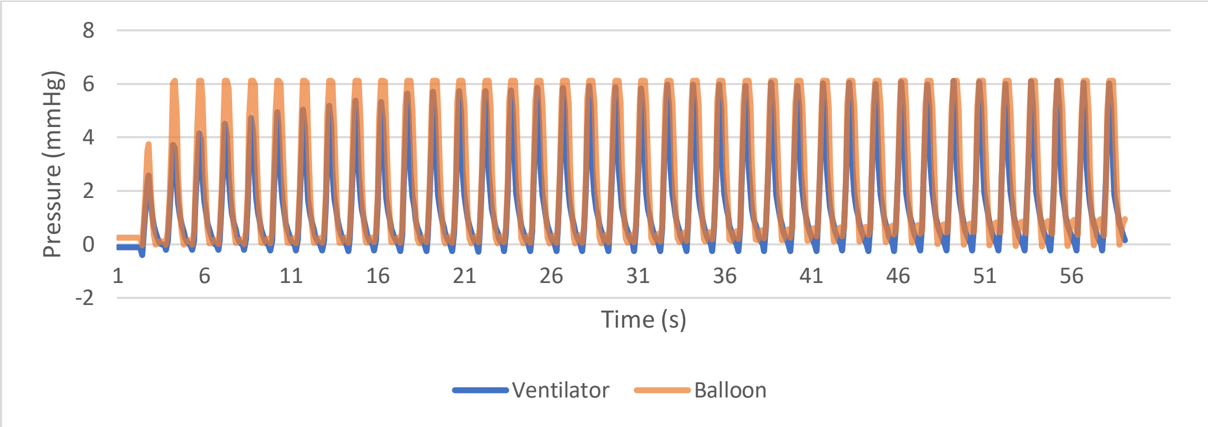

Figure 77: Respiration curve of the square measuring balloon made from TPU 92A

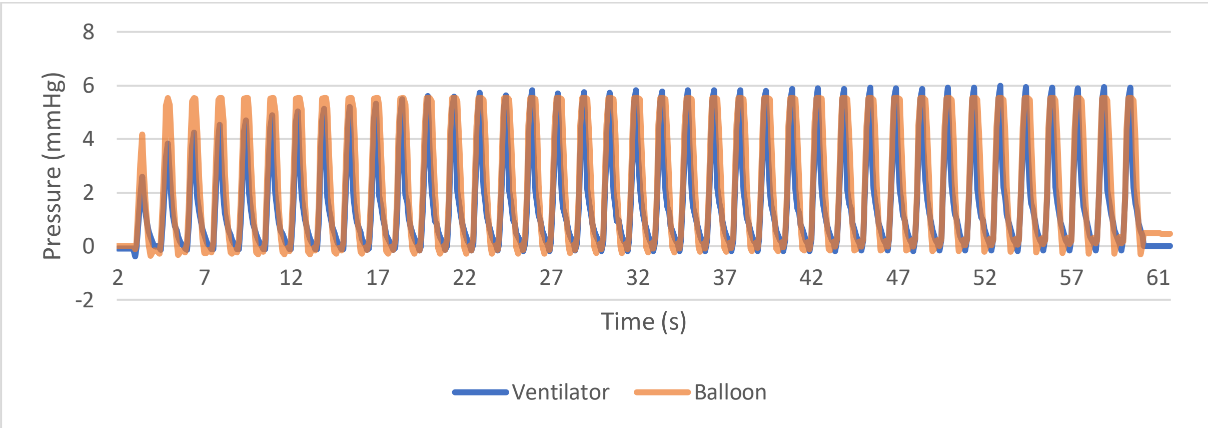

Figure 78: Respiration curve of the circle measuring balloon made from TPU 92A

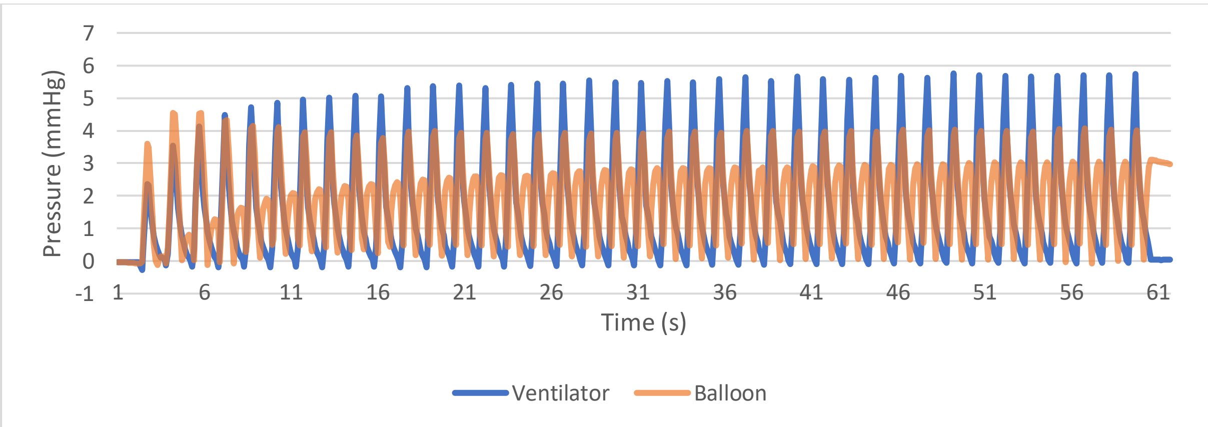

Figure 79: Respiration curve of the small triangle measuring balloon made from TPU 92A

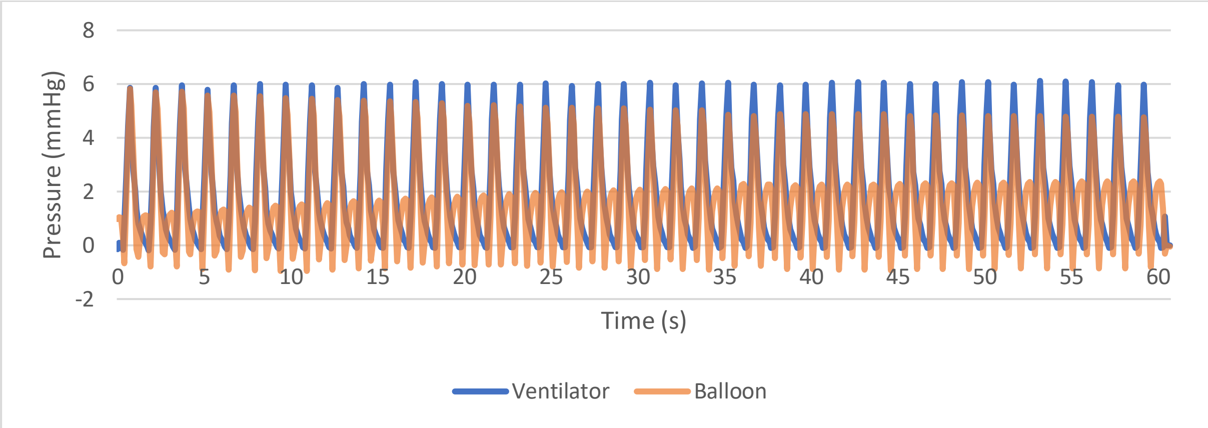

Figure 80: Respiration curve of the circle measuring balloon made from PETG

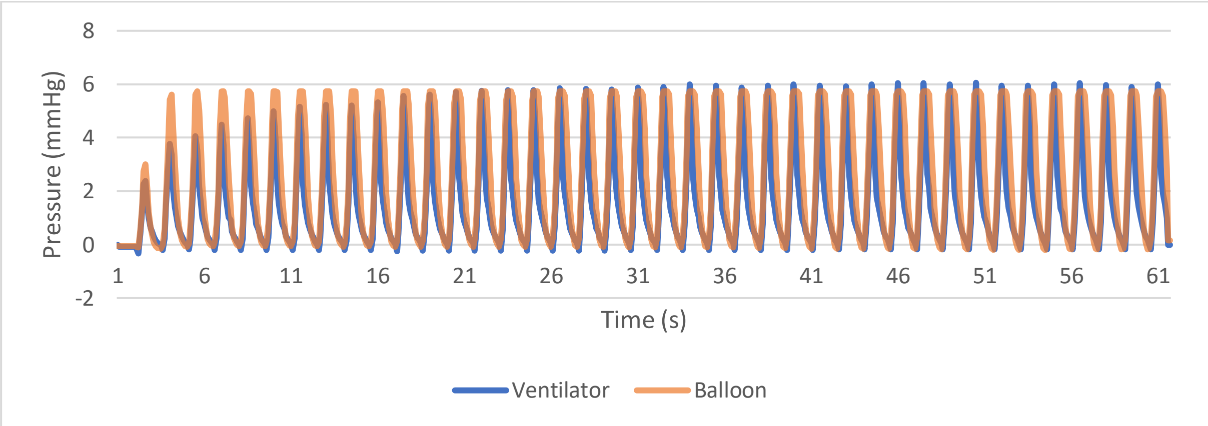

Figure 81: Respiration curve of the circle measuring balloon made from TPU resin

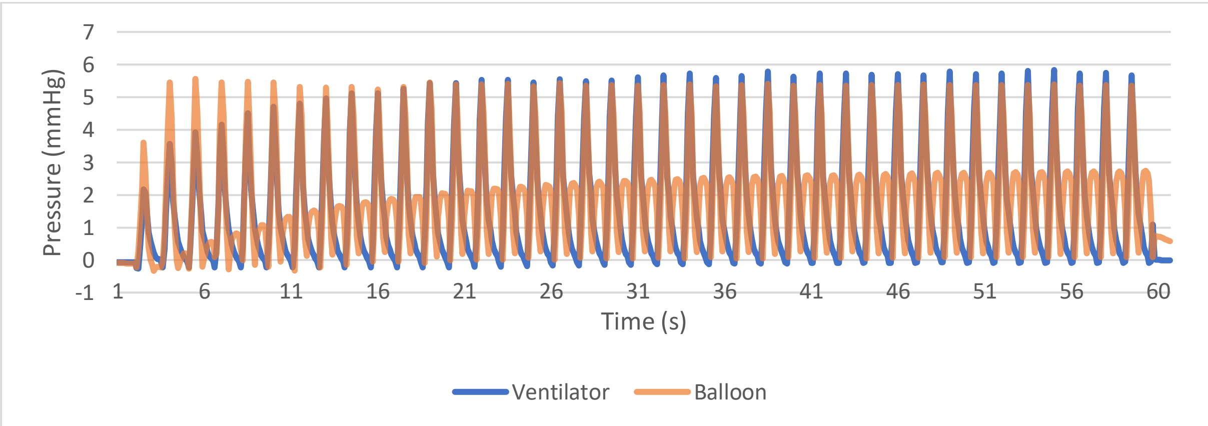

Figure 82: Respiration curve of the circle measuring balloon made from TPE 95A

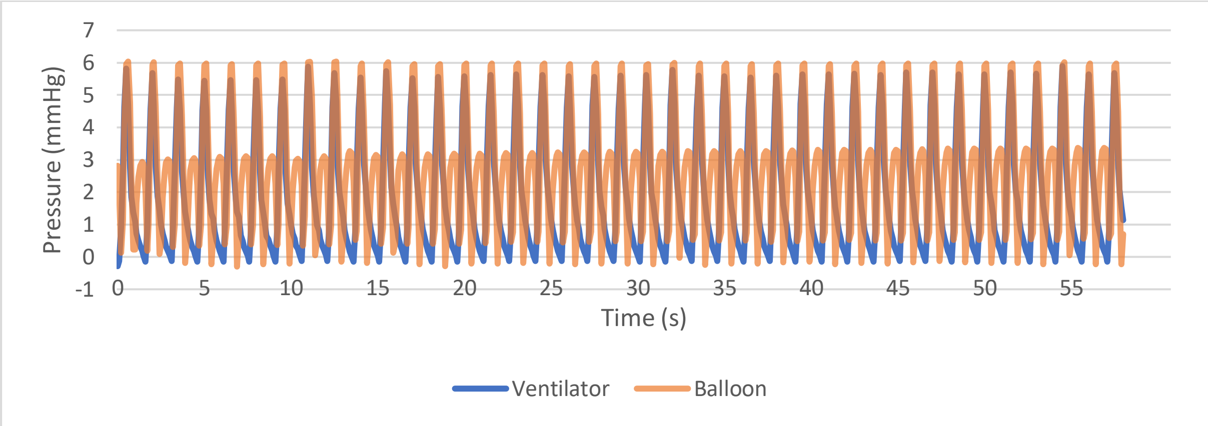

Figure 83: Respiration curve of the triangle measuring balloon made from rigid resin

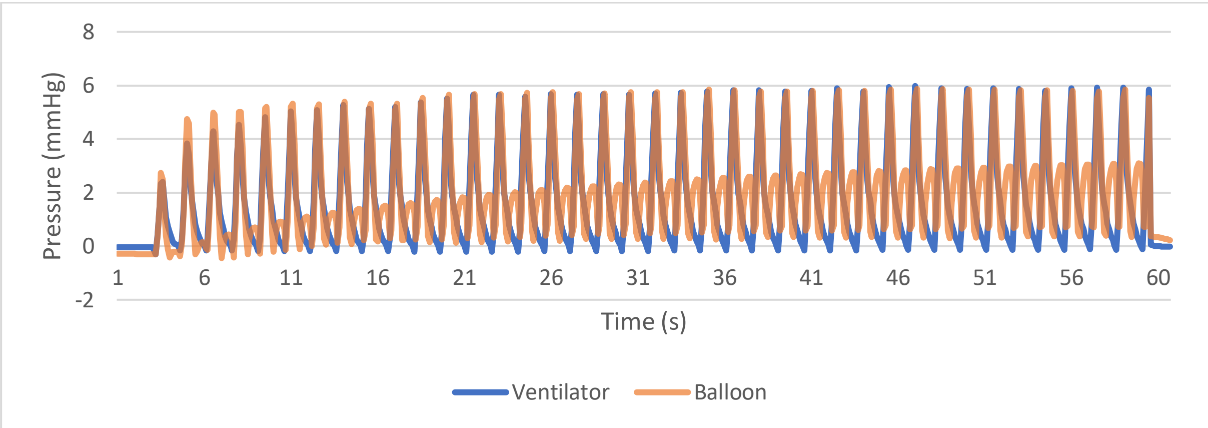

Figure 84: Respiration curve of the triangle measuring balloon made from PP

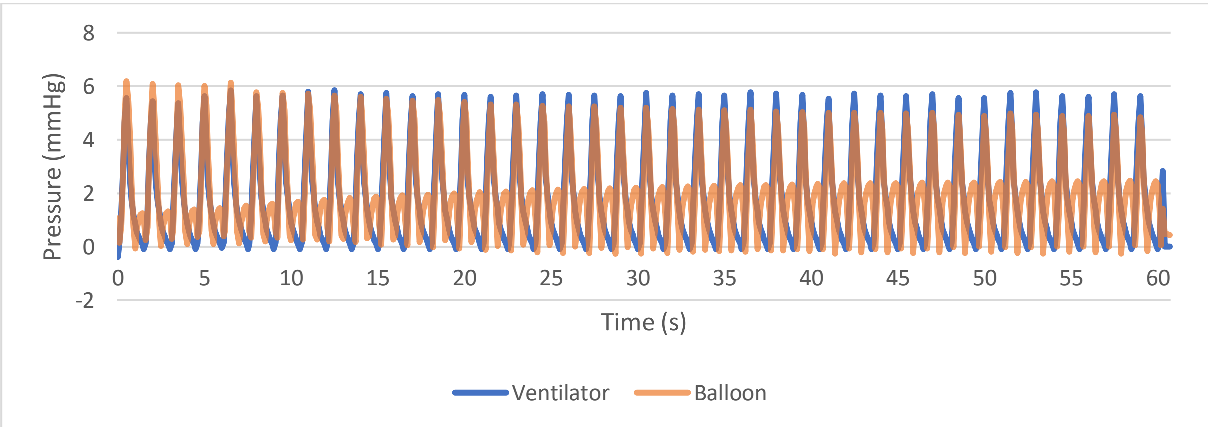

Figure 85: Respiration curve of the square measuring balloon made from PLA